AD-A115 007 NORTHEASTERN UNIV BOSTON MA F/G 12/1
RECEIVER OPTIMIZATION AND ERROR RATES FOR PSEUDO-NOISE SPREAD S--ETC(U)
FEB 82 J W KETCHUM, J G PROAKIS F30602-78-C-0102
UNCLASSIFIED RADC-TR-81-402 NL

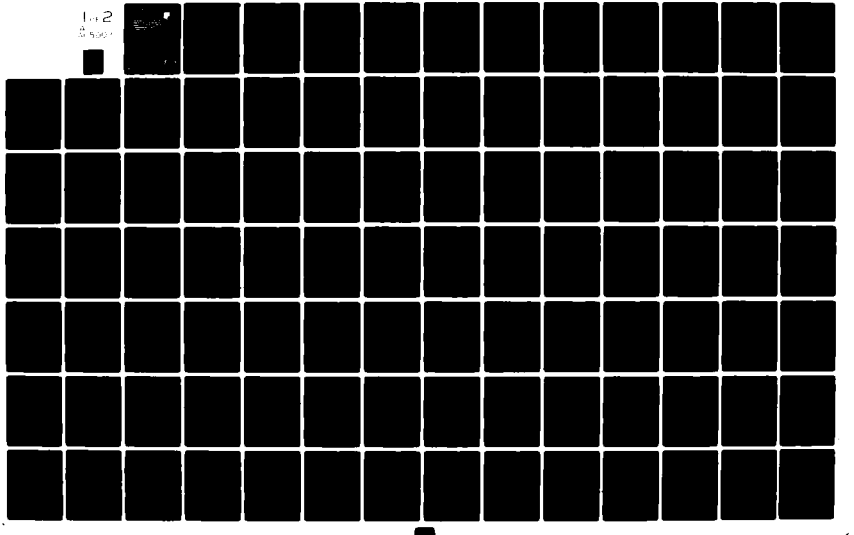

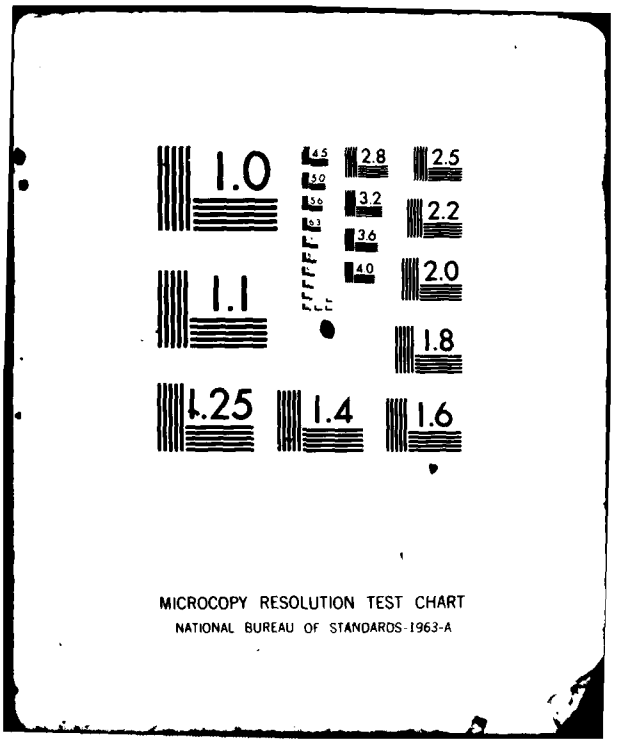
1.0
1.1
1.25
1.4
1.6
1.8
2.0
2.2
2.5
2.8
3.2
3.6
4.0
4.5
5.0
5.6
6.3
MICROCOPY RESOLUTION TEST CHART
NATIONAL BUREAU OF STANDARDS-1963-A

RADC-TR-81-402
Final Technical Report
February 1982

RECEIVER OPTIMIZATION AND ERROR RATES FOR PSEUDO-NOISE SPREAD SPECTRUM SYSTEMS WITH NARROWBAND INTERFERENCE SUPPRESSION

Northeastern University

John W. Ketchum
Dr. John G. Proakis

ROME AIR DEVELOPMENT CENTER
Air Force Systems Command
Griffiss Air Force Base, New York 13441

This report has been reviewed by the RADC Public Affairs Office (PA) and is releasable to the National Technical Information Service (NTIS). At NTIS it will be releasable to the general public, including foreign nations.

RADC-TR-81-402 has been reviewed and is approved for publication.

APPROVED: John T. Gamble

JOHN T. GAMBLE
Project Engineer

APPROVED: Bruno Beek

BRUNO BEEK
Acting Technical Director
Communications Division

FOR THE COMMANDER: John P. Huss

JOHN P. HUSS
Acting Chief, Plans Office

If your address has changed or if you wish to be removed from the RADC mailing list, or if the addressee is no longer employed by your organization, please notify RADC (DCCL) Griffiss AFB NY 13441. This will assist us in maintaining a current mailing list.

Do not return copies of this report unless contractual obligations or notices on a specific document requires that it be returned.

UNCLASSIFIED

SECURITY CLASSIFICATION OF THIS PAGE (When Data Entered)

REPORT DOCUMENTATION PAGE		READ INSTRUCTIONS BEFORE COMPLETING FORM
1. REPORT NUMBER RADC-TR-81-402	2. GOVT ACCESSION NO. AD-A115 007	3. RECIPIENT'S CATALOG NUMBER
4. TITLE (and Subtitle) RECEIVER OPTIMIZATION AND ERROR RATES FOR PSEUDO-NOISE SPREAD SPECTRUM SYSTEMS WITH NARROWBAND INTERFERENCE SUPPRESSION		5. TYPE OF REPORT & PERIOD COVERED Final Technical Report Oct 80 - Jul 81 6. PERFORMING ORG. REPORT NUMBER N/A
7. AUTHOR(s) John W. Ketchum Dr. John G. Proakis		8. CONTRACT OR GRANT NUMBER(s) F30602-78-C-0102
9. PERFORMING ORGANIZATION NAME AND ADDRESS Northeastern University Boston MA 02115		10. PROGRAM ELEMENT, PROJECT, TASK AREA & WORK UNIT NUMBERS 61102F 2305J8P5
11. CONTROLLING OFFICE NAME AND ADDRESS Rome Air Development Center (DCCL) Griffiss AFB NY 13441		12. REPORT DATE February 1982 13. NUMBER OF PAGES 128
14. MONITORING AGENCY NAME & ADDRESS(if different from Controlling Office) Same		15. SECURITY CLASS. (of this report) UNCLASSIFIED 15a. DECLASSIFICATION/DOWNGRADING SCHEDULE N/A

16. DISTRIBUTION STATEMENT (of this Report)

Approved for public release; distribution unlimited.

17. DISTRIBUTION STATEMENT (of the abstract entered in Block 20, if different from Report)

Same

18. SUPPLEMENTARY NOTES

RADC Project Engineer: Dr. John T. Gamble (DCCL)

19. KEY WORDS (Continue on reverse side if necessary and identify by block number)

Algorithms
Adaptive Algorithms
Interference Cancellation
Spread Spectrum

20. ABSTRACT (Continue on reverse side if necessary and identify by block number)

This report describes the results of a study of maximum likelihood receiver structures for direct sequence spread spectrum communications over channels with multipath distortion and narrowband interference, and several methods of assessing the bit error probability performance of bit-by-bit receivers and maximum likelihood receivers. This work is a continuation of work which focused on the performance of various methods of suppressing narrowband interference using spectral estimation. The pre-

DD FORM 1 JAN 73 1473 EDITION OF 1 NOV 65 IS OBSOLETE

UNCLASSIFIED

SECURITY CLASSIFICATION OF THIS PAGE (When Data Entered)

vious work gave performance results in terms of SNR improvement provided by interference suppression. The previous results are extended in this report by deriving a receiver structure based on the maximum likelihood (minimum probability of error) principle. Error probability results given include simulation of a bit-by-bit receiver operated in conjunction with dispersive and nondispersive channels with narrowband interference. Also, a technique for assessing the error rate by averaging conditional probabilities is stated which applies to both fixed nondispersive and fixed dispersive channels, and bit-by-bit and maximum likelihood receivers. Probability of error results obtained using this approach are given.

PREFACE

This final report describes work performed under the RADC Post Doctoral Program, Contract No. F30602-78-C-0102, during the period October 1980 to July 1981. The Principal Investigator was Professor John G. Proakis. The technical monitor at RADC was Dr. John Gamble.

The technical support and useful suggestions provided by Dr. John Gamble during the course of this work is deeply appreciated.

Table of Contents

List of Figures

I. Introduction

Adaptive interference estimation and suppression algorithms have recently been demonstrated to be an effective method of improving the performance of direct sequence spread spectrum communication systems in the presence of narrowband interference or jamming. Conventional direct sequence spread spectrum communication receivers rely on the processing gain inherent in this communication technique to provide an advantage over the intentional jammer or other co-channel users. However, Hsu and Giordano [1], and Proakis and Ketchum [2] have demonstrated that by taking advantage of the white noise-like properties of the direct sequence spread spectrum signal, any of a number of spectral estimation algorithms can be employed to estimate and suppress interference which is narrowband relative to the spread spectrum signal. By doing this, a significant additional advantage over the interferer is gained.

These estimation and suppression algorithms have in common the property that their output is a set of filter coefficients for a transversal, or finite impulse response (FIR), filter which processes the received signal prior to sequence correlation, as shown in Figure 1. The estimation and suppression

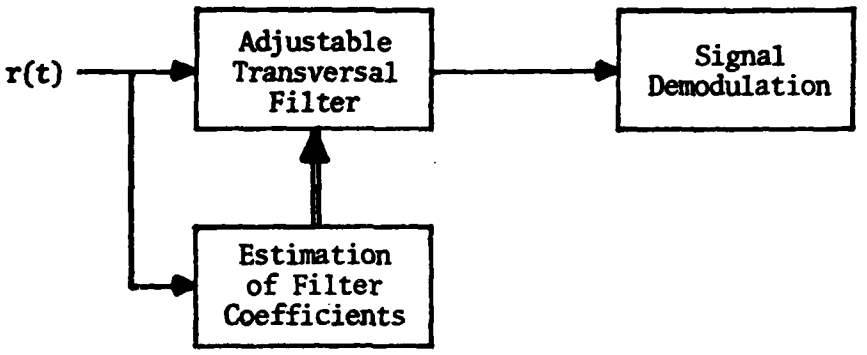

Figure 1

algorithms attempt to design a transversal filter which places a notch in the band(s) occupied by the narrowband interference. Thus these filters have the effect of significantly attenuating the interference power, as well as introducing distortion in the desired signal.

The algorithms considered in [2] fell into two classes: parametric and non-parametric. The non-parametric algorithms make use of classical frequency domain techniques, such as described in [3] to provide an estimate of the interference spectrum. This estimated spectrum is then used to compute the coefficients of a linear phase transversal filter which is the interference suppression filter.

The parametric algorithms considered in [1] and [2] are based on modeling the interference as the output of an all-pole filter which is driven by a white noise sequence. The pole positions are estimated using linear prediction, and the resulting pole positions are used as the zero locations of the FIR suppression filter. In this way, the intermediate

step of computing a spectral estimate is avoided, the suppression filter coefficients being computed directly from the data. In view of their greater simplicity, and the fact that they provide generally superior performance, the parametric methods only will be considered in this report.

Both of these methods of determining a suitable suppression filter were considered in detail in [2], and will not be considered further here. The performance of these suppression filters was given in terms of the SNR improvement factor, which is the ratio of the SNR with the suppression filter to the SNR without the filter. No explicit error rate data was given, except for the output of a simulation of a receiver which uses a decision feedback equalizer (DFE) as well as suppression filtering in a multipath environment. Another question which was not considered in [2] was the structure of the maximum likelihood receiver, assuming that some sort of discrete time interference suppression, or noise whitening, filter is used. It is these two subjects, the maximum likelihood receiver, and error rate performance, which are the subject of this report. In addition, some corrections to results contained in [2] are given in the appendices of this report. The errors involve a change in the improvement factor in the case when the suppression filter is linear phase. However, they in no way alter the conclusion that adaptive interference cancellation is an effective way of improving the performance of direct sequence spread spectrum receivers in the presence of

narrowband interference.

Before proceeding with the body of this report, we make some definitions which are useful in the derivations which follow.

Some Definitions

Throughout this report, equivalent lowpass representation of bandpass signals and systems is used. Thus the bandpass signal, $y(t)$, is represented by the lowpass equivalent signal, $x(t)$, satisfying the following relation:

$$y(t) = \mathrm{Re}[x(t)\ e^{j2\pi f_c t}]$$

If $y(t)$ is a deterministic signal, then its energy is given by:

$$E_y = \int_{-\infty}^{\infty} y^2(t)\ dt = \frac{1}{2}\int_{-\infty}^{\infty} |x(t)|^2\ dt$$

If $y(t)$ is a wide sense stationary bandpass process, then we can define its autocorrelation function as:

$$\phi_{yy}(\tau) = E[y(t)\ y(t+\tau)]$$

The autocorrelation function of the equivalent lowpass process is

$$\phi_{xx}(\tau) = \frac{1}{2}\ E[x^*(t)\ x(t+\tau)]$$

These two autocorrelation functions are related by

$$\phi_{yy}(t) = \mathrm{Re}[\phi_{xx}(t)\, e^{j2\pi f_c t}]$$

The power of the bandpass process is

$$P_y = \phi_{yy}(0) = \phi_{xx}(0)$$

If $y(t)$ is a sinusoid in the band of interest, of amplitude A, and with random phase ϕ, then $y(t)$ can be expressed

$$y(t) = A \cos[2\pi(f_c + f_\Delta)\, t + \phi]$$

and the lowpass equivalent signal is

$$x(t) = A \exp\{j[2\pi(f_\Delta)\, t + \phi]\}$$

The respective autocorrelation functions of $y(t)$ and $x(t)$ are

$$\phi_{yy}(\tau) = \frac{A^2}{2} \cos[2\pi(f_c + f_\Delta)\, \tau]$$

and

$$\phi_{xx}(\tau) = \frac{A^2}{2} \exp[j2\pi(f_\Delta)\, \tau]$$

The power is

$$P_y = \frac{A^2}{2}$$

Assume that a binary baseband communications system using antipodal signals with pulse waveform p(t) is corrupted by a single sinusoid $A \cos[2\pi f_\Delta t + \phi)$. The receiver consists of a filter matched to p(t). The signal component at the sampling instant at the output of the matched filter is:

$$\int_{-\infty}^{\infty} p(\tau - k\tau_c)\, p(\tau - k\tau_c)\, d\tau = E$$

The power of the interference component is:

$$\tau_c E_c \phi_{ii}(0) = \frac{A^2}{2} \tau_c E$$

Thus, the signal-to-interference ratio is

$$2E/A^2 \tau_c$$

Alternately, assume that a binary bandpass communications system uses a signaling pulse whose lowpass equivalent is $\hat{p}(t)$, and is corrupted by a single sinusoid $A \cos[2\pi(f_c + f_\Delta) t + \phi]$ whose lowpass equivalent is $A \exp[j(2\pi f_\Delta t + \phi)]$. The signal component at the output of the matched filter is

$$\int_{-\infty}^{\infty} p^*(\tau - k\tau_c)\, p(\tau - k\tau_c)\, d\tau = 2E$$

and the power of the interference component is

$$2\tau_c\, E\phi_{ii}(0) = A^2\, \tau_c\, E$$

The signal-to-interference ratio is

$$4E/A^2\, \tau_c$$

Thus, for interference with the same power, the coherent bandpass communications system achieves twice the signal-to-interference ratio as the baseband system.

We will define the signal-to-interference ratio (SIR) of a bandpass communications system as the ratio of signal power to equivalent baseband interference power in a baseband communications system. In the case of sinusoidal interference, this ratio is

$$SIR = 4E/A^2\, \tau_c$$

II. Maximum Likelihood Receiver

In this section, we consider the structure of the maximum likelihood receiver for detection of direct sequence spread spectrum signals in wideband (white) Gaussian noise, and narrowband interference. In its most general form, this

problem has no straightforward or easily implemented solution. Here, however, we make the simplifying assumption that the receiver contains a noise-whitening filter implemented with a tapped delay line, and whose coefficients are computed using one of the parametric methods given in [2]. The receiver structure for transmission over a nondispersive channel will be considered first, then these results will be generalized to include channels with multipath distortion.

Nondispersive Channel

The model used for the transmitter and nondispersive channel is shown in Figure 2. The input to the transmitter is a binary source which generates symbols u_j, chosen with equal probability from the binary alphabet (-1, +1). The source sequence u_j is multiplied by the modulating PN sequence, c_k, and the product modulates an impulse generator. The subscript j of the source sequence is related to the subscript k of the PN sequence by: $j = \lfloor k/L \rfloor$, where L is the

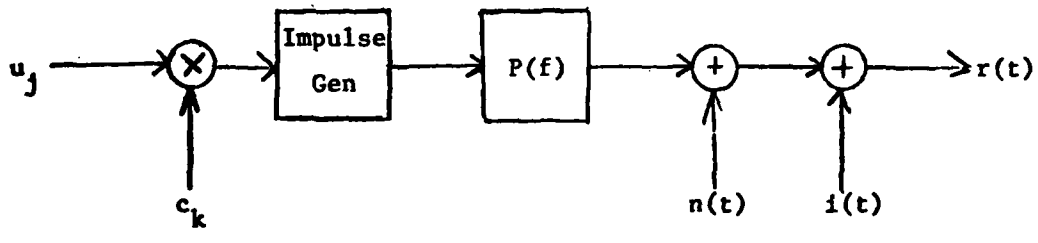

Figure 2

processing gain expressed in chips per bit, and $\lfloor x \rfloor$ denotes the greatest integer not greater than x.

The output of the impulse generator is shaped by the filter P(f), and is transmitted over the channel which is assumed to have a flat frequency response and attenuation α. The transmit filter P(f) is assumed to be such that it introduces no intersymbol interference between the elementary chip pulses transmitted on the channel (interchip interference). That is, if P(f) is followed immediately by its matched filter P*(f), whose impulse response is $p^*(-t)$, and the output of the matched filter is sampled at the appropriate moment, then energy from only one chip pulse effects the sample value. This condition can be written as:

$$\int_{-\infty}^{\infty} p(\tau)\, p^*(\tau - k\tau_c)\, d\tau = 2E_c\, \delta_{ko} \qquad (1)$$

where τ_c is the reciprocal of the chip rate, E_c is the energy in the bandpass chip pulse, and δ_{ko} is the Kronicker delta: $\delta_{ko} = \begin{cases} 1, & k = 0 \\ 0, & k \neq 0 \end{cases}$. Finally, we assume that the receiver has perfect knowledge of the phase of the received signal, so that for the purposes of this discussion, there is zero phase shift in the channel, and α is a real constant.

White Gaussian noise and narrowband interference are added to the signal at the receiver. The double-sided power spectral density of the bandpass white noise process is $N_o/2$,

and the lowpass equivalent process, n(t), has double-sided power spectral density N_o, with corresponding autocorrelation function:

$$\phi_{nn}(\tau) = \frac{1}{2} E[n(t)\ n^*(t - \tau)] = N_o\ \delta(\tau) \qquad (2)$$

The lowpass equivalent narrowband interference has autocorrelation function:

$$\phi_{ii}(\tau) = \frac{1}{2} E[i(t)\ i^*(t - \tau)] \qquad (3)$$

The received signal during the j^{th} symbol epoch is given by:

$$r_j(t) = \sum_{k=jL}^{(j+1)L-1} u_{\lfloor k/L \rfloor}\ c_k\ p(t - k\tau_c) + n(t) + i(t) \qquad (4)$$

For the purposes of deriving the maximum likelihood receiver for the transmitted message we will assume that prior to further processing, the receiver filters the received signal with a tapped delay line whitening filter whose impulse response is:

$$h(\tau) = \sum_{m=0}^{p} h(m)\ \delta(\tau - m\tau_c) \qquad (5)$$

It will be demonstrated subsequently that this is equivalent

to a receiver which contains a sampler with sampling period τ_c, followed by a sampled data FIR filter with coefficients h_m, $m = 0, \ldots, P$.

The output of the whitening filter during the j^{th} symbol epoch is given by:

$$W_j(t) = \sum_{m=0}^{P} h(m) \int_{-\infty}^{\infty} \delta(\tau - m\tau_c)\, r(t - \tau)\, d\tau$$

$$= \sum_{k+jL}^{(j+1)L-1} \sum_{m=0}^{P} h(m)\, u_{\lfloor k/L \rfloor}\, c_k\, p[t - (m + k)\, \tau_c]$$

$$+ \sum_{m=0}^{P} [n(t - m\tau_c) + i(t - m\tau_c)]\, h(m) \qquad (6)$$

It is this signal, $W_j(t)$, for all j over the message duration, to which the maximum likelihood criterion will be applied in order to determine the structure of the maximum likelihood receiver.

Before proceeding, we will make the following definitions:

$$x(t) = p(t) * h(t) \qquad (7)$$

and

$$z(t) = [n(t) + i(t)] * h(t) \qquad (8)$$

where the operation * indicates convolution. The signals x(t) and z(t) are the components at the output of the filter defined in (5) due to the transmitted signal, and the noise and interference, respectively. Furthermore, without loss of generality, we will assume that a given message has duration $-NT \leq t < NT$, or $-NL\tau_c \leq t \leq NL\tau_c - 1$, where $T = L\tau_c$ is the symbol, or bit, duration. Thus, the received signal is written:

$$r(t) = \sum_{k=-NL}^{NL-1} u_{k/L} \; c_k \; p(t - k\tau_c) + n(t) + i(t) \qquad (9)$$

and at the output of the whitening filter, the signal is:

$$w(t) = \sum_{k=-NL}^{NL-1} u_{k/L} \; c_k \; x(t - k\tau_c) + z(t) \qquad (10)$$

In order to obtain the likelihood function, $p[w(t)|\underline{u}]$, which must be maximized in order to minimize the probability of error, w(t) will first be expanded using the Karhunen-Loève series expansion as described, for example, in [3]. This process will provide a set of signal samples, w_k which are uncorrelated. We assume that z(t) is a Gaussian process; thus, the w_k are independent Gaussian random variables. The Karhunen-Loève expansion for w(t) is given by:

$$w(t) = \lim_{N\to\infty} \sum_{k=1}^{N} w_k \; f_k(t) \qquad (11)$$

where

$$w_k = \sum_{\ell=-NL}^{NL-1} u_{\lfloor \ell/L \rfloor}\, c_\ell\, x_{k,\ell} + z_k \qquad (12)$$

The functions $f_k(t)$ are an orthonormal set which satisfy:

$$\int_{-NL\tau_c}^{(NL-1)\tau_c} f_k(\tau)\, \phi_{zz}(t - \tau)\, d\tau = \lambda_k\, f_k(t)$$

and z_k and $x_{k,\ell}$ are given by:

$$z_k = \int_{-NL\tau_c}^{(NL-1)\tau_c} z(t)\, f_k^*(t)\, dt$$

and

$$x_{k,\ell} = \int_{-NL\tau_c}^{(NL-1)\tau_c} x(t - \ell\tau_c)\, f_k^*(t)\, dt$$

Thus the likelihood function for the p^{th} possible transmitted sequence, $\underline{u}_p$, can be written:

$$p(\underline{w}|\underline{u}_p) = \lim_{N\to\infty} \left[\prod_{k=1}^{N} 2\pi\, \lambda_k\right]^{-1/2}$$

$$\cdot \exp\left[-\frac{1}{2} \sum_{k=1}^{N} \left| w_k - \sum_{\ell=-NL}^{NL-1} u_{p,\, \ell/L}\; c_\ell\, x_{k,\ell} \right|^2 / \lambda_k\right] \qquad (13)$$

If we assume that the whitening filter, h(t), has done its job perfectly, so that z(t) is a white Gaussian process, it can be shown that

$$p(\underline{w}|\underline{u}_p) = \int_{-\infty}^{\infty} \exp\left[-\tfrac{1}{2}\left|w(t) - \sum_{\ell=-NL}^{NL-1} u_{\lfloor \ell/L \rfloor}\ c_\ell\ x(t - \ell\tau_c)\right|^2 dt\right] \tag{14}$$

Maximizing (14) over all possible transmitted sequences, $\underline{u}_p$, can be accomplished by maximizing $\ell n[p(\underline{w}|\underline{u}_p)]$ which is equivalent to minimizing the metric

$$\begin{aligned} \Lambda_p &= 2\mathrm{Re}\left[\sum_{k=-NL}^{NL-1} u_{p,\lfloor k/L \rfloor}^*\ c_k^* \int_{-\infty}^{\infty} w(t)\ x^*(t - k\tau_c)\ dt\right] \\ &\quad - \sum_{k=-NL}^{NL-1} \sum_{\ell=-NL}^{NL-1} u_{p,\lfloor k/L \rfloor}^*\ u_{p,\lfloor \ell/L \rfloor}\ c_k^*\ c_\ell \\ &\quad \cdot \int_{-\infty}^{\infty} x^*(t - k\tau_c)\ x(t - \ell\tau_c)\ dt \end{aligned} \tag{15}$$

Note that since both u_j and c_k are chosen from a binary real alphabet, (-1, 1), the complex conjugate indications for the u's and c's in (15) can be dropped.

Next, we define the sample value y_k:

$$y_k = \mathrm{Re} \int_{-\infty}^{\infty} w(\tau)\, x^*(\tau - k\tau_c)\, d\tau$$

$$= \sum_{\ell=-NL}^{NL-1} \alpha u_{\lfloor \ell/L \rfloor}\, c_\ell \int_{-\infty}^{\infty} x(\tau - \ell\tau_c)\, x^*(\tau - k\tau_c)\, d\tau$$

$$+ \int_{-\infty}^{\infty} z(\tau)\, x^*(\tau - k\tau_c)\, d\tau$$

$$= \mathrm{Re}[2\alpha E_c \sum_{m=0}^{P} \sum_{n=0}^{P} u_{\lfloor (k+n-m)/L \rfloor}\, c_{k+n-m}\, h(m)\, h^*(n)]$$

$$+ \mathrm{Re}\{\sum_{m=0}^{P} \sum_{n=0}^{P} h_m\, h_n^* \int_{-\infty}^{\infty} [n(\tau - m\tau_c) + i(\tau - m\tau_c)]$$

$$\cdot\, p^*[\tau - (n + k)\, \tau_c]\, d\tau\}$$

$$= \mathrm{Re}[2\alpha E_c \sum_{m=-p}^{P} u_{\lfloor (k-m)/L \rfloor}\, c_{k-m}\, g(m)$$

$$+ \sum_{m=-p}^{P} g(m) \int_{-\infty}^{\infty} [n(\tau - m\tau_c) + i(\tau - m\tau_c)]$$

$$\cdot\, p^*(\tau - k\tau_c)\, d\tau] \qquad (16)$$

where

$$g(m) \triangleq \sum_{n=0}^{P} h(m + n)\, h^*(n),\ m = -P, \ldots, P \qquad (17)$$

The sample value y_k can be obtained by passing $r(t)$ through the whitening filter $h(\tau)$ given in (5) (see Figure 3), then through its matched filter, $h^*(-\tau)$, and through the chip pulse matched filter, $p^*(-\tau)$. The output of this filter would be sampled at τ_c second intervals, and the real part of the sample values taken, thus forming y_k. However, since the desired signal, $u_{\lfloor k/L \rfloor}\ c_k$, is real, there is an alternate strategy which is preferable, shown in Figure 4. The first filtering operation to be performed in the receiver is the matched filter operation, $\int_{-\infty}^{\infty} r(\tau)\, p^*(\tau - k\tau_c)\, d\tau$. The output of the matched filter is sampled, and the real part of the sampler output is taken. Thus, we have eliminated the need to perform spectral estimation on a complex valued signal and can now use a discrete time whitening filter with real valued tap weights.

Next, noting that

$$\int_{-\infty}^{\infty} x^*(t - k\tau_c)\, x(t - \ell\tau_c)\, dt = \sum_{m=0}^{P} \sum_{n=0}^{P} h(m)\, h(n)$$

$$\cdot \int_{-\infty}^{\infty} p^*[t - (k + n)\, \tau_c]\, p[t - (\ell + m)\, \tau_c]\, dt$$

$$= 2E_c \sum_{m=-p}^{P} g(m)\, \delta_{\ell k+m} \qquad (18)$$

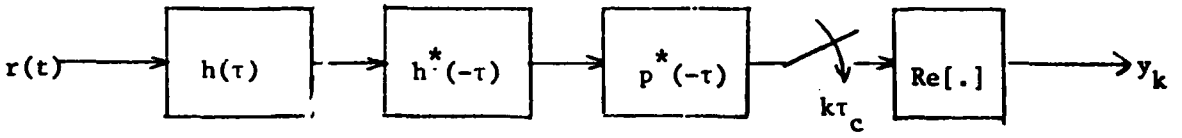

Figure 3

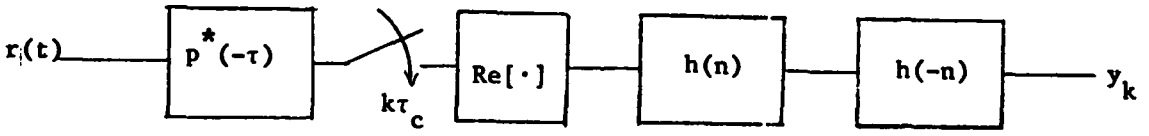

Figure 4

we can write the likelihood function as:

$$\Lambda_p = \sum_{k=-NL}^{NL-1} [2u_{p,\lfloor k/L \rfloor}\ c_k\ y_k - 2\alpha E_c \sum_{m=-p}^{p} u_{p,\lfloor k/L \rfloor}$$

$$\cdot\ u_{p,\lfloor (k-m)/L \rfloor}\ c_k\ c_{k-m}\ g(m)]$$

$$= \sum_{j=-N}^{N-1} [\sum_{k=jL}^{(j+1)L-1} 2u_{p,j}\ c_k\ y_k$$

$$- 2\alpha E_c (u_{p,j}\ c_k)^2\ g(0)$$

$$- 4\alpha E_c \sum_{m=1}^{p} \sum_{k=jL}^{(j+1)L-1} u_{p,j}\ u_{p,\lfloor (k-m)/L \rfloor}\ c_k\ c_{k-m}\ g(m)] \qquad (19)$$

The first term inside the brackets in (19) indicates that the output of the composite whitening filter-matched filter is processed by a sequence correlator which multiplies y_k by the PN sequence c_k, and sums over the bit interval T. If there were no interference, and therefore the whitening filter was such that $g(m) = 0$, $m \neq 0$, then this operation alone would constitute the maximum likelihood receiver and the output of the sequence correlator would form the decision variable on which bit decisions would be made, on a bit-by-bit basis.

However, because of the dispersion caused by the noise-whitening filter, y_k depends not only on the bit currently being transmitted, but also on adjacent bits. For this reason, it is necessary to consider the received sequence in its entirety, rather than on a bit-by-bit basis, when deciding which transmitted sequence was most likely to have been transmitted.

The Viterbi algorithm is an efficient method of accomplishing this maximum likelihood sequence estimation without waiting for the entire sequence $\underline{u}$ to be transmitted. If we wait for the entire sequence of 2N bits to be transmitted, and consider the metric, Λ_p, for each of 2^{2N} possible transmitted sequences, the result is a very complex receiver with large decoding delay. The Viterbi algorithm reduces the delay and complexity at the receiver by constructing a state trellis through which the receiver moves as it performs the maximum likelihood detection. The trellis has 2N stages with $2^{\lceil P/L \rceil}$ nodes at each stage, where P is the memory, in chip intervals, introduced by the whitening filter; L is the processing gain; and $\lceil x \rceil$ denotes the least integer not less than x. At each stage in the trellis, which corresponds to processing of a single received bit, the receiver computes two branch metrics for each node. Thus at each stage, the receiver considers $2^{\lceil P/L \rceil + 1}$ sequences, and $(2N)2^{\lceil P/L \rceil + 1}$ for the entire sequence. The branch metric which must be computed for the P^{th} branch at the j^{th} stage is:

$$\lambda_{pj} = \sum_{k=jL}^{(j+1)L-1} 2u_{p,j}\, c_k\, y_k - 2E_c\alpha(u_{p,j}\, c_k)^2\, g(0)$$

$$- 4\alpha E_c \sum_{k-jL}^{(j+1)L-1} \sum_{m=1}^{P} u_{p,j}\, u_{p,\lfloor (k-m)/L \rfloor}\, c_k\, c_{k-m}\, g(m) \qquad (20)$$

A block diagram of the receiver which results from the maximum likelihood criterion is shown in Figure 5, as well as a state trellis for $P/L = 1$ in Figure 6.

It is interesting to note that the maximum likelihood criterion leads to a branch metric which does nothing to counter the effects of pulse dispersion on the chip level. To see this, assume that $L >> P$, so that the contribution to the rightmost term in (20) due to summands where $\lfloor (k - m)/L \rfloor \neq j$ is negligible. If this is the case, for a given j this term is constant over all sequences, and for this reason it has no effect on the sequence decision. In other words, the inter-symbol interference is negligible. In this case, the branch metric reduces to:

$$\lambda_{pj} = \sum_{k=jL}^{(j+1)L-1} 2u_{p,j}\, c_k\, y_k$$

$$= \sum_{k=jL}^{(j+1)L-1} 2u_{p,j}\, c_k [2\alpha E_c\, u_j\, c_k\, g(0)]$$

$$+ \sum_{k=jL}^{(j+1)L-1} 2u_{p,j}\, c_k [2\alpha E_c \sum_{\substack{m=-p \\ m\neq 0}}^{P} u_{\lfloor (k-m)/L \rfloor}\, c_{k-m}\, g(m)]$$

$$+ \text{noise term} \qquad (21)$$

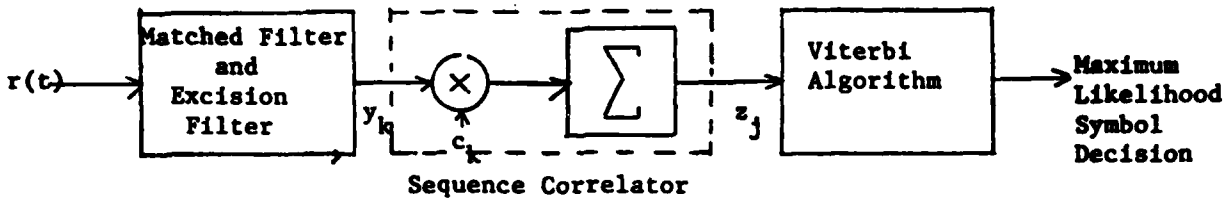

Figure 5

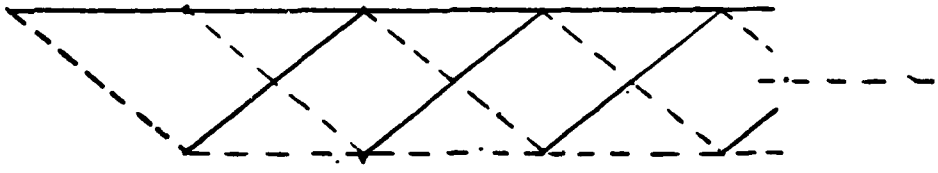

Figure 6

The first term in (21) is the desired signal, while the second term is a self-noise or "interchip" interference term which is always present whether or not there is intersymbol interference. This self-noise term can seriously degrade, and in many cases turns out to limit, the performance of maximum likelihood detection.

In a sense, the fact that the ML criterion does nothing to mitigate "interchip" interference is due to the fact that over a given bit interval, there is only one possible chip sequence (assuming that the receiver is synchronized to the transmitted PN sequence). Once the receiver has considered the two possible symbol values for that interval, it has extracted all available information about the channel from the received sequence. This view leads to the speculation that it may be desirable to introduce coding that will increase the number of possible sequences during a given bit interval.

Another observation which can be made about (21) is that this metric is the same metric which is obtained by applying the maximum likelihood criterion to transmission over a dispersive channel corrupted by white noise at the receiver input when the channel is modeled as a tapped delay line with weights h(m). In other words, for the purposes of digital transmission and maximum likelihood detection, a dispersive channel corrupted by white noise is equivalent to a nondispersive channel corrupted by colored noise whose power spectral density is the inverse of the magnitude squared frequency response of the

equivalent dispersive channel.

Dispersive Channel

To obtain the maximum likelihood receiver for the dispersive channel, corrupted by white noise and narrowband interference, we replace p(t) by p'(t)*c(t), where p'(t) is the transmitted pulse, and c(t) is the channel impulse response. The impulse response c(t) is in general a complex valued function, and is also possibly time-varying. In this case x(t) and r(t) are given by:

$$x(t) = p'(t)*c(t)*h(t) \tag{22}$$

and

$$r(t) = \sum_{k=-NL}^{NL-1} u_{\lfloor k/L \rfloor}\, c_k \int_{-\infty}^{\infty} p'(\tau)\, c(t - \tau - k\tau_c)\, d\tau \tag{23}$$

The input to the sequence correlator, y_k, is given by:

$$y_k = 2E_c \sum_{m=-L}^{L} u_{\lfloor (k-m)/L \rfloor}\, c_{k-m}\, R_{xx}(m)$$

$$+ \text{Re} \sum_{m=-p}^{P} g_m \int_{-\infty}^{\infty} [n(\tau - m\tau_c) + i(\tau - m\tau_c)]$$

$$\cdot\, p^*(\tau - k\tau_c)\, d\tau \tag{24}$$

where

$$R_{xx}(k) = \frac{1}{2E_c} \int_{-\infty}^{\infty} x(\tau)\ x^*(\tau - k\tau_c)\ d\tau \qquad (25)$$

Note that since c(t) is in general complex, we can no longer take the real part of the output of the chip pulse matched filter. If we follow the chip pulse matched filter with the channel matched filter, whose impulse response is $c^*(-n\tau_c)$, then we can take the real part of the channel matched filter output, and can still use an interference suppression filter with real valued tap weights. This receiver structure is shown in Figure 7.

Placing the channel matched filter prior to the noise-whitening filter has some disadvantages, however. The first is that since we no longer have a nondispersive channel, the component of the received signal due to the transmitted signal no longer has a flat power spectral density. The spectral estimation algorithm which determines the noise-whitening filter tap weights will now react to the channel-induced distortion of the signal as well as to the interference. The channel-matched filter, having the same magnitude response as the channel, will reinforce any distortion caused by the channel and thus increase the undesired response of the whitening filter to the channel. The second disadvantage of this structure is that if the channel is not known *a priori* at the receiver then it must be estimated. A straightforward

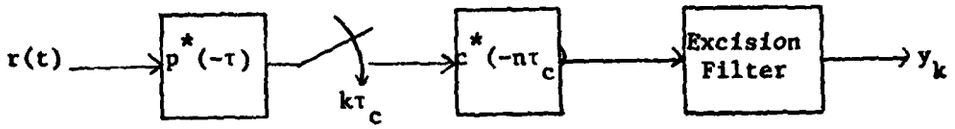

Figure 7

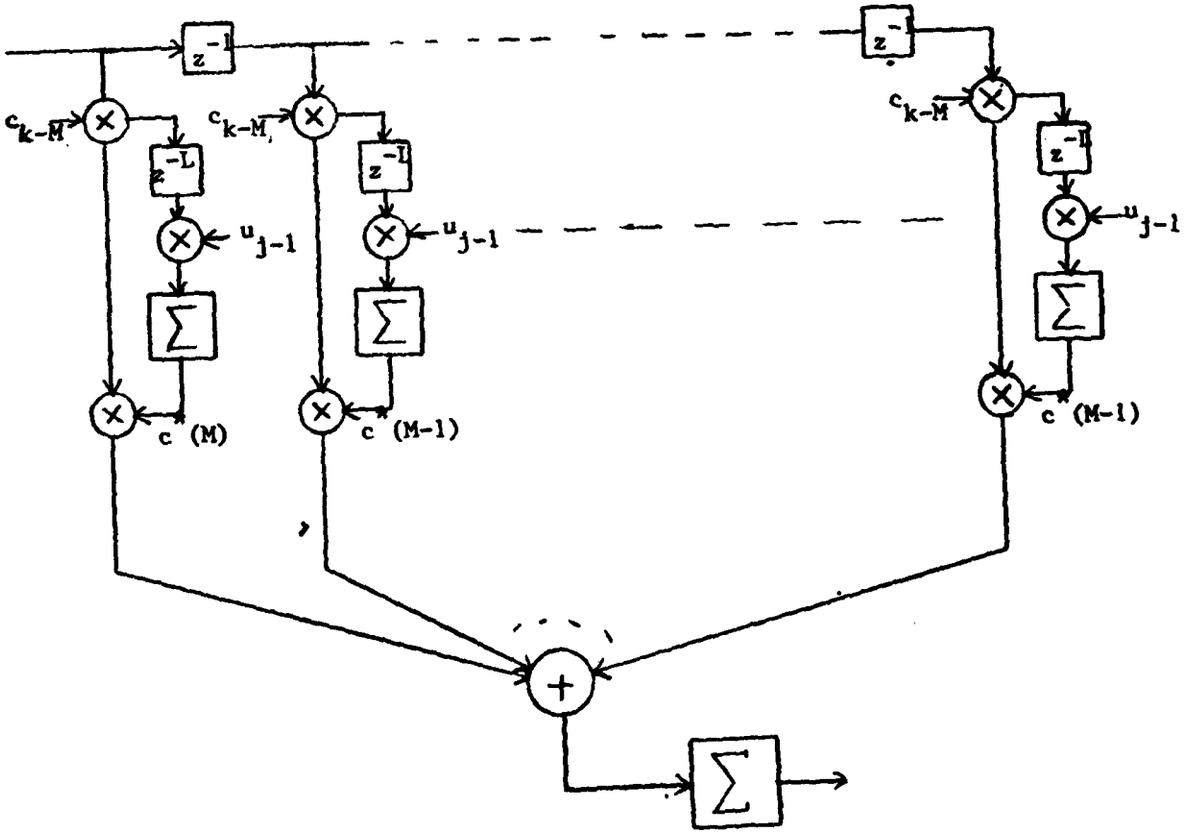

Figure 8

way of doing this is to use a RAKE (Figure 8) matched filter [4]; however, it is not practical to implement the RAKE prior to the noise-whitening filter for two reasons. The first is that the PN sequence correlation is performed internally to the RAKE so that its output is the narrowband data signal, and it is no longer possible to perform noise-whitening on this signal. Even if it were possible to remove the sequence correlator from the RAKE, this structure would still be undesirable because the large interference component at the RAKE input makes the job of channel estimation unnecessarily difficult.

A more desirable arrangement is shown in Figure 9. Here the chip pulse matched filter is followed by a sampler and then the noise-whitening filter. The noise-whitening filter must now have complex valued tap weights since we are dealing with complex valued signal samples. The noise-whitening filter is followed by a RAKE matched filter which adapts itself to have the response of a filter matched to the cascade of the channel and the noise-whitening filter. Although it may seem unnecessary to have the RAKE adapt itself to the whitening matched filter as well as the channel matched filter, there is no other straightforward way of obtaining filters matched to both the channel and the whitening filter. The RAKE operates in such a way that it adapts its filter response to match the total response of the channel and receiver between the transmitter and the RAKE. For example, if the whitening filter

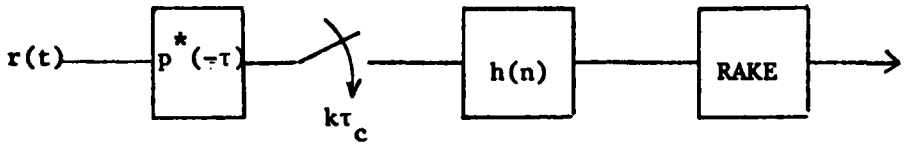

Figure 9

were followed by its matched filter, and then by the RAKE, the RAKE would adapt itself to the response of a filter matched to the channel, the whitening filter, and its matched filter. For this reason, we must allow the RAKE to match the channel and the whitening filter. Simulation results, which will be presented in a subsequent section demonstrate that the penalty for implementing the noise-whitening matched filter adaptively within the RAKE in this way is negligible.

III. Bit Error Probability for Symbol-by-Symbol Detection

The first results given in this section are bit error probability expressions for symbol-by-symbol detection based on a Gaussian assumption about the total noise, including self-noise, at the sequence correlator output. Two receivers are considered: the conventional direct sequence spread spectrum receiver shown in Figure 10 which consists of a filter matched to the chip pulse and a sequence correlator; and an enhanced spread spectrum receiver shown in Figure 11 which in addition to the chip pulse matched filter and sequence

correlator also has an interference suppression filter. The interference suppression filter consists of a noise-whitening filter, or a noise-whitening filter in cascade with its matched filter.

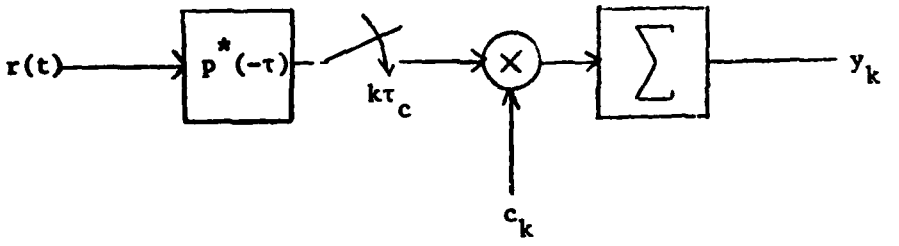

Figure 10

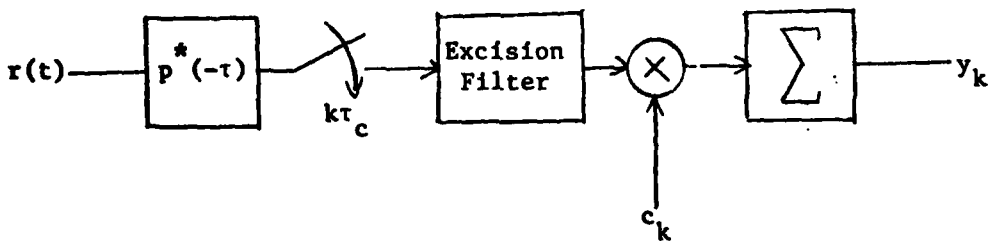

Figure 11

Receiver with No Suppression Filter

The decision variable at the output of the sequence correlator in Figure 10 is given by:

$$z_j = \mathrm{Re}\left[\sum_{\ell=jL}^{(j+1)L-1} c_\ell \int_{-\infty}^{\infty} r_j(\tau)\, p^*(\tau - \ell\tau_c)\, d\tau\right]$$

$$= \alpha u_j\, \mathrm{Re}\left[\sum_{\ell=jL}^{(j+1)L-1} \sum_{k=jL}^{(j+1)L-1} c_\ell\, c_k \int_{-\infty}^{\infty} p(\tau - k\tau_c)\right.$$

$$\cdot\, p^*(\tau - \ell\tau_c)\, d\tau$$

$$\left. + \sum_{k=jL}^{(j+1)L-1} c_k \int_{-\infty}^{\infty} [n(\tau) + i(\tau)]\, p^*(\tau - k\tau_c)\, d\tau\right]$$

$$= 2\alpha E_c\, Lu_j + \mathrm{Re}\left\{\sum_{k=jL}^{(j+1)L-1} c_k \int_{-\infty}^{\infty} [n(t) + i(t)]\right.$$

$$\left. \cdot\, p^*(\tau - k\tau_c)\, d\tau\right\} \qquad (26)$$

If we make the reasonable assumption that z_j is a Gaussian random variable, then the mean and variance of (26) are sufficient to give the error rate. These are:

$$E(z_j) = 2\alpha E_c\, Lu_j \qquad (27a)$$

$$\text{var}(z_j) = N_j + I_j \tag{27b}$$

where $N_j = 2L\, E_c\, N_o$ is the variance of the white noise term at the output of the sequence, and

$$I_j = \frac{1}{2} \sum_{\ell=jL}^{(j+1)L-1} \sum_{k=jL}^{(j+1)L-1} \overline{c_k\, c_\ell} \iint_{-\infty}^{\infty} 2\phi_{ii}(t - \tau)$$

$$\cdot\, p^*(t - k\tau_c)\, p(\tau - \ell\tau_c)\, dt\, d\tau \tag{28}$$

is the variance of the interference term. The double integral in (28) can be evaluated first by noting that it represents the autocorrelation of the interference component of the output of the chip pulse matched filter, $p^*(-\tau)$. Denoting this signal component by $\hat{i}(t)$, this autocorrelation function can be written:

$$\phi_{\hat{i}\hat{i}}(\tau) = \int_{-\infty}^{\infty} |P(f)|^2\, S_i(f)\, e^{j2\pi f\tau}\, df \tag{29}$$

where $|P(f)|^2$ is the magnitude squared frequency response of the chip pulse matched filter, and $S_i(f)$ is the power spectral density of the interference at the input of the chip pulse matched filter. Assuming that the chip pulse satisfies the Nyquist criterion for lack of intersymbol interference, and that $|P(f)|^2 \simeq$ constant, $-\frac{1}{2\tau_c} \leq f \leq \frac{1}{2\tau_c}$, then $|P(f)|^2 = 2\tau_c\, E_c$, so

$$\phi_{\hat{i}\hat{i}}(\tau) = 2\tau_c E_c \int_{-\infty}^{\infty} S_i(f)\, e^{j2\pi f\tau}\, df$$

$$= 2\tau_c E_c \phi_{ii}(\tau) \qquad (30)$$

Thus, I_j is given by:

$$I_j = 2\tau_c E_c L\phi_{ii}(0) \qquad (31)$$

The bit error probability is then given by:

$$P_b = \Pr(z_j < 0 \mid u_j = +1) = \frac{1}{2}\,\mathrm{erfc}\,\sqrt{\gamma} \qquad (32)$$

where

$$\gamma = \frac{[E(z_j)]^2}{2\mathrm{var}(z_j)} = \frac{L E_c \alpha^2}{N_o + \tau_c \phi_{ii}(0)} \qquad (33)$$

Receiver with Suppression Filter

The decision variable at the output of the sequence correlator in Figure 11 when the excission filter consists of the noise-whitening filter plus its matched filter is:

$$z_j = 2\alpha E_c Lg(0)\, u_j + 2\alpha E_c \sum_{k=jL}^{(j+1)L-1} \sum_{\substack{\ell=-p \\ \ell\neq 0}}^{p} u_{\lfloor (k-\ell)/L \rfloor} \cdot c_k c_{k-\ell} g(\ell)$$

$$+ \sum_{k=jL}^{(j+1)L-1} \sum_{\ell=-p}^{p} c_k g(\ell)\, \mathrm{Re}\left\{ \int_{-\infty}^{\infty} [n(\tau) + i(\tau)] \right.$$

$$\cdot\ p^*[\tau - (k - \ell)\ \tau_c]\ d\tau\Bigg\} \qquad (34)$$

When the noise-whitening filter alone is used, the decision variable is:

$$z_j = 2\alpha E_c\ Lh(0)\ u_j + 2\alpha E_c \sum_{k=jL}^{(j+1)L-1} \sum_{\ell=1}^{P} u_{\lfloor (k-\ell)/L \rfloor}$$

$$\cdot\ c_k\ c_{k-\ell}\ h(\ell)$$

$$+ \sum_{k=jL}^{(j+1)L-1} \sum_{\ell=0}^{P} c_k\ h(\ell)\ \mathrm{Re}\Bigg\{\int_{-\infty}^{\infty} [n(\tau) + i(\tau)]$$

$$\cdot\ p^*[\tau - (k - \ell)\ \tau_c]\ d\tau\Bigg\} \qquad (35)$$

In finding the mean and variance of z_j, we assume that the starting phase of the PN sequence is a uniformly distributed random variable, which is uncorrelated with the phase of the information sequence, so that the first PN chip in any given information bit occurs with equal probability at any position in the PN sequence. We also assume that the autocorrelation of the PN sequence is $E[c_k\ c_\ell] = \delta_{k\ell}$. Another way of stating these assumptions is that the channel symbol for the j^{th} transmitted bit is given by $u_j\ \underline{c}_j$, where u_j is the information bit and $\underline{c}_j$ is a random binary vector of length L with elements chosen from the binary alphabet (-1, 1). The vector $\underline{c}_j$ can be any of the 2^L possible binary vectors of length L, with equal

probability.

Thus, in the whitening filter only receiver, the mean and variance of z_j are:

$$E(z_j) = 2\alpha E_c \, L \, h(0) \, u_j \tag{36}$$

$$\begin{aligned} \mathrm{var}(z_j) = {} & 2L \, N_o \, E_c \sum_{\ell=0}^{P} [h(\ell)]^2 \\ & + 2L \, \tau_c \, E_c \sum_{\ell=0}^{P} \sum_{m=0}^{P} h(\ell) \, h(m) \, \phi_{ii}[(m-\ell) \, \tau_c] \\ & + 4\alpha^2 \, L \, E_c^2 \sum_{\ell=1}^{P} [h(\ell)]^2 \end{aligned} \tag{37}$$

The signal-to-noise ratio, defined as $E^2(z_j)/2\mathrm{var}(z_j)$ is then:

$$\gamma_j = \frac{L \, E_c \, h^2(0) \, \alpha^2}{N_o \sum_{\ell=0}^{P} h^2(\ell) + \tau_c \sum_{\ell=0}^{P} \sum_{m=0}^{P} h(\ell) h(m) \phi_{ii}[(m-\ell)\tau_c] + 2\alpha^2 E_c \sum_{\ell=1}^{P} h^2(\ell)} \tag{38}$$

and the bit error probability is again given by:

$$P_b = \frac{1}{2} \, \mathrm{erfc} \, \sqrt{\gamma_j}$$

When the receiver contains the filter matched to the whitening filter as well as the whitening filter, the mean and variance of z_j are:

$$E(z_j) = 2\alpha E_c \, Lg(0) \, u_j \tag{39a}$$

$$\text{var}(z_j) = 2L \, N_o \, E_c \sum_{\ell=-p}^{P} g^2(\ell)$$

$$+ 2L \, E_c \, \tau_c \sum_{\ell=-p}^{P} \sum_{m=-p}^{P} g(\ell) \, g(m) \, \phi_{ii}[(m - \ell) \, \tau_c]$$

$$+ 8\alpha^2 \, E_c^2 \sum_{\ell=1}^{P} (2L - \ell) \, g^2(\ell) \tag{39b}$$

The signal-to-noise ratio in this case is:

$$\gamma_j = \frac{L \, E_c \, g^2(0) \, \alpha^2}{N_o \sum_{\ell=-p}^{P} g^2(\ell) + \tau_c \sum_{\ell=-p}^{P} \sum_{m=-p}^{P} g(\ell) g(m) \phi_{ii}[(m-\ell)\tau_c] + 4\alpha^2 E_c \sum_{\ell=1}^{P} \frac{(2L-\ell)}{L} g^2(\ell)} \tag{40}$$

For a detailed derivation of these formulas, see Appendix A.

We next give some performance results obtained by use of these bit error probability expressions. In all of these results, we have taken $\tau_c = 1$, and $\alpha = 1$. The results are plotted against E_b/N_o to aid in comparison with the performance of ideal antipodal signaling without interference. The interference is a sum of 100 sinusoids occupying 20% of the band, between 0 and 0.1 Hz. The results are given for processing gains of 10, 20, 30, and 60 chips per bit. The performance of

the receiver without interference suppression as given by (32) and (33) is not plotted since at an SIR of -20dB and the processing gains given above this probability of error is not much below 0.5 for any E_b/N_o.

Figure 12 shows the performance with a suppression filter which uses a 4-tap predictor, and no matched filter, at an SIR of -20dB/chip. At the low processing gain of 10 the suppression filter has provided only slight improvement over the receiver with no suppression; at a processing gain of 60 there is a significant improvement over the receiver without suppression, but clearly there is room for improvement relative to the performance without interference.

Next, Figure 13 gives the performance arrived at by the Gaussian assumption for the same interference and receiver as that in Figure 12, with the exception that now the receiver includes a filter matched to the suppression filter. This has provided a marked improvement in performance over that obtained without the matched filter, particularly at the higher processing gains. It is notable, however, that for all these processing gains the bit error rate always bottoms out at some finite probability of error. The source of this behavior will be addressed presently.

Figure 14 shows the performance of the same receiver with lower interference power resulting in an SIR of -10dB/chip. This drop in interference power results in an expected performance improvement. The performance bottoms out at lower

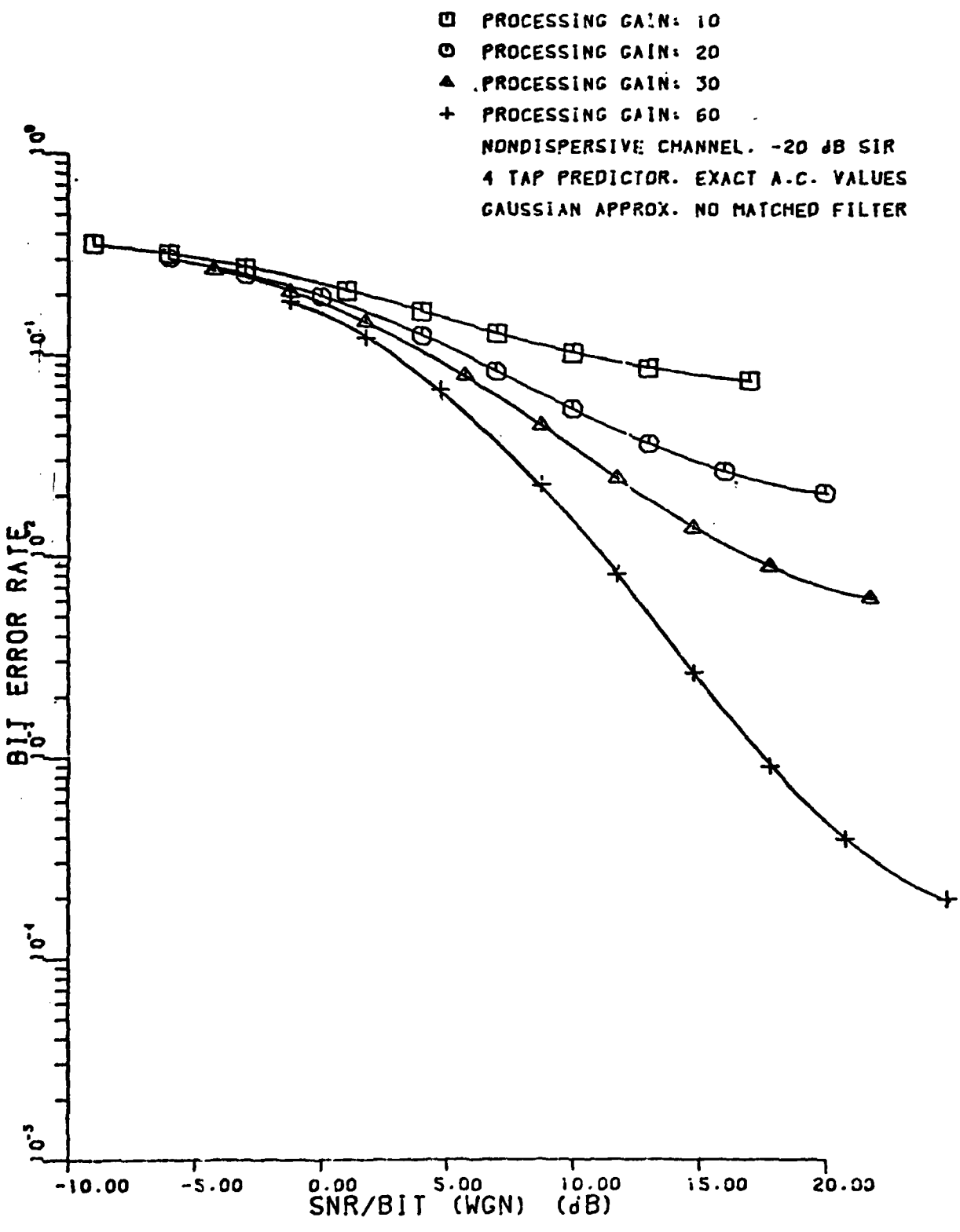
PROCESSING GAIN: 10
PROCESSING GAIN: 20
PROCESSING GAIN: 30
PROCESSING GAIN: 60
NONDISPERSIVE CHANNEL. -20 dB SIR
4 TAP PREDICTOR. EXACT A.C. VALUES
GAUSSIAN APPROX. NO MATCHED FILTER
BIT ERROR RATE
10^0
10^-1
10^-2
10^-3
-10.00
-5.00
0.00
5.00
10.00
15.00
20.00
SNR/BIT (WGN) (dB)

Figure 12

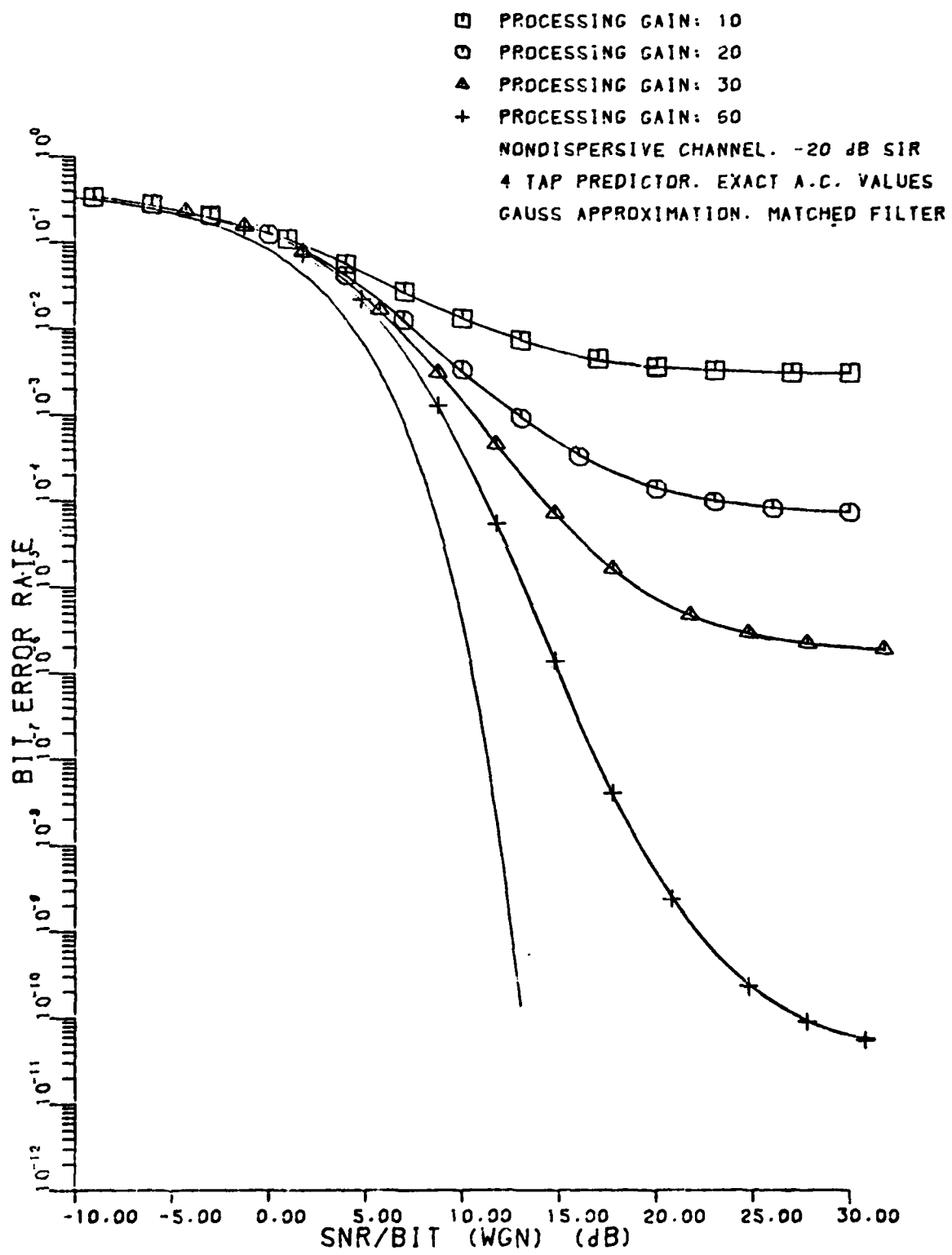
PROCESSING GAIN: 10
PROCESSING GAIN: 20
PROCESSING GAIN: 30
PROCESSING GAIN: 60
NONDISPERSIVE CHANNEL. -20 dB SIR
4 TAP PREDICTOR. EXACT A.C. VALUES
GAUSS APPROXIMATION. MATCHED FILTER
BIT ERROR RATE
SNR/BIT (WGN) (dB)
-10.00
-5.00
0.00
5.00
10.00
15.00
20.00
25.00
30.00

Figure 13

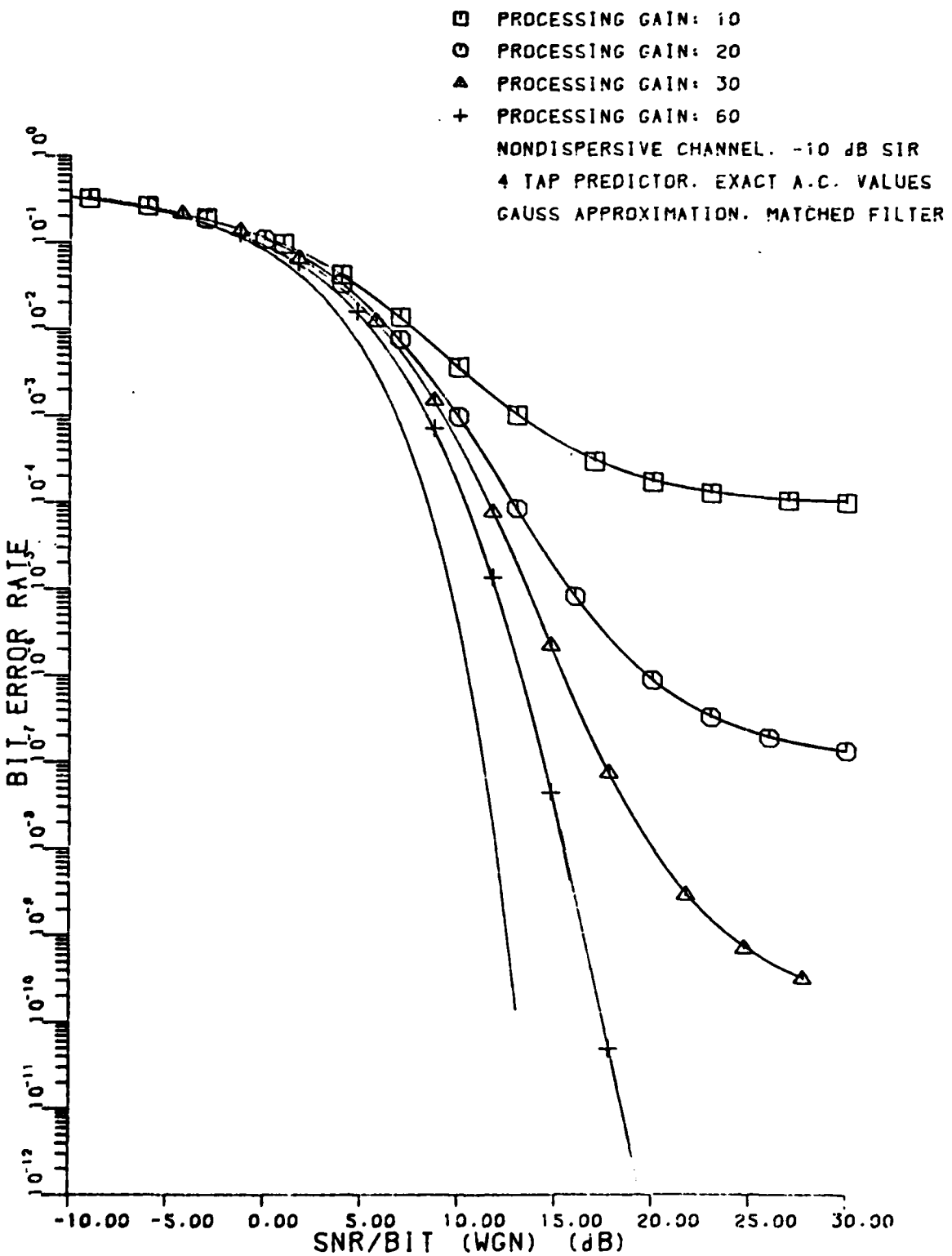
PROCESSING GAIN: 10
PROCESSING GAIN: 20
PROCESSING GAIN: 30
PROCESSING GAIN: 60
NONDISPERSIVE CHANNEL. -10 dB SIR
4 TAP PREDICTOR. EXACT A.C. VALUES
GAUSS APPROXIMATION. MATCHED FILTER
BIT ERROR RATE
SNR/BIT (WGN) (dB)
-10.00
-5.00
0.00
5.00
10.00
15.00
20.00
25.00
30.00

Figure 14

error probabilities at all processing gains; at a processing gain of 60, the bottoming out is off the scale of the plot. At the higher processing gain, the E_b/N_o requirement for 10^{-7} bit error probability is degraded by about 3dB from ideal binary signalling, compared with about 6dB for an SIR of -20dB.

The 4-tap predictor used so far is close to the minimum order filter required to place a notch in the band occupied by the interference and thus approximate a noise-whitening filter, as established in a previous report [2]. It was also shown that by increasing the filter order modest gains in the SNR improvement factor could be obtained over the 4-tap predictor. In the frequency domain, the effect of increasing the predictor order is a notch which more closely approximates the spectral shape and location of the interference. Figure 15 shows the error probability for the same interference as Figure 13, except now the predictor is a 15-tap predictor. This has led to a significant gain in performance over Figure 13; in fact, the performance of a 15-tap predictor in -20dB of interference is slightly superior to that of a 4-tap predictor in -10dB of interference.

We have only considered here the performance of narrowband interference suppression when the interference is contained within a single band. However, it was demonstrated in [2] that similar values of the SNR improvement factor, which is proportional to the SNR, γ_j, can be obtained when

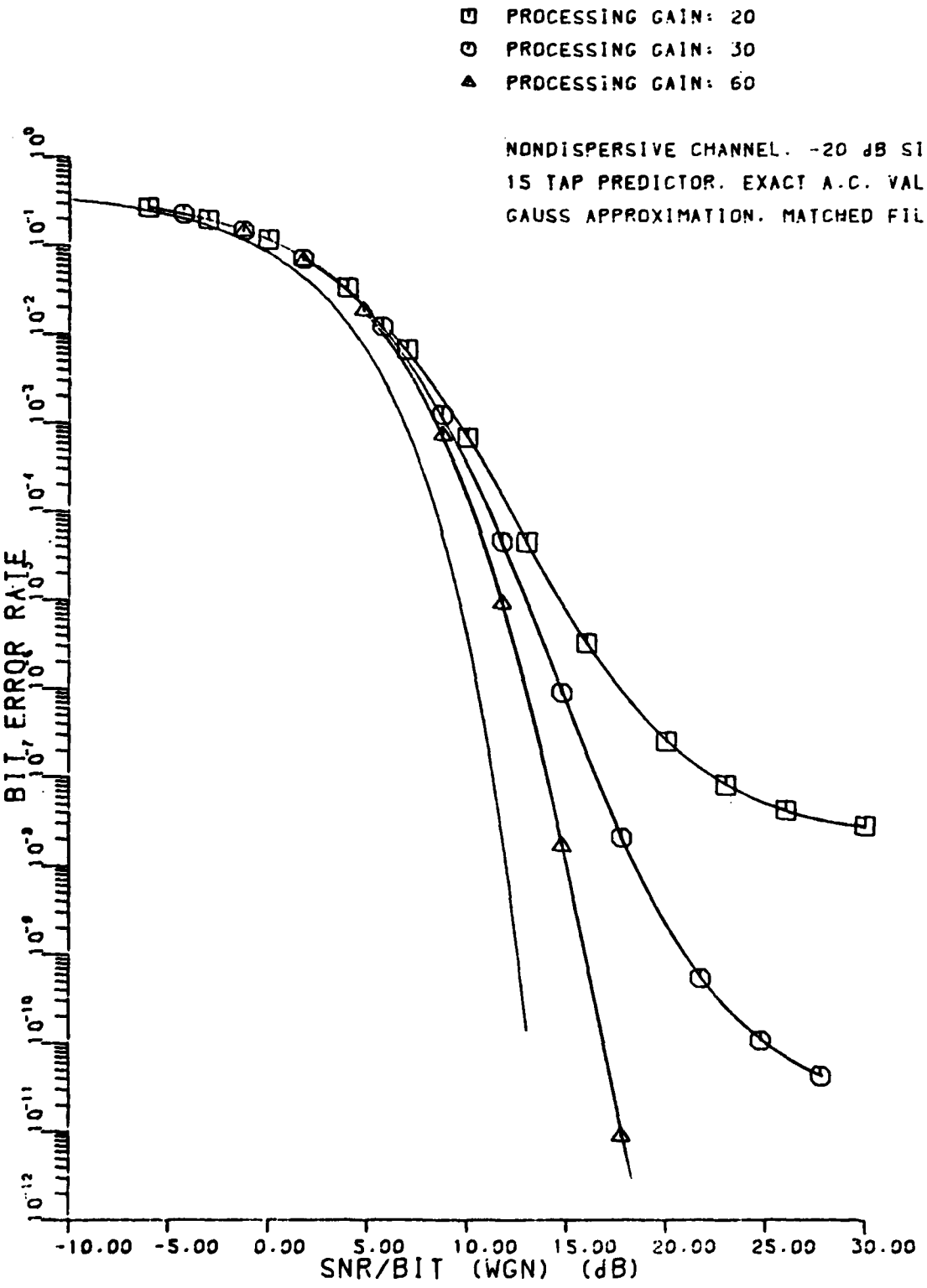
PROCESSING GAIN: 20
PROCESSING GAIN: 30
PROCESSING GAIN: 60
NONDISPERSIVE CHANNEL. -20 dB SIR
15 TAP PREDICTOR. EXACT A.C. VALUES
GAUSS APPROXIMATION. MATCHED FILTER
BIT ERROR RATE
SNR/BIT (WGN) (dB)
-10.00 -5.00 0.00 5.00 10.00 15.00 20.00 25.00 30.00

Figure 15

the interference is split into multiple bands, provided that the suppression filter order is sufficiently large. We would expect then that the probability of error performance for multiple-band interference would also be similar to that given here for single-band interference when the conditions given in [2] are met.

In order to gain some insight into the "bottoming out" behavior of the performance obtained using the Gaussian assumption, we performed the following experiment. First we assumed that we had a noiseless estimate of the transmitted signal plus interference for the purpose of computing the suppression filter coefficients, but that the decision variable at the output of the sequence correlator is still corrupted by a white noise term, as well as the interference and self-noise terms. The resulting error probability performance is the top curve in Figure 16. We next assumed that the filter coefficients were computed from a noisy received signal, but that the decision variable at the output of the sequence correlator was missing its white noise term. The resulting error probability is the lower curve in Figure 16.

We note first that the top curve in Figure 16 is very little different from the performance given in Figure 13 for the real world case where both the filter estimates and the decision variable are noisy. This implies that noisy estimates of the interference have very little effect on the

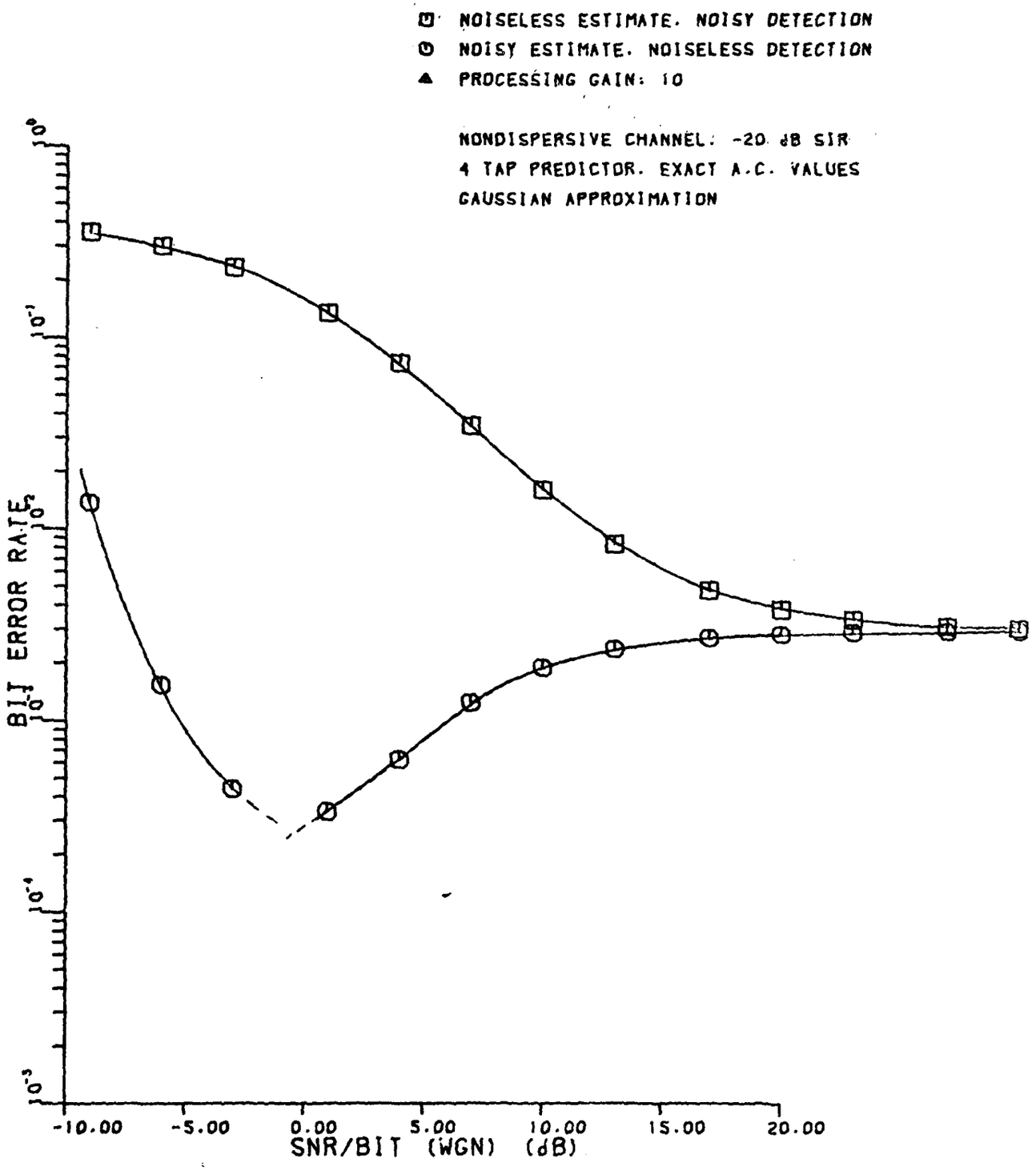
NOISELESS ESTIMATE. NOISY DETECTION
NOISY ESTIMATE. NOISELESS DETECTION
PROCESSING GAIN: 10
NONDISPERSIVE CHANNEL: -20 dB SIR
4 TAP PREDICTOR. EXACT A.C. VALUES
GAUSSIAN APPROXIMATION
BIT ERROR RATE
10^0
10^-1
10^-2
10^-3
10^-4
-10.00
-5.00
0.00
5.00
10.00
15.00
20.00
SNR/BIT (WGN) (dB)

Figure 16

performance of the receiver with interference suppression.

At very low values of E_b/N_o, the lower curve falls off rapidly until it reaches a minimum at roughly 0dB. The error rate increases for higher values of E_b/N_o, until it reaches a saturation value of about 3×10^{-3}. This behavior can be explained as follows. At very low E_b/N_o, the interference estimate is very noisy, and the resulting suppression filter has a nearly flat frequency characteristic, thus introducing very little pulse dispersion. As E_b/N_o is increased, the interference estimate improves, and the interference is suppressed more effectively. At about 0dB, however, the self-noise component due to the increased dispersion caused by the improving interference estimate begins to wash out the effect of the residual interference. As the E_b/N_o is increased, the self-noise increases until the interference estimate approaches its almost noiseless, high E_b/N_o value, at which point the error rate given by the lower curve becomes constant.

The conclusion that we draw from this experiment is that the performance as given by the Gaussian approximation is limited by the pulse dispersion caused by the excision filter.

Alternate Bit Error Probability Method for Symbol-by-Symbol Detection

Application of the Gaussian assumption to the decision variable, z_j, as was considered in the previous section, is a useful approach to evaluating the performance of adaptive interference cancellation in a spread spectrum communications

receiver. However, it is desirable for several reasons to drop this assumption and investigate other ways of determining the error rate performance of such a receiver. The validity of the Gaussian assumption is uncertain, and if we can find a second method which does not depend on this assumption, we can get some idea of its validity. Moreover, in the process of applying this assumption we also made a fairly strong assumption about the statistics of the PN sequence, i.e., that $E[c_k\ c_j] = 0$ for $k \neq j$. This is a valid assumption for very long sequences, but it would be interesting and useful to be able to evaluate the error probability when sequences which do not satisfy this property are employed. Finally, the error probability expressions given in the previous section apply only to spread spectrum communications over nondispersive channels. It is desirable to have a more general result which applies to the dispersive channel as well.

In the previous section, the error probability was found by averaging the mean and variance of the decision variable over all possible locations in the PN sequence, and assuming that the results were the mean and variance of a Gaussian random variable. In this section, we will reverse the process. We will find the conditional error probability when a given subsequence of the PN sequence occurs during a given symbol transmission, and this probability will be averaged over all possible subsequences, or locations, in the PN sequence, as well as all possible transmitted sequences. The resulting

error probability expression is completely general in that it can be applied to any PN sequence of interest, and does not make any assumptions about the properties of the PN sequence, or the self-noise caused by dispersion of the PN sequence. The drawback of this method is that we lose the generality of the Gaussian assumption and must now evaluate the error rate numerically for a given PN code of interest.

To evaluate the probability of error in this way, we start with the expression for the decision variable given by (34). The mean value of z_j is now given by:

$$E(z_j) = 2\alpha E_c \, L \, g(0) \, u_j$$

$$+ 2\alpha E_c \sum_{k=jL}^{(j+1)L-1} \sum_{\ell=-p}^{p} u_{\lfloor (k-\ell)/L \rfloor} \, c_k \, c_{k-\ell} \, g(\ell)$$

$$= 2\alpha E_c \, u_j [L \, g(0) + 2 \sum_{\ell=1}^{P} \sum_{k=jL+i}^{(j+1)L-1} c_k \, c_{k-\ell} \, g(\ell)]$$

$$+ 2\alpha E_c \sum_{\ell=1}^{P} g(\ell) [u_{j+1} \sum_{k=(j+1)L-\ell}^{(j+1)L-1} c_k \, c_{k+\ell}$$

$$+ u_{j-1} \sum_{k=jL}^{jL+\ell-1} c_k \, c_{k-\ell}] \qquad (41)$$

and the variance is:

$$\text{var}(z_j) = \frac{1}{2} E\Bigg\{ \sum_{k=jL}^{(j+1)L-1} \sum_{n=jL}^{(j+1)L-1} \sum_{\ell=-p}^{P} \sum_{m=-p}^{P} c_k \, c_n \, g(\ell) \, g(m)$$

$$\cdot \iint_{-\infty}^{\infty} [i(t) \, i^*(\tau) + n(t) \, n^*(\tau)] \, p^*[t - (k - \ell) \, \tau_c]$$

$$\cdot \, p[\tau - (m - n) \, \tau_c] \, dt \, d\tau \Bigg\} \qquad (42)$$

The effects of both self-noise ("interchip" interference) and intersymbol interference are apparent in (41). The first term within the first brackets, $Lg(0)$, represents the desired signal. The second term in the first brackets represents the chip pulse dispersion within a bit interval, the effect which we have been referring to as self-noise. The righthand term in (41) represents the signal component due to chip pulse dispersion which overlaps the bit boundaries. This component is intersymbol interference. We have made the assumption in (41) that the dispersion caused by the interference suppression spans less than a single bit duration, i.e., $P < L$.

There are several ways of evaluating the variance of z_j as given by (42), the most general of which yields an expression not much simpler than (42). Here we will make the simplifying assumption that the noise and interference term of the sample value at the output of the whitening filter is, in fact, white.

In other words, defining

$$e(k) = \sum_{\ell=0}^{P} h(\ell)\ \mathrm{Re} \int_{-\infty}^{\infty} [n(\tau) + i(\tau)]\ p^*[\tau - (k - \ell)\ \tau_c]\ d\tau \tag{43}$$

and

$$\phi_{ee}(n) = E[e(k)\ e(k + n)]\ , \tag{44}$$

$\phi_{ee}(n) = 0$, for $n \neq 0$.

Evaluating $\phi_{ee}(0)$ yields:

$$\phi_{ee}(0) = E[e^2(k)] = \frac{1}{2} \sum_{\ell=0}^{P} \sum_{m=0}^{P} h(\ell)\ h(m)$$

$$\cdot \iint_{-\infty}^{\infty} [\overline{n(t)\ n^*(\tau)} + \overline{i(t)\ i^*(\tau)}]\ p^*[t - (k - \ell)\ \tau_c]$$

$$\cdot\ p[\tau - (k - m)\ \tau_c]\ dt\ d\tau$$

$$= 2E_c\ N_o\ g(0) + 2E_c\ \tau_c \sum_{\ell=-p}^{P} g(\ell)\ \phi_{ii}(\ell\tau_c) \tag{45}$$

The noise and interference term in the decision variable can now be written:

$$\sum_{k=jL}^{(j+1)L-1} \sum_{m=0}^{P} c_k\ h(m)\ e(k + m)$$

and the variance of z_j is

$$\text{var}(z_j) = \sum_{k=jL}^{(j+1)L-1} \sum_{n=jL}^{(j+1)L-1} \sum_{m=0}^{P} \sum_{\ell=0}^{P} c_k \, c_n$$

$$\cdot \, h(\ell) \, h(m) \, \overline{e(k+m) \, e(n+\ell)}$$

$$= \phi_{ee}(0) \sum_{k=jL}^{(j+1)L-1} \sum_{n=jL}^{(j+1)L-1} \sum_{m=0}^{P} c_k \, c_n$$

$$\cdot \, h(k+m-n) \, h(m)$$

$$= \phi_{ee}(0) \left[Lg(0) + 2 \sum_{m=1}^{P} \sum_{k=jL+m}^{(j+1)L-1} c_k \, c_{k-m} \, g(m) \right] \tag{46}$$

Next, define the normalized noise variance,

$$\sigma_e^2 = \phi_{ee}(0)/2E_c \tag{47}$$

Then the signal-to-noise ratio, $\gamma_j(u_{j-1}, u_j, u_{j+1})$, is

$$\gamma_j(u_{j-1}, u_j, u_{j+1}) = [E(z_j)]^2/2 \, \text{var}(z_j)$$

$$= \alpha^2 E_c \left\{ \frac{(u_j)^2}{\sigma_e^2} \left[Lg(0) + 2 \sum_{\ell=1}^{P} \sum_{k=jL+\ell}^{(j+1)L-1} c_k \, c_{k-\ell} \, g(\ell) \right] \right.$$

$$+ \frac{2u_j}{\sigma_e^2} \left[\sum_{\ell=1}^{P} g(\ell) \left[u_{j+1} \sum_{k-(j+1)L-\ell}^{(j+1)L-1} c_k \, c_{k+\ell} \right. \right.$$

$$\left. + u_{j-1} \sum_{k=jL}^{jL+\ell-1} c_k \, c_{k-\ell} \right] \Bigg]$$

$$+ \frac{1}{2\sigma_e^2} \left[Lg(0) + 2 \sum_{\ell=1}^{P} \sum_{k=jL+\ell}^{(j+1)L-1} c_k \, c_{k-\ell} \, g(\ell) \right]^{-1}$$

$$\cdot \left\{ \left[\sum_{\ell=1}^{P} g(\ell) \left[u_{j+1} \sum_{k=(j+1)L-\ell}^{(j+1)L-1} c_k \, c_{k+\ell} \right. \right. \right.$$

$$\left. \left. \left. + u_{j-1} \sum_{k=jL}^{jL+\ell-1} c_k \, c_{k-\ell} \right] \right]^2 \right\} \qquad (48)$$

The bit error probability, conditioned on a given location in the sequence, is

$$P(\text{error}|j) = \frac{1}{2} \operatorname{erfc}\left[\sqrt{\gamma_j(u_{j-1}, u_j, u_{j+1})}\right] \qquad (49a)$$

and the average bit error probability is:

$$P_b = \frac{1}{2} \sum_{\ell} p_\ell(jL = \ell) \sum_{\underline{u}} p_{\underline{u}}(u_{j-1}, u_j, u_{j+1})$$

$$\cdot \operatorname{erfc}\left[\sqrt{\gamma_j(u_{j-1}, u_j, u_{j+1})}\right] \qquad (49b)$$

where $p_{\ell}(jL = \ell)$ is the probability that the symbol u_j starts at chip jL in the PN sequence, and $p_{\underline{u}}(u_{j-1}, u_j, u_{j+1})$ is the probability associated with the subsequence (u_{j-1}, u_j, u_{j+1}) of the total transmitted message, $\underline{u}$.

Evaluation of (49) depends on specific knowledge of the PN sequence employed and must be performed with the aid of a digital computer. Our ability to do so is limited by the length of the sequence in question. For increasing sequence lengths, at some point the computation time required to consider every starting point will become unreasonable. If, on the other hand, we assume that the sequence is sufficiently long that all subsequences of length L + 2P are equally likely, then we can evaluate (49) by averaging over all possible sequences of length L + 2P. The processing time required to accomplish this, however, quickly becomes unreasonable as well. For example, with a modest processing gain of 20, and a 4-tap predictor, we need to average over $2^{28} \approx 3 \times 10^8$ sequences. If the PN sequence in use is a maximal length sequence of length $2^K - 1$, in order to satisfy this randomness property, K must be greater than L + 2P.

Equation (49) has been evaluated for a maximal length sequence of length 1023, i.e., K = 10. Although this sequence does not satisfy the randomness property stated above, it is sufficiently long that the resulting performance estimate is quite close to that provided by the Gaussian assumption. Figure 17 is a plot of this performance estimate for the same

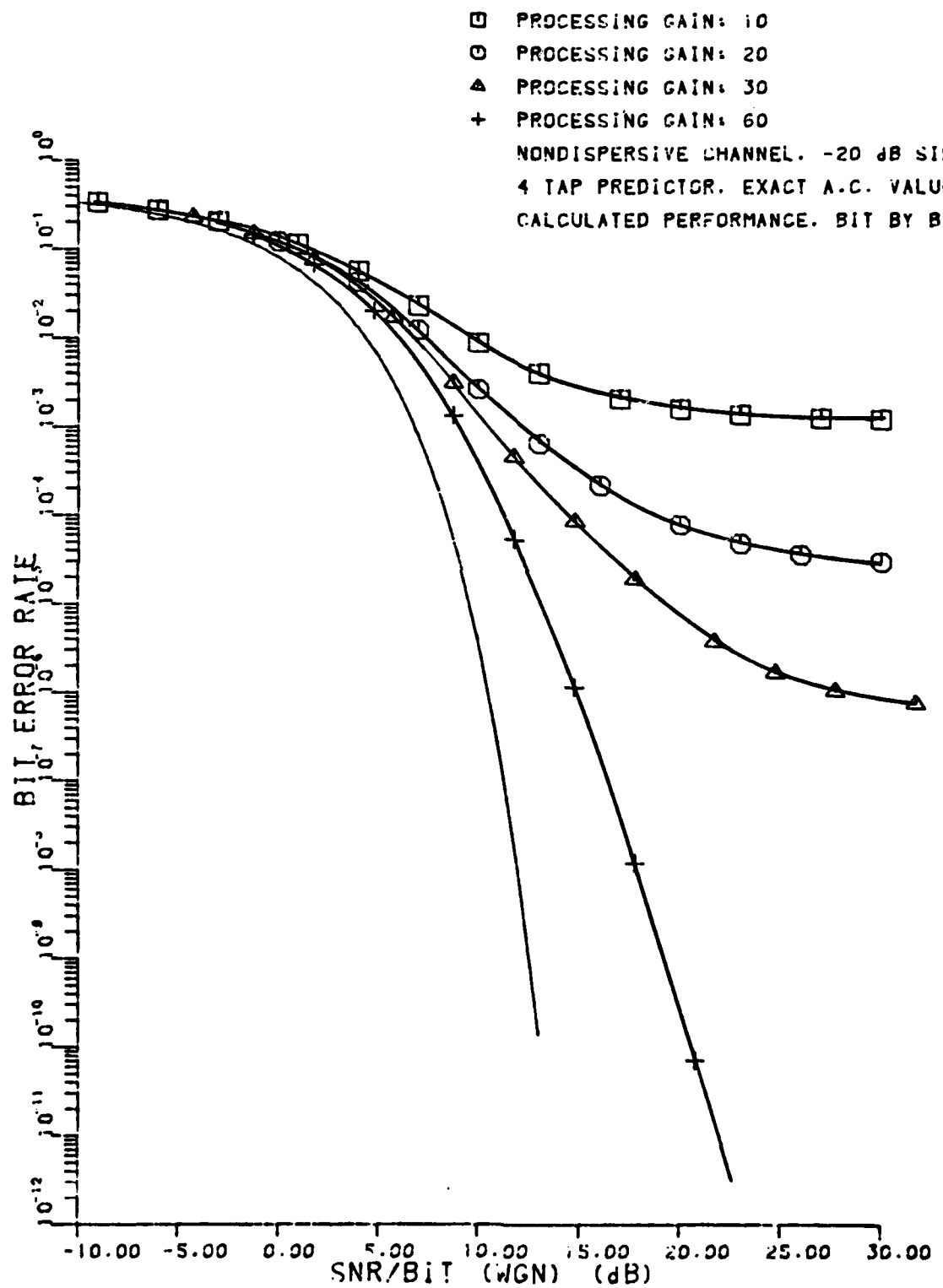
PROCESSING GAIN: 10
PROCESSING GAIN: 20
PROCESSING GAIN: 30
PROCESSING GAIN: 60
NONDISPERSIVE CHANNEL. -20 dB SIR
4 TAP PREDICTOR. EXACT A.C. VALUES
CALCULATED PERFORMANCE. BIT BY BIT
BIT ERROR RATE
SNR/BIT (WGN) (dB)
-10.00
-5.00
0.00
5.00
10.00
15.00
20.00
25.00
30.00

Figure 17

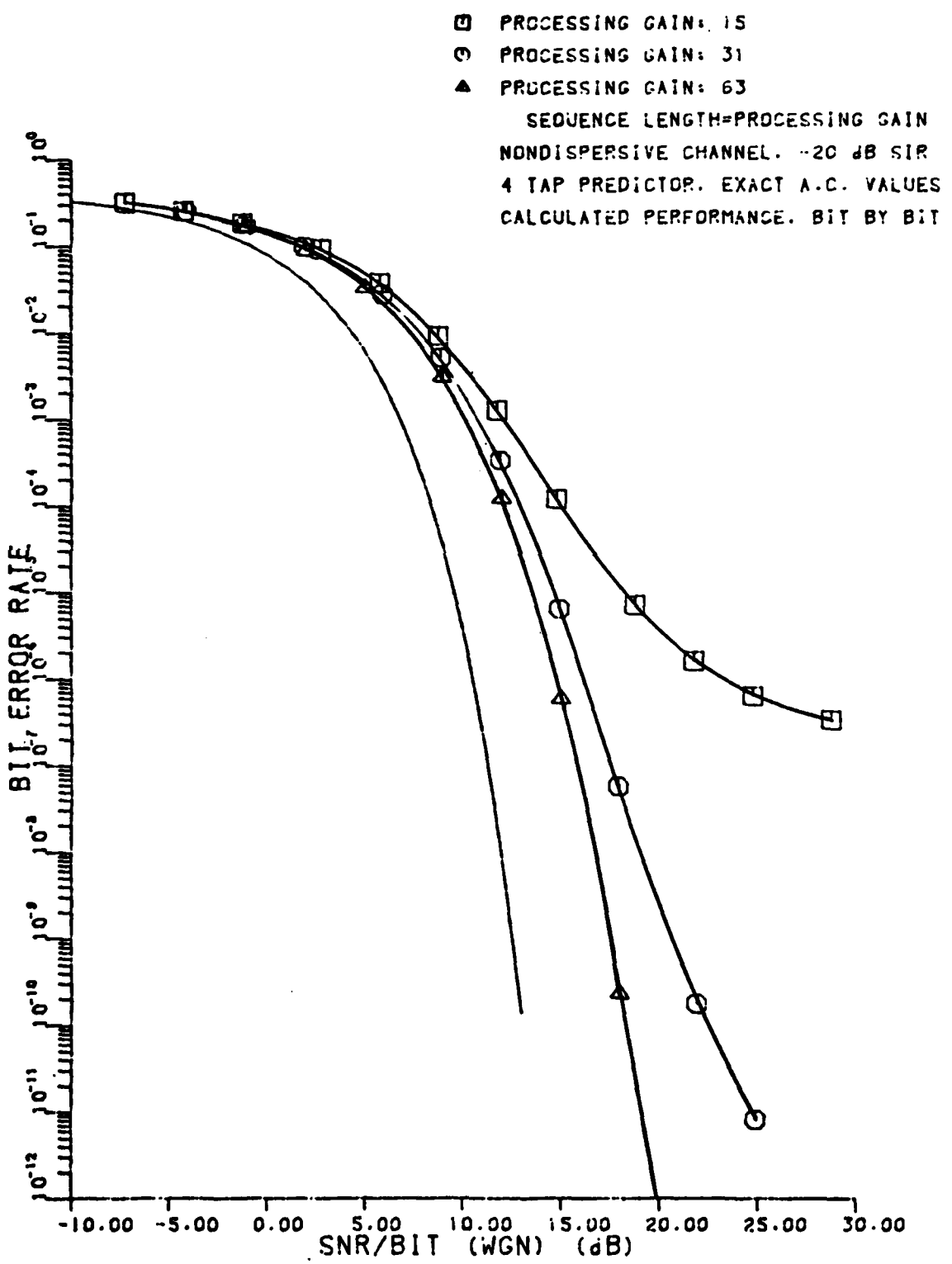
PROCESSING GAIN: 15
PROCESSING GAIN: 31
PROCESSING GAIN: 63
SEQUENCE LENGTH=PROCESSING GAIN
NONDISPERSIVE CHANNEL. -20 dB SIR
4 TAP PREDICTOR. EXACT A.C. VALUES
CALCULATED PERFORMANCE. BIT BY BIT
BIT ERROR RATE
10^{0}
10^{-1}
10^{-2}
10^{-3}
10^{-4}
10^{-5}
10^{-6}
10^{-7}
10^{-8}
10^{-9}
10^{-10}
10^{-11}
10^{-12}
-10.00
-5.00
0.00
5.00
10.00
15.00
20.00
25.00
30.00
SNR/BIT (WGN) (dB)

Figure 18

interference, suppression filter, and processing gains as those used to obtain Figure 13. Comparison of these figures shows that the performance obtained in this case is quite close to, but a bit superior to that given by the Gaussian assumption.

To illustrate the performance dependence on PN code attributes, we have evaluated (49) for the same interference as shown in Figure 17, but now using a maximal length sequence whose length is equal to the processing gain. In this case one complete cycle of the sequence makes up the transmitted waveform for each bit. Evaluation of (49) was carried out by averaging over each possible phase shift of the PN sequence. This process was carried out for sequence lengths and processing gains of 15, 31, and 63; and the results are plotted in Figure 18. It is evident from comparison of Figures 17 and 18 that use of the shorter codes yields superior performance to that provided by the longer codes.

Simulation of a Bit-by-Bit Detection on the Nondispersive Channel

Another set of performance data was obtained for the nondispersive channel and the bit-by-bit receiver by a Monte Carlo simulation. The conditions which were simulated were identical to those for which the calculated performance is given in Figure 17, with the exception that, in order to simplify the simulation, the transmitted information sequence

in the simulation consisted of all "1's". The simulation processed a simulated received sequence of approximately 100,000 chips, corrupted by white Gaussian noise and interference consisting of a sum of 10 real sinusoids with random phase uniformly distributed over $(0, 2\pi)$ and occupying 20% of the band. The received sequence was processed in blocks of 1,200 chips; whitening filter coefficients were computed from each block of 1,200 samples, using the least squares algorithm, and the 1,200 samples were processed using the resulting filter coefficients. The processing of each block was overlapped in such a way that there was no loss of data at the ends of the blocks, and phase continuity in the PN sequence was maintained from block to block so that each simulated bit waveform would contain as many subsequences of the 1023-chip PN sequence as possible.

In order to obtain a highly accurate simulation, it is necessary to average over a sufficient number of samples of each possible subsequence of the PN sequence to obtain a good estimate of the conditional error probability given that the given subsequence was transmitted, as expressed in (49a). At higher SNR, however, it is usually the case that one or a few of the subsequences dominate the error probability, so that it is sufficient to average over a sufficient number of samples of each subsequence to obtain a good estimate of the worst case conditional error probabilities. In our simulations, at a processing gain of 10, we are processing roughly 10,000

simulated information bits. Since the PN sequence used is 1023 chips long there are 1023 possible subsequences of length 10. For this reason, we are averaging over only about 10 samples of each possible subsequence. Since the dominating conditional error probabilities at high SNR are on the order of 10^{-1}, this yields only a very rough estimate of the conditional error probabilities, and thus a rough estimate of the total error probability.

This argument is borne out by Figure 19, which is a plot of the results of this simulation. The results are in general agreement with those obtained by the Gaussian approach and the conditional probability averaging approach, but appear more optimistic. This is probably a consequence of the poor estimates noted above. A more accurate simulation could be obtained by increasing the sample size by perhaps a factor of ten. The cost in computer time and storage would be prohibitive, however, and it is not clear that there is a real need to do so since we have demonstrated a more efficient analytical method of assessing performance.

Dispersive Channel

For operation over a dispersive channel, the receiver which performs symbol-by-symbol detection will consist of the whitening filter and its matched filter, as well as a filter matched to the channel, followed by the sequence correlator. If the channel is time-varying, the filter matched

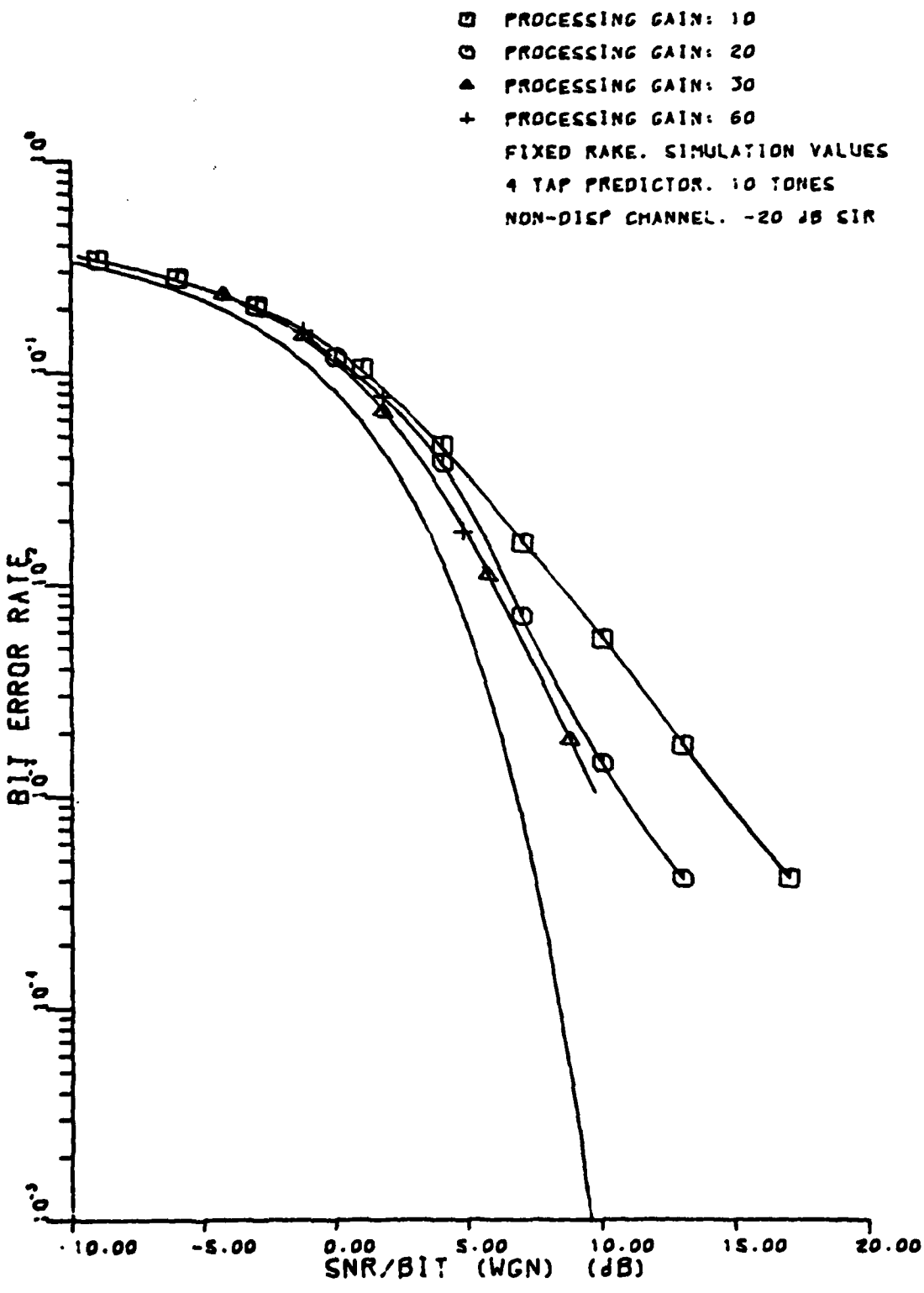
PROCESSING GAIN: 10
PROCESSING GAIN: 20
PROCESSING GAIN: 30
PROCESSING GAIN: 60
FIXED RAKE. SIMULATION VALUES
4 TAP PREDICTOR. 10 TONES
NON-DISP CHANNEL. -20 dB SIR
BIT ERROR RATE
10^0
10^-1
10^-2
10^-3
-10.00
-5.00
0.00
5.00
10.00
15.00
20.00
SNR/BIT (WGN) (dB)

Figure 19

to the whitening filter, and the filter matched to the channel can be realized in a unit as the RAKE correlator, as discussed in the section on the maximum likelihood receiver. In order to derive the performance of this receiver, we will follow the procedure outlined in the previous section for the non-dispersive channel.

As before, the noise at the output of the whitening filter,

$$e(k) = \sum_{\ell=0}^{P} h(\ell) \int_{-\infty}^{\infty} [n(\tau) + i(\tau)]\, p^*[\tau - (k - \ell)\, \tau_c]\, d\tau \tag{50}$$

is assumed to be white. In this case, however, the real part of the output of the chip pulse matched filter is not taken, since the channel impulse response is in general complex, and taking the real part at this point would lead to a loss of some of the desired signal. The variance of e(k) is:

$$\begin{aligned}
\phi'_{ee}(0) &= E[|e(k)|^2] \\
&= \sum_{\ell=0}^{P} \sum_{m=0}^{P} h(\ell)\, h^*(m) \iint_{-\infty}^{\infty} [\overline{n(t)\, n^*(\tau)} + \overline{i(t)\, i^*(\tau)}] \\
&\quad \cdot p^*[t - (k - \ell)\, \tau_c]\, p[\tau - (k - m)\, \tau_c]\, dt\, d\tau \\
&= 4N_o\, E_c\, g(0) + 4E_c\, \tau_c \sum_{\ell=-p}^{P} g(\ell)\, \phi_{ii}(\ell\tau_c)
\end{aligned} \tag{51}$$

The mean of the decision variable is

$$E(z_j) = 2E_c\, u_j \Big[LR_{xx}(0) + 2\mathrm{Re}\Big\{ \sum_{\ell=1}^{L} \sum_{k=jL+i}^{(j+1)L-1} c_k\, c_{k-\ell}\, R_{xx}(\ell) \Big\} \Big]$$

$$+ 2E_c\, R_e \Big\{ \sum_{\ell=1}^{L} R_{xx}(\ell) \Big[u_{j+1} \sum_{k=(j+1)L-\ell}^{(j+1)L-1} c_k\, c_{k+\ell}$$

$$+ u_{j-1} \sum_{k=jL}^{jL+\ell-1} c_k\, c_{k-\ell} \Big] \Big\} \qquad (52)$$

where $R_{xx}(k)$ is as defined in (25), and L is the span of the convolution of the channel with the whitening filter.

The noise and interference term in the decision variable is:

$$\mathrm{Re}\left[\sum_{k=jL}^{(j+1)L-1} \sum_{m=0}^{L} c_k\, h'^*(m)\, e(k+m) \right]$$

where $h'(m)$, $m = 0, \ldots, L$, are the filter coefficients of the cascade of the channel and the whitening filter. The variance of z_j is then

$$\mathrm{var}(z_j) = \frac{1}{2}\, \phi'_{ee}(0) \Big[LR_{xx}(0)$$

$$+ 2\mathrm{Re} \sum_{m=1}^{L} \sum_{k=jL+m}^{(j+1)L-1} c_k\, c_{k-m}\, R_{xx}(m) \Big] \qquad (53)$$

We can form a signal-to-noise ratio from (52) and (53) similar to that in (48) and use this expression to find the average bit error probability, as in (49).

The resulting expression for bit error probability applies to the fixed channel case. If the channel is time-varying, then $h'(m)$ and $R_{xx}(m)$ are functions of time, since $h'(m)$ is the convolution of the channel and the whitening filter, and $x(t)$ is the convolution of the transmitter pulse conditioning, the channel, and the whitening filter. Now the bit error probability given in (49) is only the error probability conditioned on a given channel, i.e.,

$$P_b = P[\text{bit error} | c(t,\tau)] \tag{54}$$

Conceptually, at least, it is possible to average the conditional probability given in (54) over the channel statistics to arrive at an average error probability. If we model the channel as a tapped delay line with time-varying coefficients,

$$c(t,\tau) = \sum_{k=1}^{M} c_k(t)\ \delta(\tau - k\tau_c) \tag{55}$$

the average probability of error is given by

$$P_{ave} = \iint \ldots \int p(\underline{c})\ P[\text{bit error} | c(t,\tau)]\ d\underline{c} \tag{56}$$

where (56) is an M-dimensional integral and $p(\underline{c})$ is the

M-dimensional probability density function of the channel tap weights. Since the conditional probability has to be evaluated numerically, the integral must be evaluated numerically, and in general the computation time required to perform the integration would be completely unreasonable.

Using the technique just outlined for evaluating bit error rate for a fixed multipath channel, error probabilities for signaling over a two-path channel with tap weights of equal magnitude have been calculated for several different interference realizations. In these calculations, complex channel coefficients and interference realizations were used. Figure 20 shows the calculated bit error rate when the interference consists of a sum of 100 complex sinusoids occupying the band between -0.1 and +0.1 with random Hz, phases uniformly distributed between 0 and 2π, and the SIR is -20dB. The PN sequence used was the same maximal length sequence of length 1023 used previously. The performance in this case is degraded by roughly 10dB compared to that obtained with ideal antipodal binary signaling and no interference at an error probability of 10^{-7} and a processing gain of 60, and by roughly 5dB relative to the nondispersive channel case shown in Figure 17. Figure 21 is the same channel and interference, except that the SIR is -10dB here. In this case the performance is about 2dB better than when the SIR is -20dB, when the processing gain is 60, at a 10^{-7} BER. At higher values of E_b/N_o the curves in Figures 20 and 21 for a processing gain

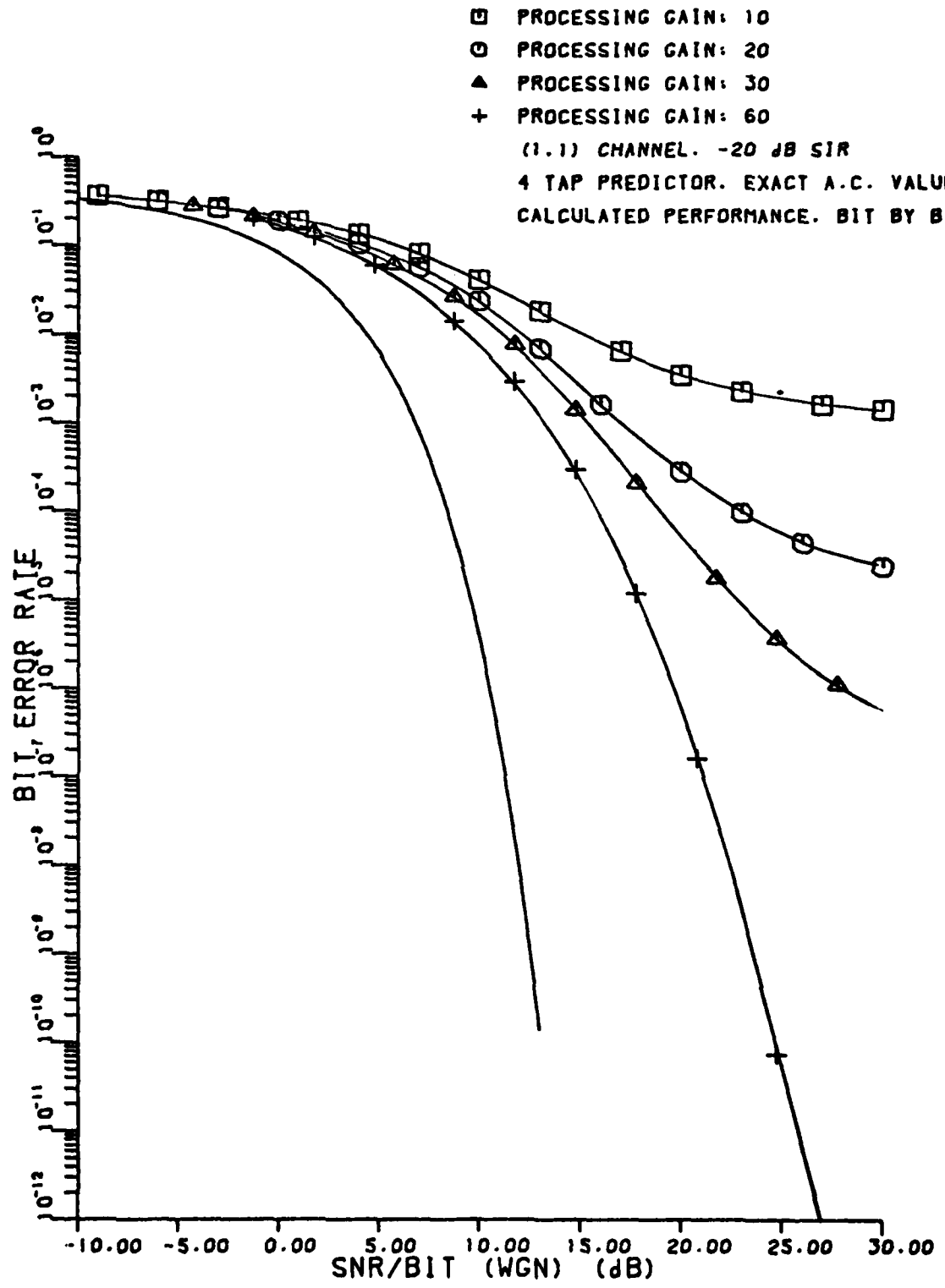
PROCESSING GAIN: 10
PROCESSING GAIN: 20
PROCESSING GAIN: 30
PROCESSING GAIN: 60
(1,1) CHANNEL. -20 dB SIR
4 TAP PREDICTOR. EXACT A.C. VALUES
CALCULATED PERFORMANCE. BIT BY BIT
BIT ERROR RATE
SNR/BIT (WGN) (dB)
-10.00 -5.00 0.00 5.00 10.00 15.00 20.00 25.00 30.00

Figure 20

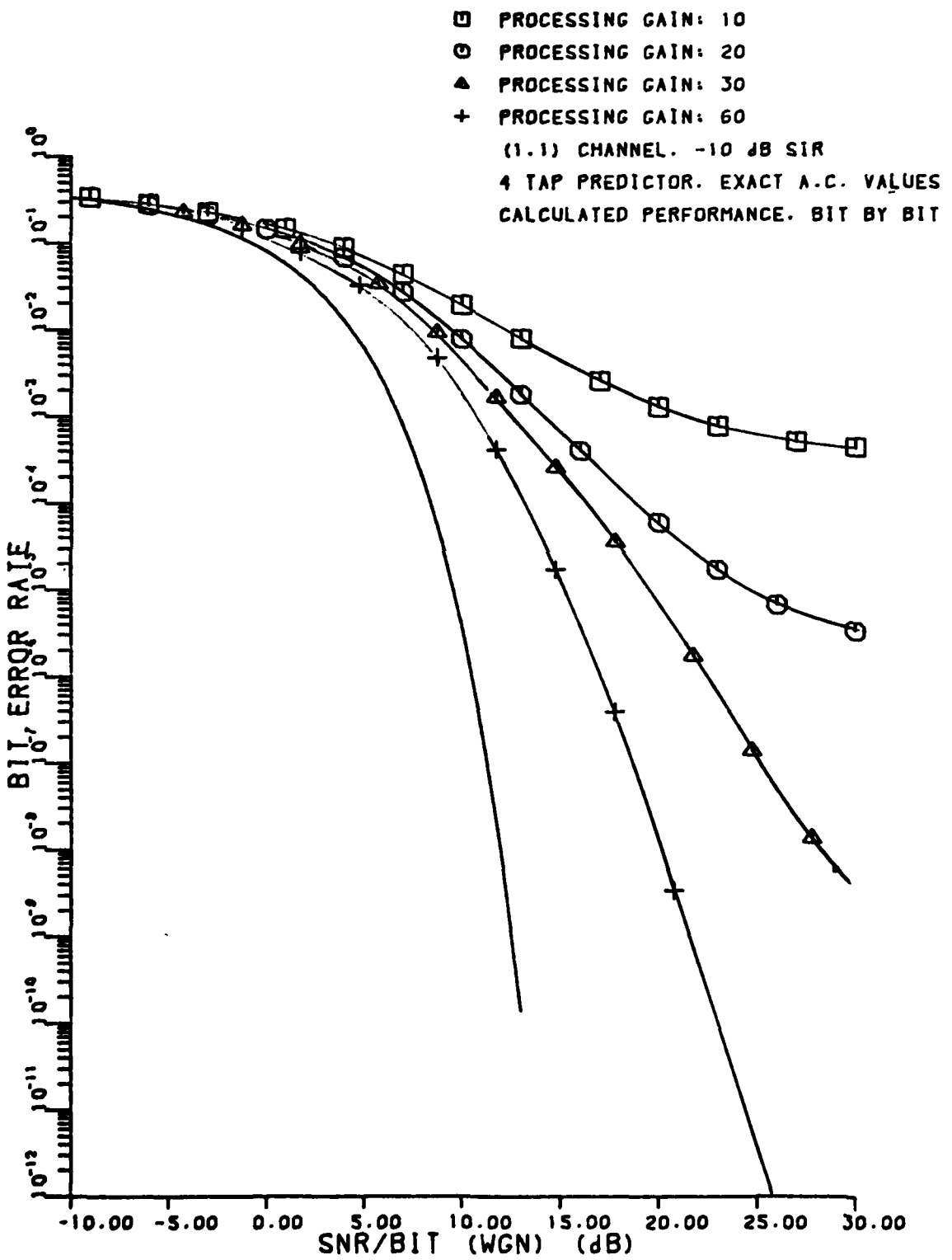
PROCESSING GAIN: 10
PROCESSING GAIN: 20
PROCESSING GAIN: 30
PROCESSING GAIN: 60
(1,1) CHANNEL. -10 dB SIR
4 TAP PREDICTOR. EXACT A.C. VALUES
CALCULATED PERFORMANCE. BIT BY BIT
BIT ERROR RATE
SNR/BIT (WGN) (dB)
-10.00 -5.00 0.00 5.00 10.00 15.00 20.00 25.00 30.00

Figure 21

of 60 appear to converge.

Figure 22 shows the calculated performance when the channel is the same as previously given, but now the interference is 100 complex sinusoids with uniformly distributed phases occupying the band between 0.0 Hz and +0.1 Hz, and the SIR is again -20dB. This figure illustrates that there is a substantial performance improvement when the interference bandwidth is reduced; in this case the improvement is about 5dB at 10^{-7} BER when the processing gain is 60.

The interference examples given here are near worst case for single-band interference corrupting communications on the (1,1) channel. This is because this channel has a spectral peak at 0 Hz, and spectral nulls at $\pm$0.5 Hz, and thus the chosen interference examples concentrate the interference power in the band where the signal power density reaches a peak. For this reason, interference which occupies the same bandwidth in other parts of the spectrum can be expected to cause less severe performance degradation relative to ideal binary communications than the examples chosen here.

Simulation of Bit-by-Bit Detection on the Dispersive Channel

A Monte Carlo simulation of the bit-by-bit receiver for the (1,1) channel was performed in a manner similar to that used for the nondispersive channel, with the exception that phase continuity in the PN sequence from block to block was not maintained. Instead, each block of 1,200 samples which

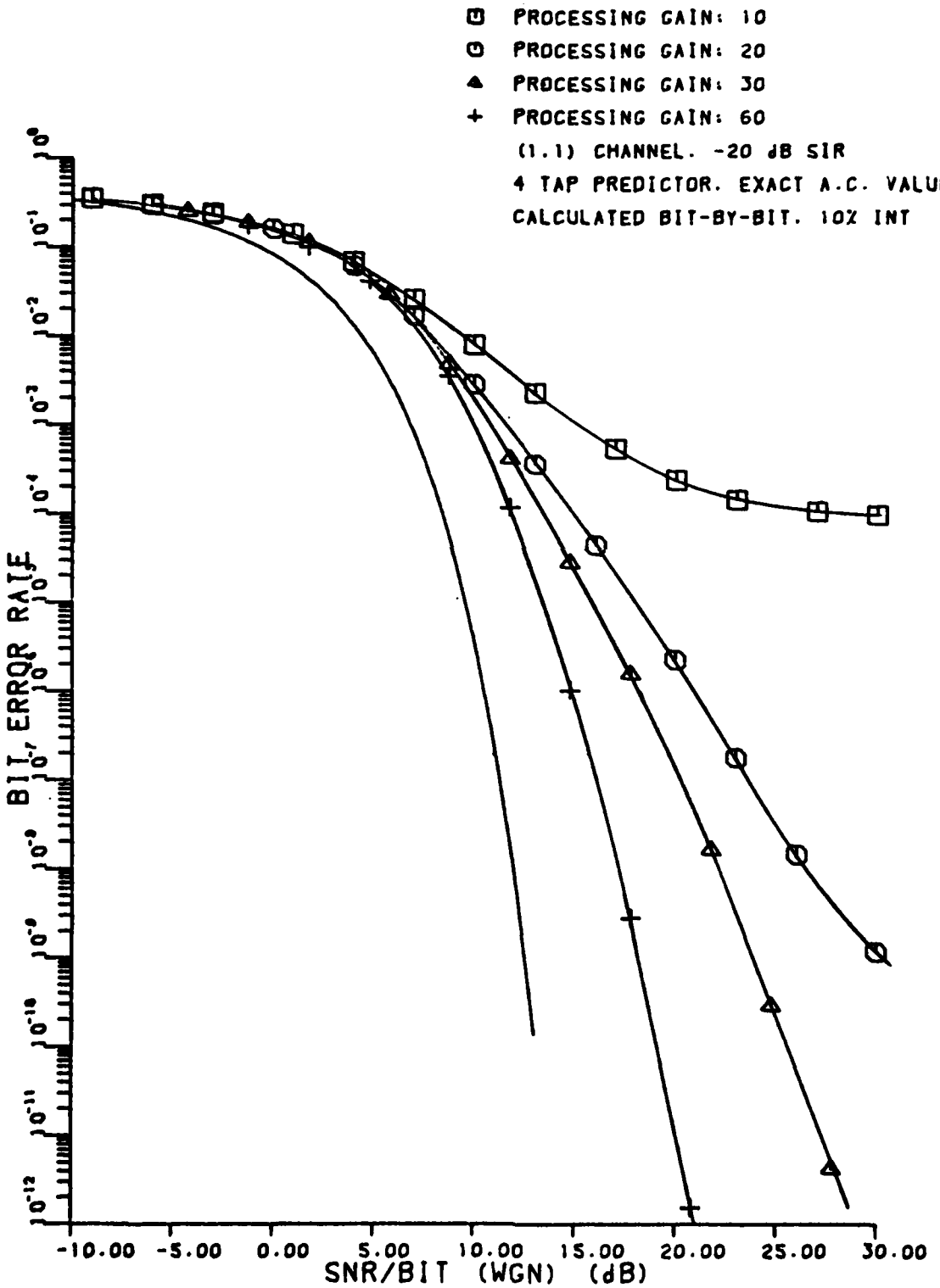
PROCESSING GAIN: 10
PROCESSING GAIN: 20
PROCESSING GAIN: 30
PROCESSING GAIN: 60
(1,1) CHANNEL. -20 dB SIR
4 TAP PREDICTOR. EXACT A.C. VALUES
CALCULATED BIT-BY-BIT. 10% INT
BIT ERROR RATE
SNR/BIT (WGN) (dB)
-10.00
-5.00
0.00
5.00
10.00
15.00
20.00
25.00
30.00

Figure 22

was processed in the simulation started at the same location in the PN sequence, and as a result only a subset of all possible subsequences in the PN sequence were transmitted in the simulation. We would expect that for this reason the complete set of worst case subsequences was not used, and the resulting performance estimate would be optimistic. Figure 23 shows the results of this simulation. The interference used in this simulation was a sum of 10 complex sinusoids with random phases occupying 10% of the band (0.0 Hz to 0.1). Comparing Figure 23 with Figure 22 confirms that the simulated performance exhibits generally the same sort of behavior as the calculated performance, although somewhat more optimistic.

A Monte Carlo simulation of the bit-by-bit receiver for fading multipath was also performed. This receiver was realized using a RAKE correlator, and simulations have been performed using both an adaptive RAKE and a fixed RAKE. The adaptive RAKE simulation was implemented using a "snapshot" approach. In this technique a set of channel coefficients are chosen pseudo-randomly and a block of 2,000 chips are transmitted through the resulting channel. At the receiver, the interference suppression filter coefficients are computed from the block of data. The first 1,000 chips are then used to train the RAKE and the next 1,000 chips are used for collecting error rate data. The simulation of the fixed RAKE was performed in a similar manner except that the full 2,000

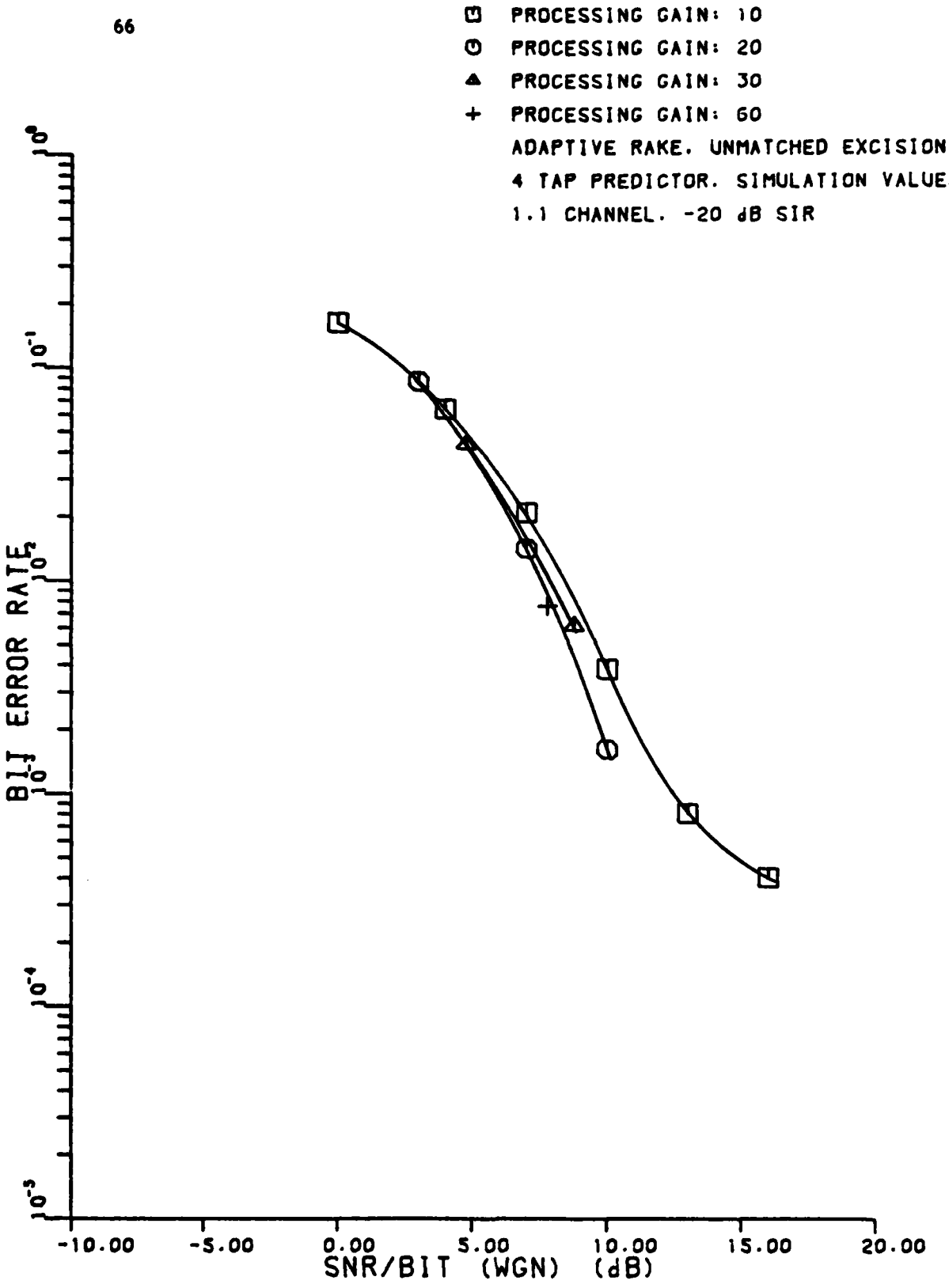
PROCESSING GAIN: 10
PROCESSING GAIN: 20
PROCESSING GAIN: 30
PROCESSING GAIN: 60
ADAPTIVE RAKE. UNMATCHED EXCISION
4 TAP PREDICTOR. SIMULATION VALUES
1.1 CHANNEL. -20 dB SIR
BIT ERROR RATE
10^{0}
10^{-1}
10^{-2}
10^{-3}
10^{-4}
10^{-5}
-10.00
-5.00
0.00
5.00
10.00
15.00
20.00
SNR/BIT (WGN) (dB)

Figure 23

chips in each block were used for collecting error rate data, and the exact matched filter coefficients were used for the RAKE coefficients instead of estimates obtained from the RAKE adaptation process. This method has the advantage of providing a larger sample size for the purpose of estimating the error rate. Both simulation methods were used, and it was found that the adaptive RAKE exhibited performance which was only slightly degraded from that of the fixed RAKE.

Figure 24 shows the results of the fixed RAKE simulation, using 100,000 chips of data processed in 50 blocks of 2,000 chips each. Thus there were 50 channel realizations. The channels had two active taps, the first and the fourth, which were chosen pseudo-randomly from a complex Gaussian distribution with zero mean and unit variance. The interference was a sum of 20 complex sinusoids with random phases occupying 20% of the band (-0.1 to +0.1 Hz). Also plotted in Figure 24 is performance of ideal dual diversity communications with no interference. It is seen from this figure that the performance in the presence of interference tracks that of ideal dual diversity, except that it is degraded by a few dB. Figure 25 shows the simulated performance for the same set of channels, but with interference which covers 10% of the band (0.0 to 0.1 Hz). The performance in this case is improved over that of the 20% interference, as would be expected.

All the limitations of our simulation technique which

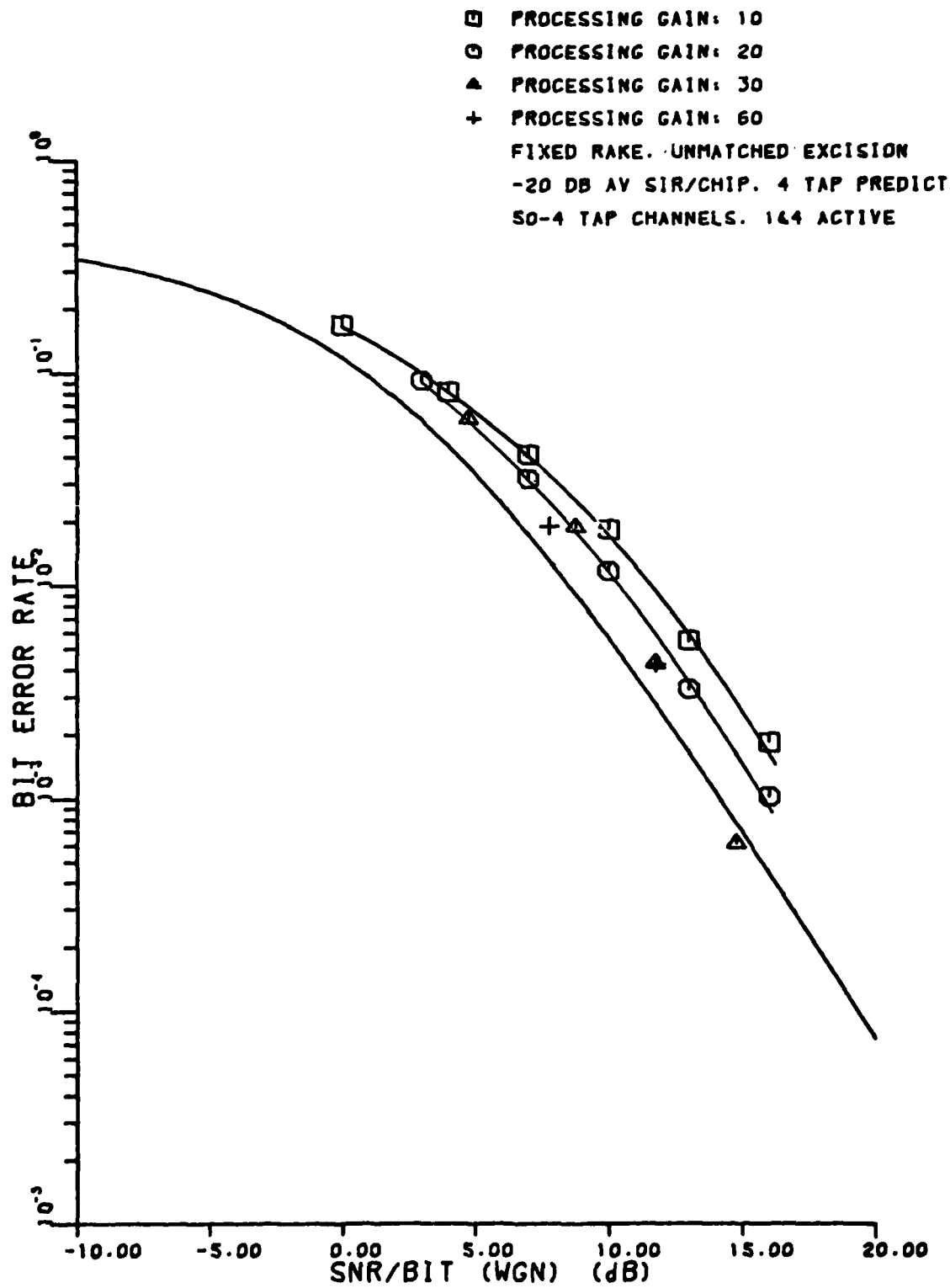
PROCESSING GAIN: 10
PROCESSING GAIN: 20
PROCESSING GAIN: 30
PROCESSING GAIN: 60
FIXED RAKE. UNMATCHED EXCISION
-20 DB AV SIR/CHIP. 4 TAP PREDICTOR
50-4 TAP CHANNELS. 144 ACTIVE
BIT ERROR RATE
10^0
10^-1
10^-2
10^-3
10^-4
-10.00
-5.00
0.00
5.00
10.00
15.00
20.00
SNR/BIT (WGN) (dB)

Figure 24

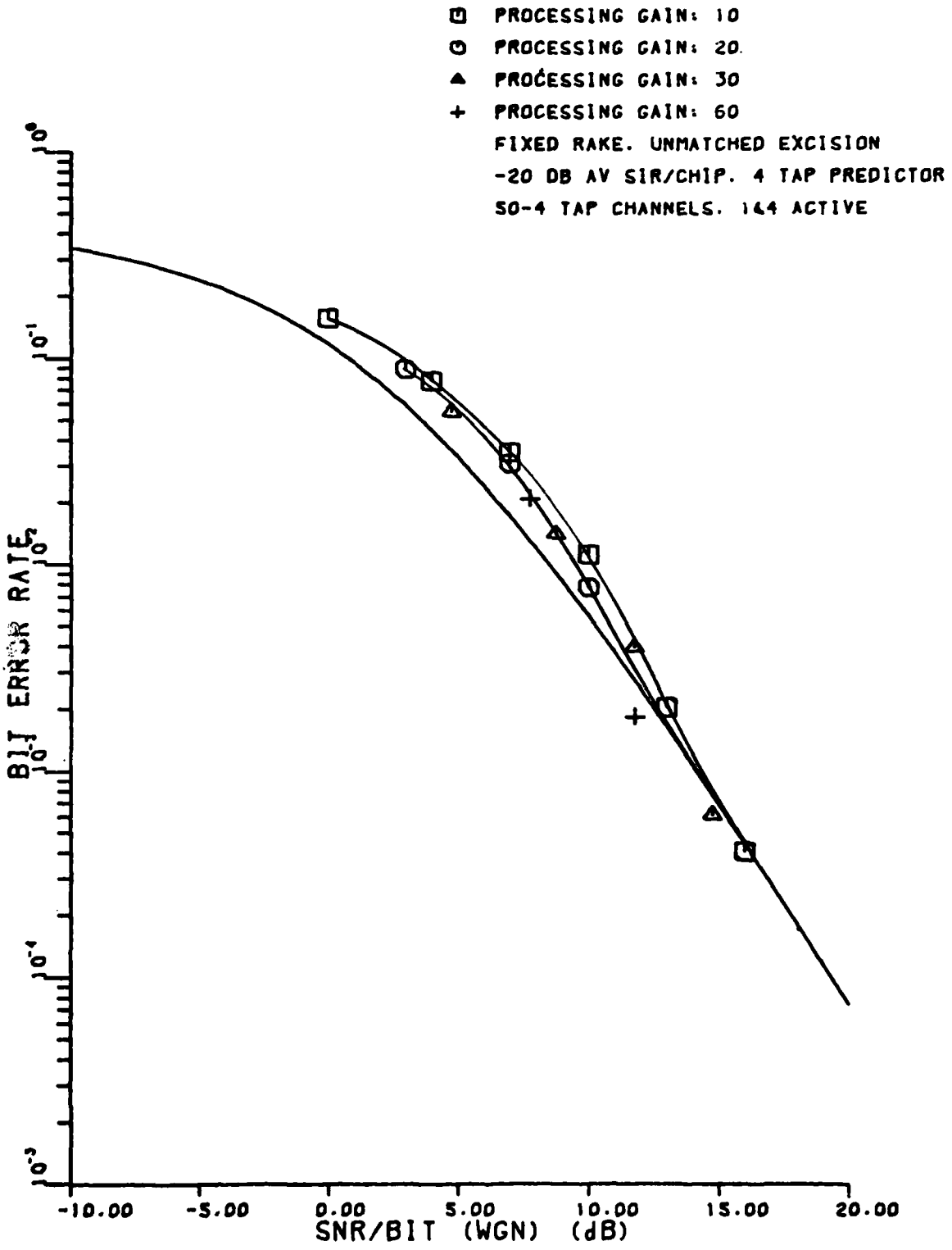
PROCESSING GAIN: 10
PROCESSING GAIN: 20
PROCESSING GAIN: 30
PROCESSING GAIN: 60
FIXED RAKE. UNMATCHED EXCISION
-20 DB AV SIR/CHIP. 4 TAP PREDICTOR
50-4 TAP CHANNELS. 144 ACTIVE
BIT ERROR RATE
10^0
10^-1
10^-2
10^-3
10^-4
-10.00
-5.00
0.00
5.00
10.00
15.00
20.00
SNR/BIT (WGN) (dB)

Figure 25

were stated for the nondispersive channel and the fixed multipath channel apply even more strongly for this simulation since now we need not only average over the noise and interference density functions and the subsequences of the PN sequence, but we must average over the complex, two-dimensional probability distribution of the channel as well. Since we have not increased the sample size over that of the fixed channel simulation, we would expect that the performance estimate given by the simulation would be less accurate than that given by the fixed channel simulations. For this reason it is not surprising that a few of the data points in these simulations fall below the double diversity performance. This is presumably a consequence of the limitations of the simulation. A considerable increase in sample size would be required to provide an accurate estimate of performance, and unfortunately, the resulting storage and computation time requirements would be prohibitive. However, the simulations which we have performed indicate that adaptive interference suppression techniques can be used with good results in a fading multipath environment.

IV. Error Probability Bounds for Maximum Likelihood Detection

In order to establish error rate bounds for maximum likelihood sequence detection of direct sequence spread spectrum signals with receiver processing of the type considered in this report, we first consider the probability of

a pair-wise sequence error. This is the probability that the transmitted information sequence, $\underline{u}$, is decoded at the receiver as the sequence $\underline{u}'$, where $\underline{u}'$ is identical to $\underline{u}$ in all but a given number of bit positions. We then make use of this pair-wise sequence error probability to establish bounds on the bit error probability. The arguments given here follow fairly closely those given in [5] for probability of error on an intersymbol interference channel.

In order to find the probability of a pair-wise sequence error, we start by defining the decision variable $z = \Lambda - \Lambda'$, where Λ is the likelihood function given in (19) for the correct transmitted sequence decision $\underline{u}$ and Λ' is the likelihood function for some incorrect sequence decision, $\underline{u}'$. Thus the probability of a pair-wise error is given by

$$\Pr(\underline{\varepsilon}) = \Pr(z < 0)$$

where $\underline{\varepsilon}$ is the error sequence $\underline{\varepsilon} = \frac{1}{2}(\underline{u} - \underline{u}')$. Again we assume that the decision variable z is a Gaussian random variable, so that we only need to find the mean and variance of z to have the desired probability of error. The mean of z is

$$E(z) = \sum_{j=-N}^{N-1} \Bigg[\sum_{k=jL}^{(j+1)L-1} 2(u_j - u_j') \, c_k \, E(y_k)$$

$$- 2\alpha E_c \sum_{k=jL}^{(j+1)L-1} \sum_{m=-p}^{P} (u_j \, u_{\lfloor (k-m)/L \rfloor}$$

$$- u_j' \, u'_{\lfloor (k-m)/L \rfloor}) \, c_k \, c_{k-m} \, g(m) \Bigg]$$

$$= \sum_{j=-N}^{N-1} \Bigg[4\alpha E_c \sum_{k=jL}^{(j+1)L-1} \sum_{m=-p}^{P} (u_j - u_j')$$

$$\cdot \, u_{\lfloor (k-m)/L \rfloor} \, c_k \, c_{k-m} \, g(m)$$

$$- 2\alpha E_c \sum_{k=jL}^{(j+1)L-1} \sum_{m=-p}^{P} (u_j \, u_{\lfloor (k-m)/L \rfloor}$$

$$- u_j' \, u'_{\lfloor (k-m)/L \rfloor}) \, c_k \, c_{k-m} \, g(m)$$

$$= \sum_{j=-N}^{N-1} \Bigg[2\alpha E_c \sum_{k=jL}^{(j+1)L-1} \sum_{m=-p}^{p} (u_j - u_j')$$

$$\cdot \, (u_{\lfloor (k-m)/L \rfloor} - u'_{\lfloor (k-m)/L \rfloor}) \, c_k \, c_{k-m} \, g(m) \Bigg]$$

(57)

Substituting the error sequence $\underline{\varepsilon}$ into (57):

$$E(z) = 8\alpha E_c \sum_{j=-N}^{N-1} \sum_{k=jL}^{(j+1)L-1} \sum_{m=-p}^{P} \varepsilon_j \, \varepsilon_{\lfloor (k-m)/L \rfloor} \, c_k \, c_{k-m} \, g(m)$$

$$= 8\alpha E_c \sum_{j=-N}^{N-1} [L(\varepsilon_j)^2 \, g(0)$$

$$+ 2 \sum_{m=1}^{p} \sum_{k=jL}^{(j+1)L-1} \varepsilon_j \, \varepsilon_{\lfloor (k-m)/L \rfloor} \, c_k \, c_{k-m} g(m)] \qquad (58)$$

We will next evaluate the variance of z on the assumption, used in the previous section, that the total noise at the whitening filter output, due to the white noise and the narrow-band interference, is white. Thus the noise term in z is given by:

$$N_z = 2 \sum_{k=-NL}^{NL-1} \sum_{\ell=0}^{P} (u_{\lfloor k/L \rfloor} - u'_{\lfloor k/L \rfloor}) \, c_k \, h(\ell) \, e(k - \ell) \qquad (59)$$

and the variance of z is given by

$$\text{var}(z) = E(N_z^2)$$

$$= 4 \sum_{k=-NL}^{NL-1} \sum_{\ell=0}^{P} \sum_{n=-NL}^{NL-1} \sum_{m=0}^{P} (u_{\lfloor k/L \rfloor} - u'_{\lfloor k/L \rfloor})$$

$$\cdot (u_{\lfloor n/L \rfloor} - u'_{\lfloor n/L \rfloor}) \, c_k \, c_n \, h(\ell) \, h(m) \, E[e(k-\ell) \, e(n-m)]$$

$$= 16 \sum_{k=-NL}^{NL-1} \sum_{\ell=0}^{P} \sum_{m=0}^{P} \varepsilon_{\lfloor k/L \rfloor} \varepsilon_{\lfloor (k+m-\ell)/L \rfloor}$$

$$\cdot c_k c_{k+m-\ell} h(\ell) h(m) \phi_{ee}(0)$$

$$= 16\phi_{ee}(0) \sum_{j=-N}^{N-1} [L(\varepsilon_j)^2 g(0)$$

$$+ 2 \sum_{m=1}^{P} \sum_{k=jL}^{(j+1)L-1} \varepsilon_j \varepsilon_{\lfloor (k-m)/L \rfloor} c_k c_{k-m} g(m)] \quad (60)$$

Finally, defining the signal-to-noise ratio as

$$\gamma = [E(z)]^2/2 \text{ var}(z)$$

we have

$$\gamma = \frac{\alpha^2 E_c}{\sigma_e^2} \sum_{j=-N}^{N-1} [L(\varepsilon_j)^2 g(0)$$

$$+ 2 \sum_{m=1}^{P} \sum_{k=jL}^{(j+1)L-1} \varepsilon_j \varepsilon_{\lfloor (k-m)/L \rfloor} c_k c_{k-m} g(m)] \quad (61)$$

where σ_e^2 is given by (47). Thus the probability that the maximum likelihood receiver will select the sequence $\underline{u}'$ instead of $\underline{u}$ is given by:

$$P(\underline{\varepsilon}) = \frac{1}{2}\,\mathrm{erfc}[\sqrt{\gamma}]$$

In order to compute the bit error probability we start by defining the error sequence $\underline{\varepsilon}_\ell$ as any error sequence which has a non-zero element for the first time in the ℓ^{th} position, i.e., $\varepsilon_j = 0$ for $j < \ell$. Thus we can union bound the bit error probability given that the first error occurs at the ℓ^{th} node by:

$$P_b(\ell) \leq \sum_{\underline{\varepsilon}_\ell} w(\underline{\varepsilon}_\ell)\; 2^{-[w(\underline{\varepsilon}_\ell)]}\; P(\underline{\varepsilon}_\ell) \qquad (62)$$

The summation in (62) is over all possible error sequences which begin at node ℓ, and $w(\varepsilon_\ell)$ is the number of places in which $\underline{\varepsilon}_\ell$ is non-zero. In order to obtain a union bound on the total probability of bit error, we also must average over all nodes in the sequence. This is because for a given non-zero error sequence starting at two different nodes, the value of $P(\underline{\varepsilon})$ is different, depending on the particular subsequence of the PN sequence which occurs at that node. For example, the probability that a single bit error will occur at node p depends on the PN sequence on the interval $pL \leq k < (p + 1)L$, while the probability that a single bit error will occur at node q depends on the PN sequence on the interval $qL \leq k < (q + 1)L$. In general, the PN sequence in these two intervals is not the same unless the processing gain, L, is equal to or some integer multiple of the PN sequence length.

The bit error probability is then bounded by:

$$P_b \leq \sum_{\ell} p(\ell) \sum_{\underline{\varepsilon}_\ell} w(\underline{\varepsilon}_\ell)\ 2^{-w(\underline{\varepsilon}_\ell)}\ P(\underline{\varepsilon}_\ell) = \sum_{\ell} p(\ell)\ p_b(\ell) \qquad (63)$$

The outer summation is over all possible nodes at which an error event can start, or equivalently, over all points in the PN sequence at which the bit u_ℓ can start. The probability $p(\ell)$ is the probability that u_ℓ starts at a particular point in the PN sequence. We assume that this probability is uniformly distributed over the PN sequence, or $p(\ell) = 1/(\text{sequence length})$.

We will start by evaluating the conditional probability $P_b(\ell)$. To do so, we will need the inequality: $\text{erfc}\sqrt{x} \leq \text{erfc}\sqrt{y}\{\exp(y - x)\}$ [6]. We will also define $\gamma_\ell(\underline{\varepsilon}_\ell)$ as the signal-to-noise ratio, γ, given by (61), evaluated for $\varepsilon_j = 0$, $j < \ell$, and $\varepsilon_\ell = \pm 1$. We make the further definition that

$$\gamma_{\ell,\min} = \frac{\alpha^2 E_c}{\sigma_e^2}\left[Lg(0) + 2\sum_{m=1}^{P}\ \sum_{k=\ell L+m}^{(\ell+1)m-1} c_k\, c_{k-m}\, g(m)\right] \qquad (64)$$

By virtue of these definitions and the above inequality, we can write the following inequality:

$$P(\underline{\varepsilon}_\ell) = \tfrac{1}{2}\,\text{erfc}[\sqrt{\gamma_\ell(\underline{\varepsilon}_\ell)}] \leq \tfrac{1}{2}\,\text{erfc}\sqrt{\gamma_{\ell,\min}} \cdot \left\{e^{\gamma_{\ell,\min}}\quad e^{-\gamma_\ell(\underline{\varepsilon}_\ell)}\right\} \qquad (65)$$

In order to evaluate (65), the term $e^{-\gamma_\ell(\underline{\varepsilon}_\ell)}$ must be evaluated using an error state diagram and solving for its transfer function. This technique was developed by Forney, Viterbi and Omura, and others [5,6], for the purpose of finding error probabilities for intersymbol interference channels. Extending this technique to (65) is a bit problematic, however, since γ_ℓ depends not only on the given error sequence, but also on the timing of the PN sequence relative to the error sequence. Another way of stating the problem is that although we are employing a binary antipodal signaling scheme, the basic channel waveform varies from bit to bit. For this reason, the resulting error state diagram will have time-varying path gains. Although we know of no exact solution to such a time-varying flowgraph, we will proceed to construct the flowgraph, and write an approximate solution.

First we will substitute (65) into (62):

$$P_b(\ell) \leq \frac{1}{2}\,\mathrm{erfc}\sqrt{\gamma_{\ell,\min}}\,\exp(\gamma_{\ell,\min}) \sum_{\underline{\varepsilon}_\ell} w(\underline{\varepsilon}_\ell)$$

$$\cdot\ 2^{-w(\underline{\varepsilon}_\ell)}\,\exp[-\gamma_\ell(\underline{\varepsilon}_\ell)]$$

$$= \frac{1}{2}\,\mathrm{erfc}\sqrt{\gamma_{\ell,\min}}\,\exp(\gamma_{\ell,\min}) \sum_{\underline{\varepsilon}_\ell} w(\underline{\varepsilon}_\ell)$$

$$\cdot \prod_{j=\ell}^{N-1} \frac{1}{2^{w(\varepsilon_j)}}\,\exp\left[-\frac{\alpha^2 E_c}{\sigma_e^2}\,E(\underline{\varepsilon}_\ell, j)\right] \qquad (66)$$

where

$$E(\underline{\varepsilon}_\ell, j) = L(\varepsilon_j)^2\, g(0) + 2 \sum_{m=1}^{P} \sum_{k=jL}^{(j+1)L-1} \varepsilon_j\, \varepsilon_{\lfloor (k-m)/L \rfloor}\, c_k\, c_{k-m}\, g(m) \tag{67}$$

We have assumed that an error occurs for the first time at node ℓ, i.e., $\varepsilon_j = 0$, $j < \ell$, $\varepsilon_\ell = \pm 1$. Thus, for $j < \ell$ $E(\underline{\varepsilon}_\ell, j) = 0$, and

$$E(\underline{\varepsilon}_\ell, \ell) = Lg(0) + 2 \sum_{m=1}^{P} \sum_{k=\ell L+m}^{(\ell+1)L-1} c_k\, c_{k-m}\, g(m) \tag{68}$$

and we define the quantity $a_o(\ell)$ as

$$a_o(\ell) = \exp\left[-\frac{\alpha^2 E_c}{\sigma_e^2} E(\underline{\varepsilon}_\ell, \ell)\right] \tag{69}$$

There are three possible values for $E(\underline{\varepsilon}_\ell, \ell+i)$, for $i \geq 1$ and $\varepsilon_j \neq 0$, $\ell \leq j < \ell + i$. If $\varepsilon_{\ell+i} = \varepsilon_{\ell+i-1}$, then:

$$E(\underline{\varepsilon}_\ell, \ell+i) = Lg(0) + 2 \sum_{m=1}^{P} \sum_{k=(\ell+i)L}^{(\ell+i+1)L-1} c_k\, c_{k-m}\, g(m) \tag{70}$$

and we define the quantity $a_1(\ell + i)$ by

$$a_1(\ell + i) = \exp[-\frac{\alpha^2 E_c}{\sigma_e^2} E(\underline{\varepsilon}_\ell, \ell+i)] \tag{71}$$

If $\varepsilon_{\ell+i} = -\varepsilon_{\ell+i-1}$, then

$$E(\underline{\varepsilon}_\ell, \ell+i) = Lg(0) + 2 \sum_{m=1}^{P} [\sum_{k=(\ell+i)L+m}^{(\ell+i+1)L-1} c_k \, c_{k-m} - \sum_{k=(\ell+i)L}^{(\ell+i)L+m-1} c_k \, c_{k-m}] \, g(m) \tag{72}$$

and we define the quantity $a_2(\ell + i)$ by:

$$a_2(\ell + i) = \exp[-\frac{\alpha^2 E_c}{\sigma_e^2} E(\underline{\varepsilon}_\ell, \ell+i)] \tag{73}$$

If $\varepsilon_{\ell+i} = 0$, then $E(\underline{\varepsilon}_\ell, \ell+i) = 0$.

The resulting flowgraph is shown in Figure 26. The factors of $\frac{1}{2}$ in each branch account for the factors $2^{-w(\varepsilon_j)}$ in (66), and the factor I is also inserted into each branch to indicate that a bit error is made on every transition in the error state diagram. The variable i is incremented each time a non-zero state is passed through on a y-path from the start node to the finish node. P_b is obtained by

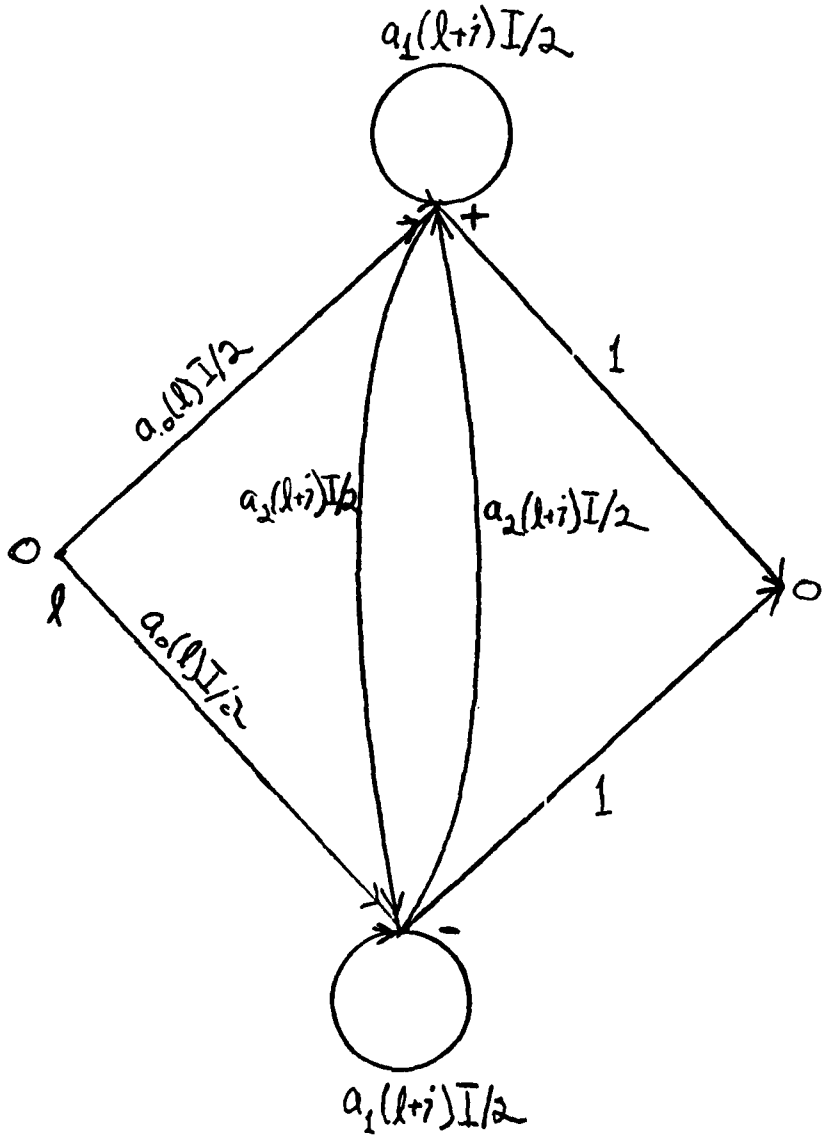

Figure 26

differentiating the resulting generating function with respect to I, as shown by Forney, and Viterbi and Omura [5,6].

As was previously mentioned, it is not possible to write a closed form expression for the transfer function of this error state diagram, since the path gains are time-varying. However, because the transfer function is the sum of all possible paths through the state diagram, we can write the first several terms of the transfer function as follows:

$$\begin{aligned} T(a_0, a_1, a_2, \ell, I) = {} & a_0(\ell) I + a_1(\ell + 1)\, a_0(\ell)\, I^2/2 \\ & + a_0(\ell)\, a_2(\ell + 1)\, I^2/2 \\ & + a_0(\ell)\, a_1(\ell + 1)\, a_1(\ell + 2)\, I^3/4 \\ & + a_0(\ell)\, a_1(\ell + 1)\, a_2(\ell + 2)\, I^3/4 \\ & + a_0(\ell)\, a_2(\ell + 1)\, a_1(\ell + 2)\, I^3/4 + \ldots \end{aligned} \tag{74}$$

We have written in (74) terms representing all possible ways of making one, two, and three bit errors. In order to find an approximate upper bound for the bit error rate, we take the derivative of (74) with respect to I and set I = 1.

$$\begin{aligned} \left.\frac{\partial T(a_0, a_1, a_2, \ell, I)}{\partial I}\right|_{I=1} = {} & a_0(\ell) + a_0(\ell)\, a_1(\ell + 1) \\ & + a_0(\ell)\, a_2(\ell + 1) + \tfrac{3}{4}\, a_0(\ell)\, a_1(\ell + 1)\, a_1(\ell + 2) + \ldots \end{aligned} \tag{75}$$

Replacing (75) in (66), we have:

$$P_b(\ell) \leq \frac{1}{2} \operatorname{erfc}\sqrt{\gamma_{\ell,\min}} \exp(\gamma_{\ell,\min}) [a_o(\ell) + a_0(\ell)\, a_1(\ell+1) + a_0(\ell)\, a_2(\ell+1) + \frac{3}{4} a_0(\ell)\, a_1(\ell+1)\, a_1(\ell+2) + \ldots] \quad (76)$$

Noting that $\gamma_{\ell,\min} = \frac{\alpha^2 E_c}{\sigma_2^2} E(\underline{\varepsilon}_\ell, \ell)$, and thus $\exp(\gamma_{\ell,\min}) = [a_0(\ell)]^{-1}$, we have

$$P_b(\ell) \leq \frac{1}{2} \operatorname{erfc}\sqrt{\gamma_{\ell,\min}} [1 + a_1(\ell+1) + a_2(\ell+1) + \frac{3}{4} a_1(\ell+1)\, a_1(\ell+2) + \ldots] \quad (77)$$

Dropping all but the first term in (77) gives the approximate upper bound:

$$P_b(\ell) \lesssim \frac{1}{2} \operatorname{erfc}\sqrt{\gamma_{\ell,\min}} \quad (78)$$

This represents the probability of error due to the minimum distance path through the error state diagram, assuming that the error event starts at node ℓ.

Finally, to find the average bit error probability, we substitute (78) into (63), yielding:

$$P_b \lesssim \frac{1}{2} \sum_{\ell} p(\ell)\ \mathrm{erfc}\sqrt{\gamma_{\ell,\min}} \qquad (79)$$

This expression has been evaluated for the nondispersive channel and several PN sequences. Figure 27 is the resulting calculated performance of the maximum likelihood receiver when the interference is a sum of 100 real sinusoids occupying the band between 0.0 and 0.1 Hz, with independent and identically, uniformly distributed phases between 0 and 2π. The SIR is -20dB, so the performance shown is for the same channel and interference as is illustrated in Figure 17 for the receiver which performs bit decisions on a bit-by-bit basis. Comparison of Figure 27 with Figure 17 reveals that the receiver which performs maximum likelihood sequence estimation has only slightly improved performance over the bit-by-bit receiver, particularly for the high processing gain. This is true because at the higher processing gain, the inequality $L >> P$ holds, i.e., the symbol duration is much greater than the dispersion caused by the interference suppression filter, and for this reason there is negligible intersymbol interference.

The remaining performance degradation relative to ideal binary signaling without interference, about 5dB at 10^{-7} BER, is due to residual interference, loss of signal power due to the notch created by the interference suppression filter, and the chip pulse dispersion or interchip interference. The loss of signal power due to the suppression filter is 20%, or

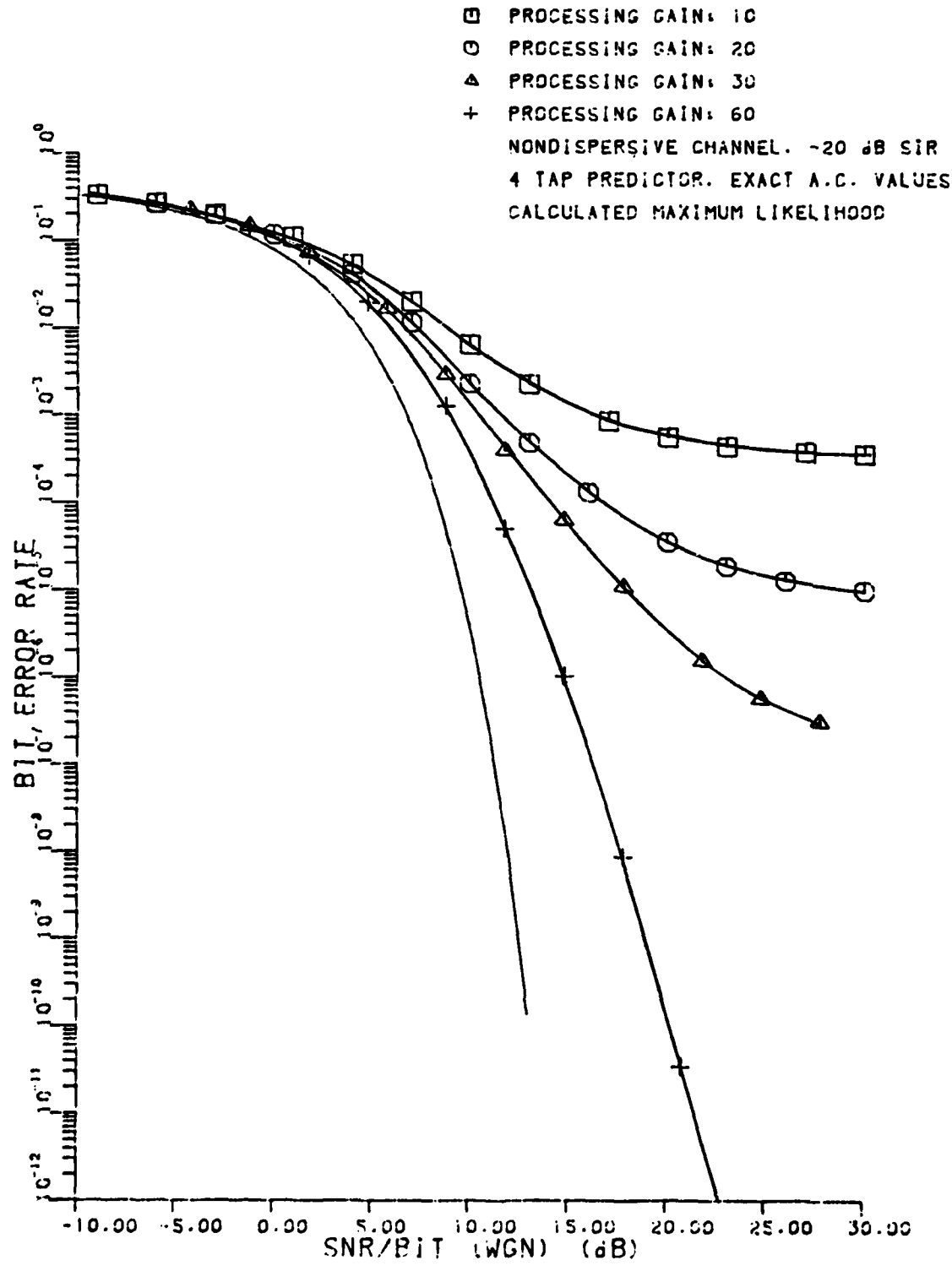
PROCESSING GAIN: 10
PROCESSING GAIN: 20
PROCESSING GAIN: 30
PROCESSING GAIN: 60
NONDISPERSIVE CHANNEL. -20 dB SIR
4 TAP PREDICTOR. EXACT A.C. VALUES
CALCULATED MAXIMUM LIKELIHOOD
BIT ERROR RATE
SNR/BIT (WGN) (dB)
-10.00
-5.00
0.00
5.00
10.00
15.00
20.00
25.00
30.00

Figure 27

1dB, since the interference occupies 20% of the band. Assuming that the residual interference at the output of the matched filter is negligible relative to the white noise, the remaining 4dB of degradation at 10^{-7} BER must be due to interchip interference. Furthermore, since the performance curve for a processing gain of 60 continues to diverge from the ideal binary curve below 10^{-7} BER, it appears that the interchip interference increases with increasing E_b/N_o.

Figure 28 shows the performance with the same channel and interference, but with an SIR of -10dB. Here, at the higher processing gain, the performance is degraded by only 1.5-2dB at 10^{-7} BER. Thus at lower levels of interference, it appears that the suppression filter contributes significantly less interchip interference than -20dB, in this case causing less than 1dB degradation above that caused by loss of signal power.

The performance bounds given in Figures 27 and 28 were obtained with a maximal length sequence of length 1023. We next consider the performance with shorter sequences. Figure 29 is the performance obtained when the channel and interference are the same as given in Figure 27, but the sequence length is now 63. We see that at the highest processing gain, the performance at error rates above 10^{-12} is not much different than that obtained with the longer sequence; however, at the lower processing gain, the BER bottoms out at a lower error rate when the shorter sequence is used.

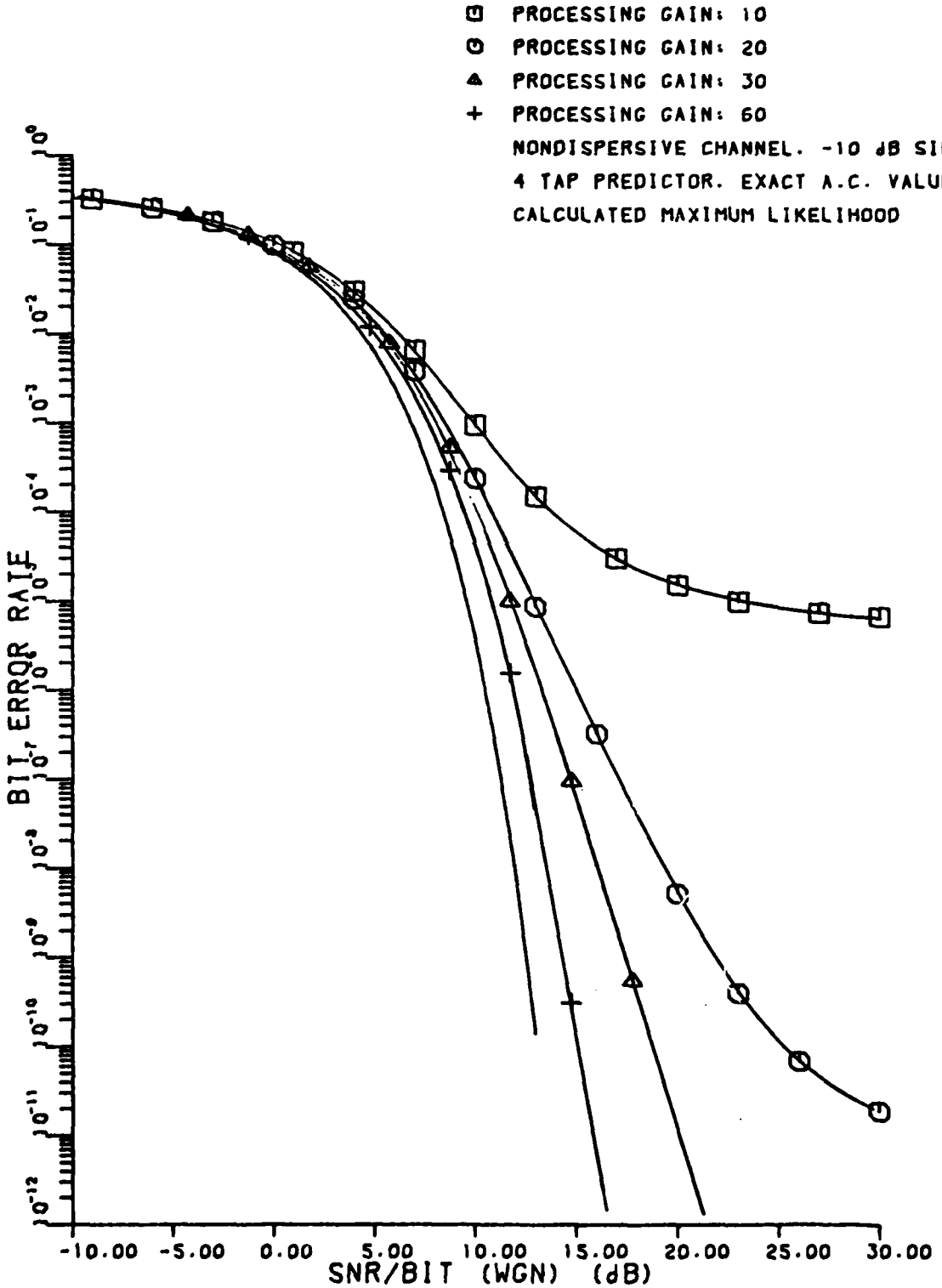
PROCESSING GAIN: 10
PROCESSING GAIN: 20
PROCESSING GAIN: 30
PROCESSING GAIN: 60
NONDISPERSIVE CHANNEL. -10 dB SIR
4 TAP PREDICTOR. EXACT A.C. VALUES
CALCULATED MAXIMUM LIKELIHOOD
BIT ERROR RATE
SNR/BIT (WGN) (dB)
-10.00
-5.00
0.00
5.00
10.00
15.00
20.00
25.00
30.00

Figure 28

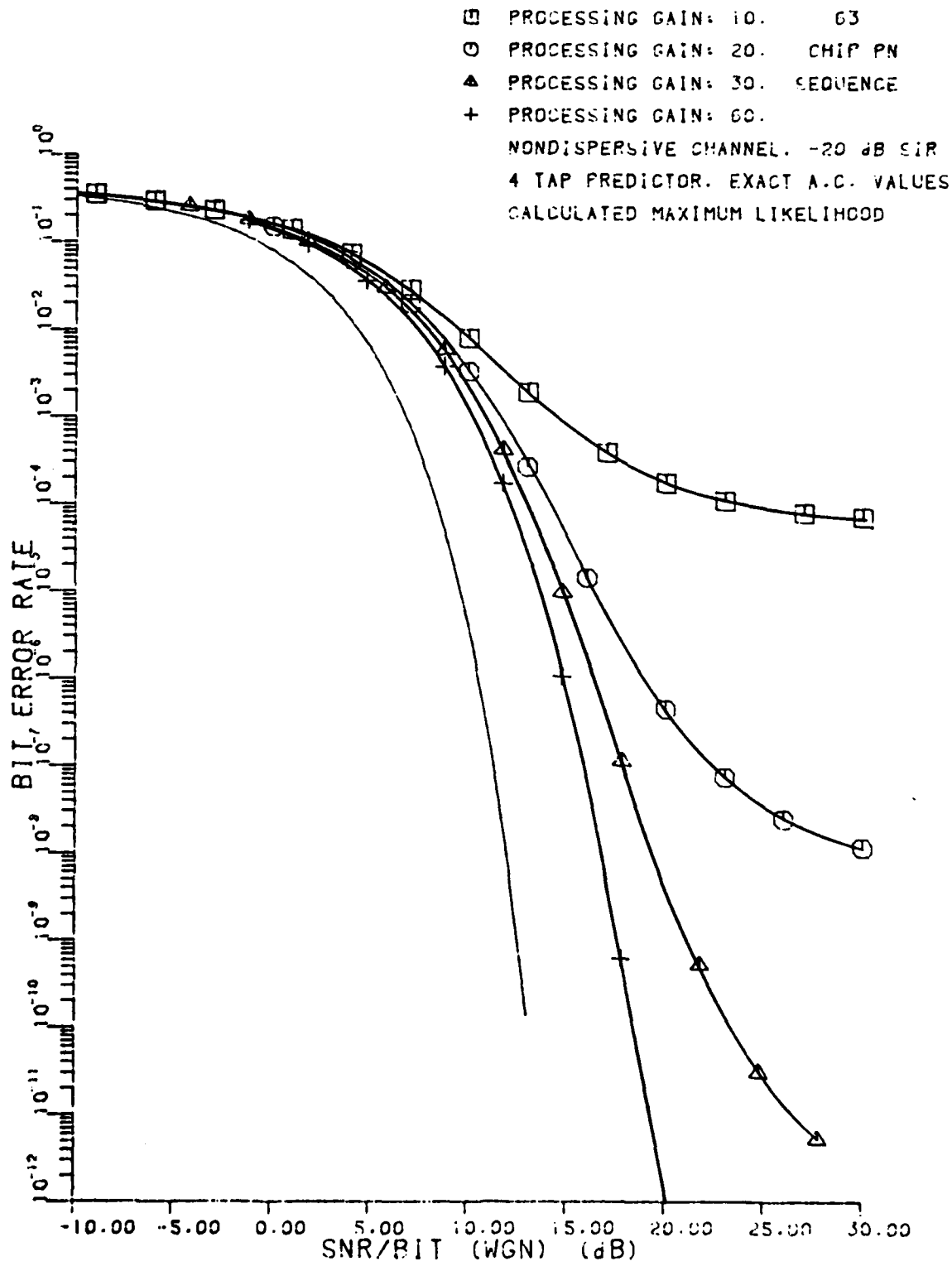
PROCESSING GAIN: 10. 63
PROCESSING GAIN: 20. CHIP PN
PROCESSING GAIN: 30. SEQUENCE
PROCESSING GAIN: 60.
NONDISPERSIVE CHANNEL. -20 dB SIR
4 TAP PREDICTOR. EXACT A.C. VALUES
CALCULATED MAXIMUM LIKELIHOOD
BIT ERROR RATE
SNR/BIT (WGN) (dB)
-10.00
-5.00
0.00
5.00
10.00
15.00
20.00
25.00
30.00

Figure 29

AD-A115 007 NORTHEASTERN UNIV BOSTON MA F/G 12/1
RECEIVER OPTIMIZATION AND ERROR RATES FOR PSEUDO-NOISE SPREAD S--ETC(U)
FEB 82 J W KETCHUM, J G PROAKIS F30602-78-C-0102
UNCLASSIFIED RADC-TR-81-402 NL

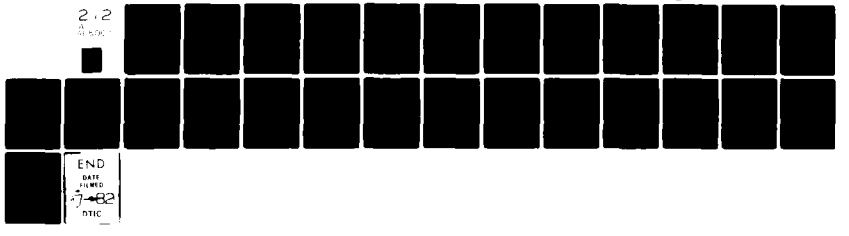

END
DATE FILMED
7-82
DTIC

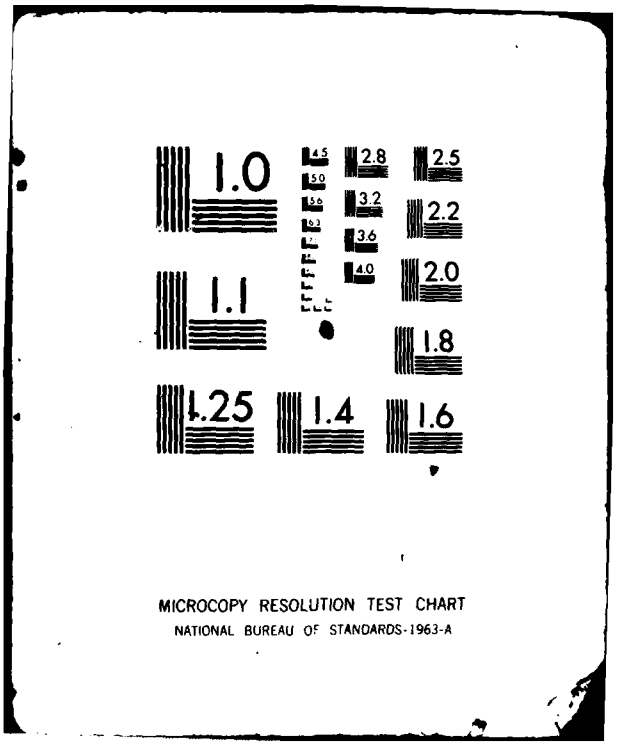
1.0
1.1
1.25
1.4
1.6
1.8
2.0
2.2
2.5
2.8
3.2
3.6
4.0
4.5
5.0
5.6
6.3
MICROCOPY RESOLUTION TEST CHART
NATIONAL BUREAU OF STANDARDS-1963-A

Finally, Figure 30 shows the performance obtained when the sequence length equals the processing gain, for sequence lengths of 15, 31, and 63. Here again, at the high processing gain, the performance is not much different from that obtained with the long spreading sequence, but at lower processing gains, the minimum achievable error rates are significantly better than those obtained with the long PN sequence.

Dispersive Channel

The upper bound on error rate performance of the maximum likelihood receiver for transmission over a nondispersive channel, which is summarized in (65) and (79) can be modified to give an upper bound on performance of the maximum likelihood receiver for transmission over a dispersive channel. This is done in a manner similar to that used to generalize the alternate method for evaluating the bit error rate performance of the bit-by-bit receiver given in Part III. This has been done, and the results have been used to evaluate the upper bound for channels with weights (1,1), (.5,.71,.5) and (.38,.6,.6,.38). These are channels given by Magee and Proakis [7] as the channels with length 2, 3, and 4 which have minimum distance of all channels of their respective lengths for binary antipodal signaling in white Gaussian noise. Although these channels will not necessarily yield minimum distance in non-white noise, they are useful as examples of the performance of the maximum likelihood receiver

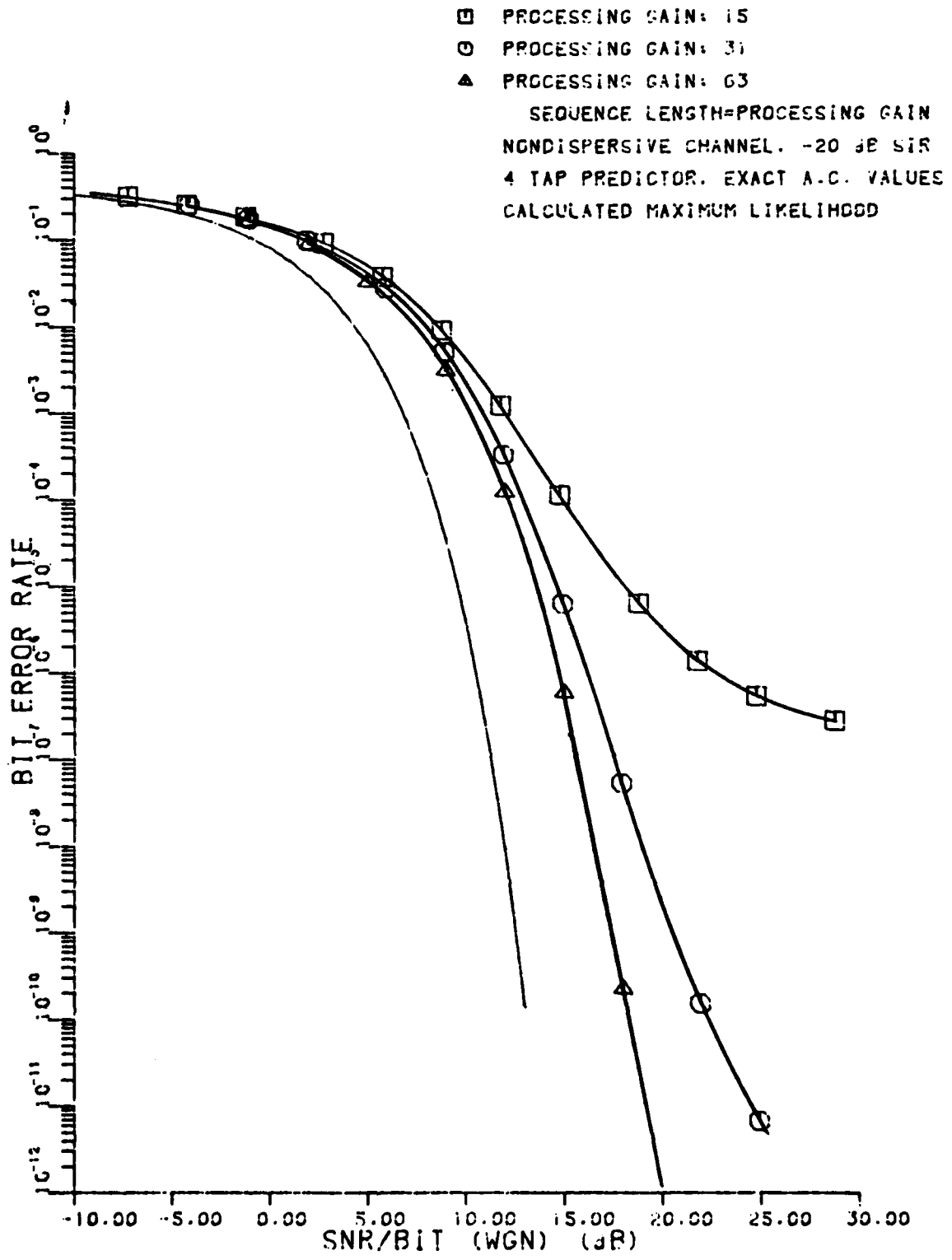
PROCESSING GAIN: 15
PROCESSING GAIN: 31
PROCESSING GAIN: 63
SEQUENCE LENGTH=PROCESSING GAIN
NONDISPERSIVE CHANNEL. -20 dB SIR
4 TAP PREDICTOR. EXACT A.C. VALUES
CALCULATED MAXIMUM LIKELIHOOD
BIT ERROR RATE
SNR/BIT (WGN) (dB)
-10.00
-5.00
0.00
5.00
10.00
15.00
20.00
25.00
30.00

Figure 30

for channels with severe multipath distortion.

Figures 31 and 32 show the performance of the maximum likelihood receiver for the channel with weights (1,1) and interference which consists of 100 complex sinusoids with random phases uniformly distributed between 0 and 2π, and occupying the band between -0.1 and +0.1 Hz. The PN sequence used in these examples is the maximal length sequence of length 1023 used in previous examples. Figure 31 illustrates the performance with -20dB SIR, 32 with -10dB SIR. Comparing these results with the corresponding results for bit-by-bit detection (Figures 20 and 21) shows that, as with the non-dispersive channel, at a processing gain of 60, there is very little difference in the performance of the maximum likelihood and bit-by-bit receivers. At the lower processing gains the maximum likelihood receiver again bottoms out at a lower error probability than the bit-by-bit receiver.

The performance of the maximum likelihood receiver for the (1,1) channel when shorter sequences are used was also considered, and the results were similar to those obtained for shorter sequences with a nondispersive channel. At a processing gain of 60, the performance differs little from that of the longer sequence. At smaller processing gains, the bottoming out behavior is considerably less severe than that exhibited when the longer (1023 chips) sequence is used. Figure 33 shows the performance for the same channel, interference, and processing gains as Figure 31, but with a 63-chip

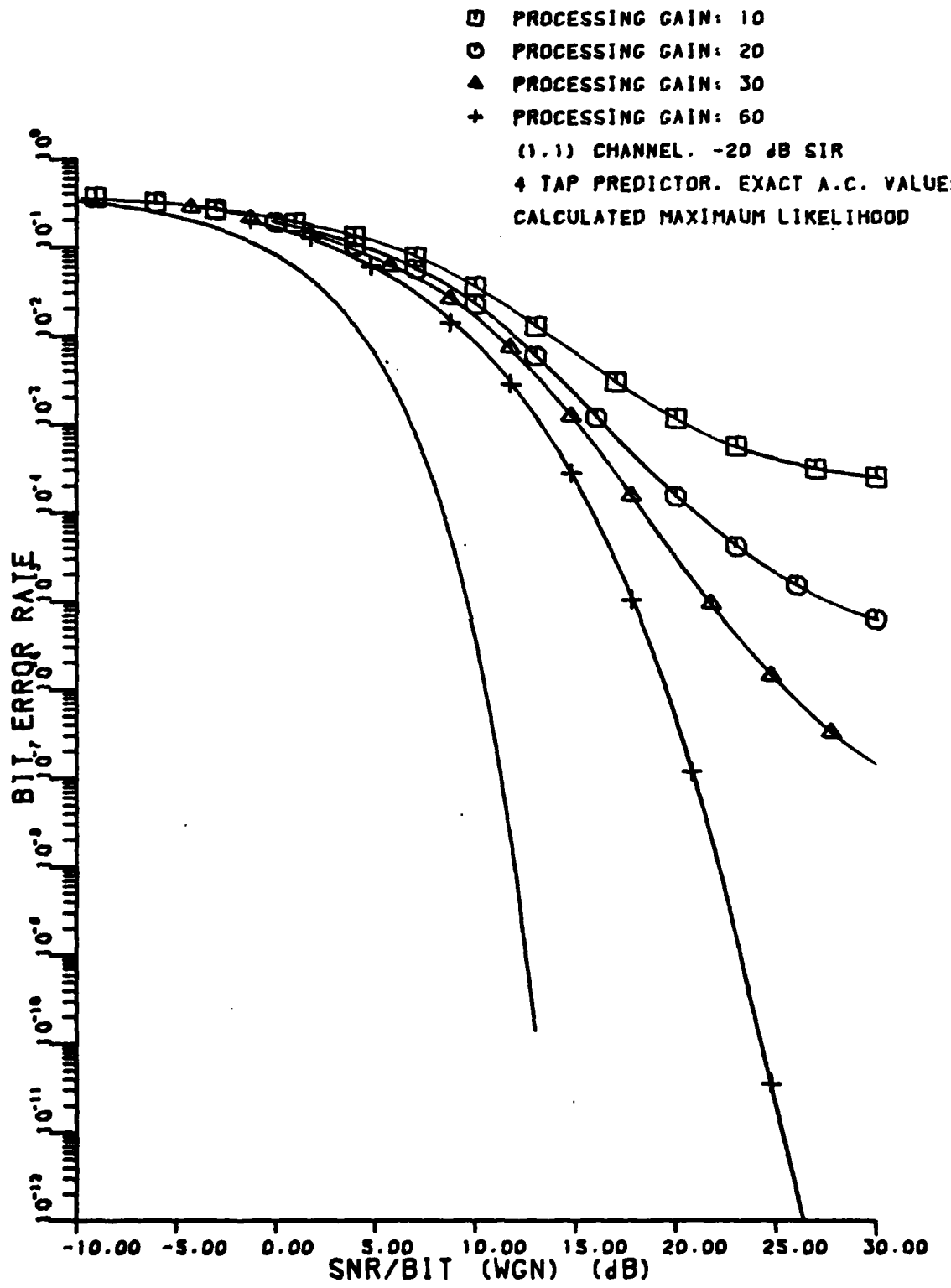
PROCESSING GAIN: 10
PROCESSING GAIN: 20
PROCESSING GAIN: 30
PROCESSING GAIN: 60
(1.1) CHANNEL. -20 dB SIR
4 TAP PREDICTOR. EXACT A.C. VALUES
CALCULATED MAXIMAUM LIKELIHOOD
BIT ERROR RATE
SNR/BIT (WGN) (dB)
-10.00
-5.00
0.00
5.00
10.00
15.00
20.00
25.00
30.00

Figure 31

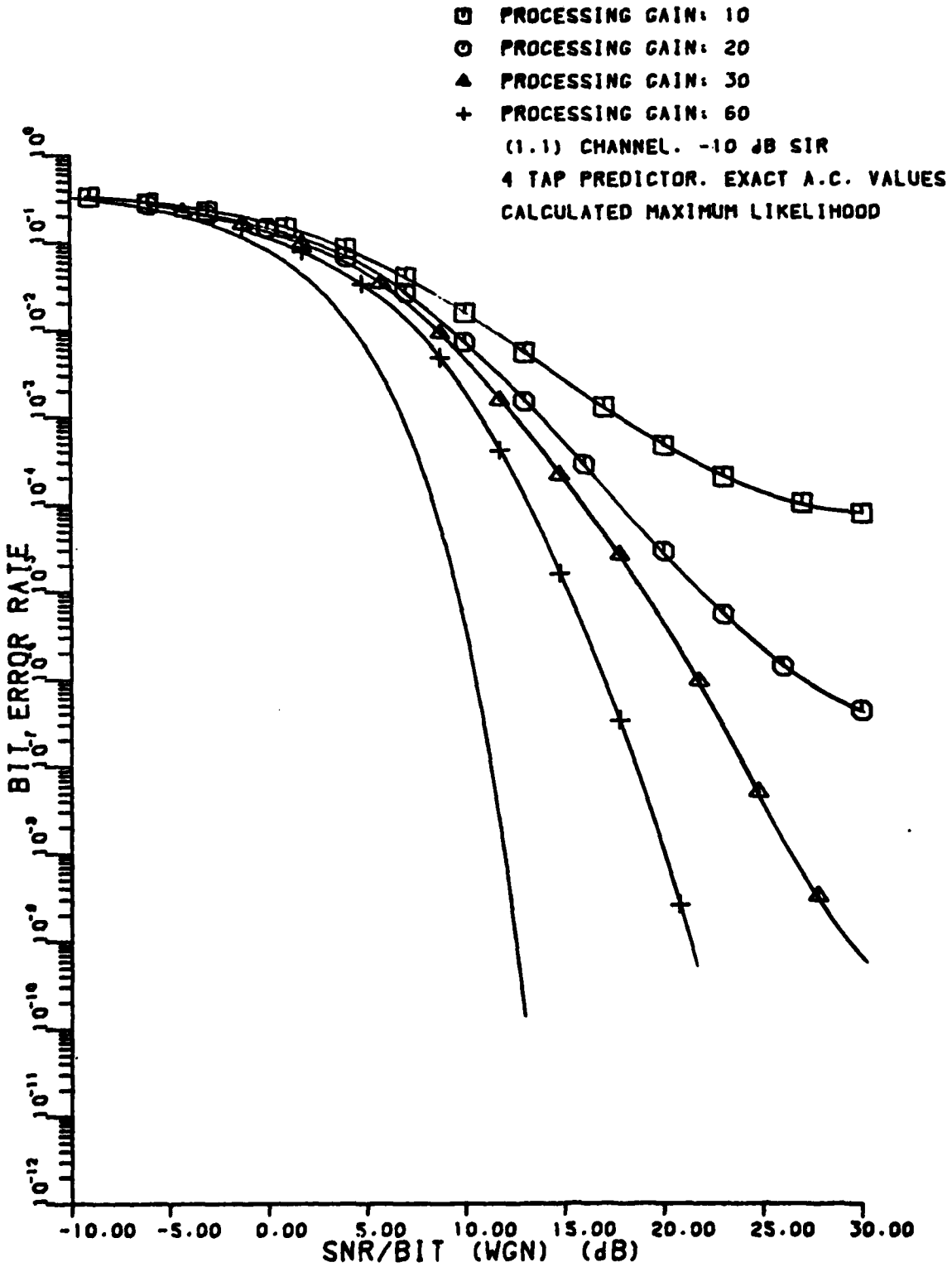
PROCESSING GAIN: 10
PROCESSING GAIN: 20
PROCESSING GAIN: 30
PROCESSING GAIN: 60
(1,1) CHANNEL. -10 dB SIR
4 TAP PREDICTOR. EXACT A.C. VALUES
CALCULATED MAXIMUM LIKELIHOOD
BIT ERROR RATE
SNR/BIT (WGN) (dB)
-10.00
-5.00
0.00
5.00
10.00
15.00
20.00
25.00
30.00

Figure 32

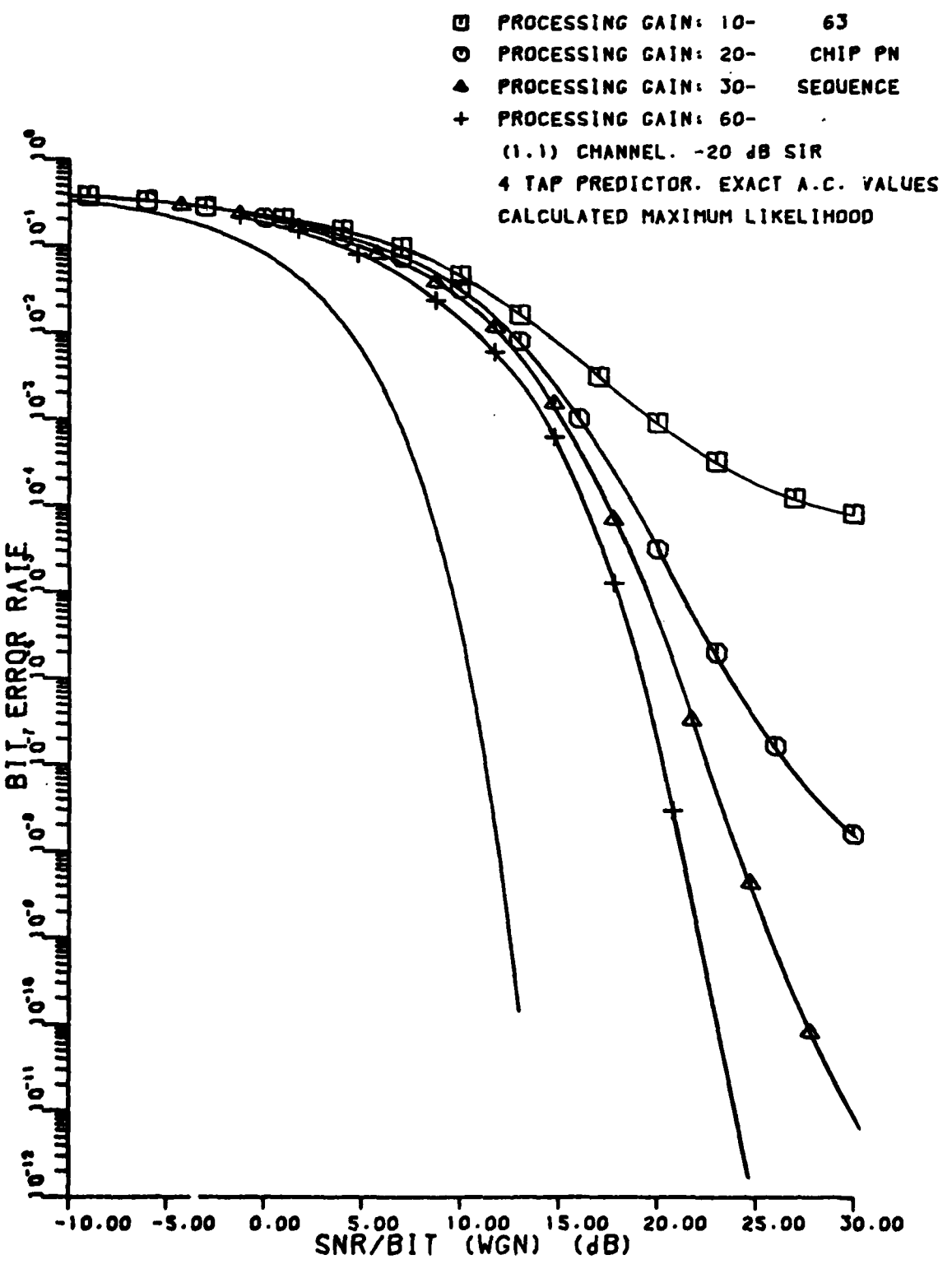
PROCESSING GAIN: 10- 63
PROCESSING GAIN: 20- CHIP PN
PROCESSING GAIN: 30- SEQUENCE
PROCESSING GAIN: 60-
(1,1) CHANNEL. -20 dB SIR
4 TAP PREDICTOR. EXACT A.C. VALUES
CALCULATED MAXIMUM LIKELIHOOD
BIT ERROR RATE
SNR/BIT (WGN) (dB)
-10.00 -5.00 0.00 5.00 10.00 15.00 20.00 25.00 30.00

Figure 33

PN sequence. Figure 34 is the performance with same channel and interference, but now the processing gain and sequence length are the same, with values of 15, 31, and 63.

Finally, Figures 35 and 36 show the performance obtained with the 3- and 4-tap channels given above. In these computations the interference, sequence length and processing gains are the same as those which yielded the performance curves in Figure 31. These curves exhibit behavior similar to that of the nondispersive and (1,1) channel except that as the span of the dispersion increases, the degradation relative to ideal binary antipodal signaling increases, reaching approximately 16dB at 10^{-7} BER for the 4-tap channel with a processing gain of 60. Although this is a severe degradation, we have demonstrated that the performance of the maximum likelihood receiver using autoregressive spectral estimation techniques for suppressing narrowband interference in an environment of severe multipath distortion exhibits error probability performance which decreases exponentially as a function of E_b/N_o. This is a significant improvement over performance which is achievable even on a nondispersive channel without interference suppression.

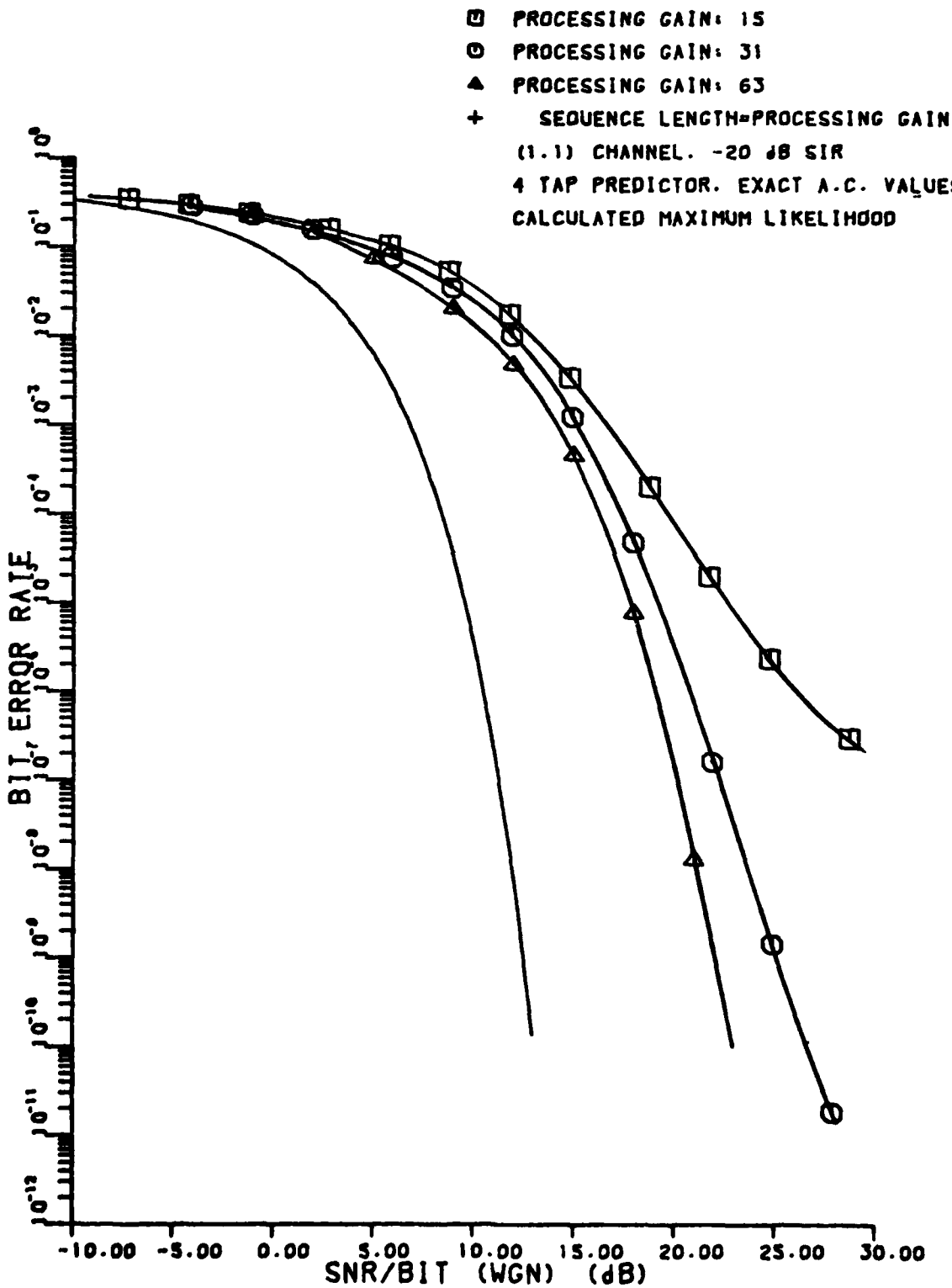
PROCESSING GAIN: 15
PROCESSING GAIN: 31
PROCESSING GAIN: 63
SEQUENCE LENGTH=PROCESSING GAIN
(1,1) CHANNEL. -20 dB SIR
4 TAP PREDICTOR. EXACT A.C. VALUES
CALCULATED MAXIMUM LIKELIHOOD
BIT ERROR RATE
SNR/BIT (WGN) (dB)
-10.00
-5.00
0.00
5.00
10.00
15.00
20.00
25.00
30.00

Figure 34

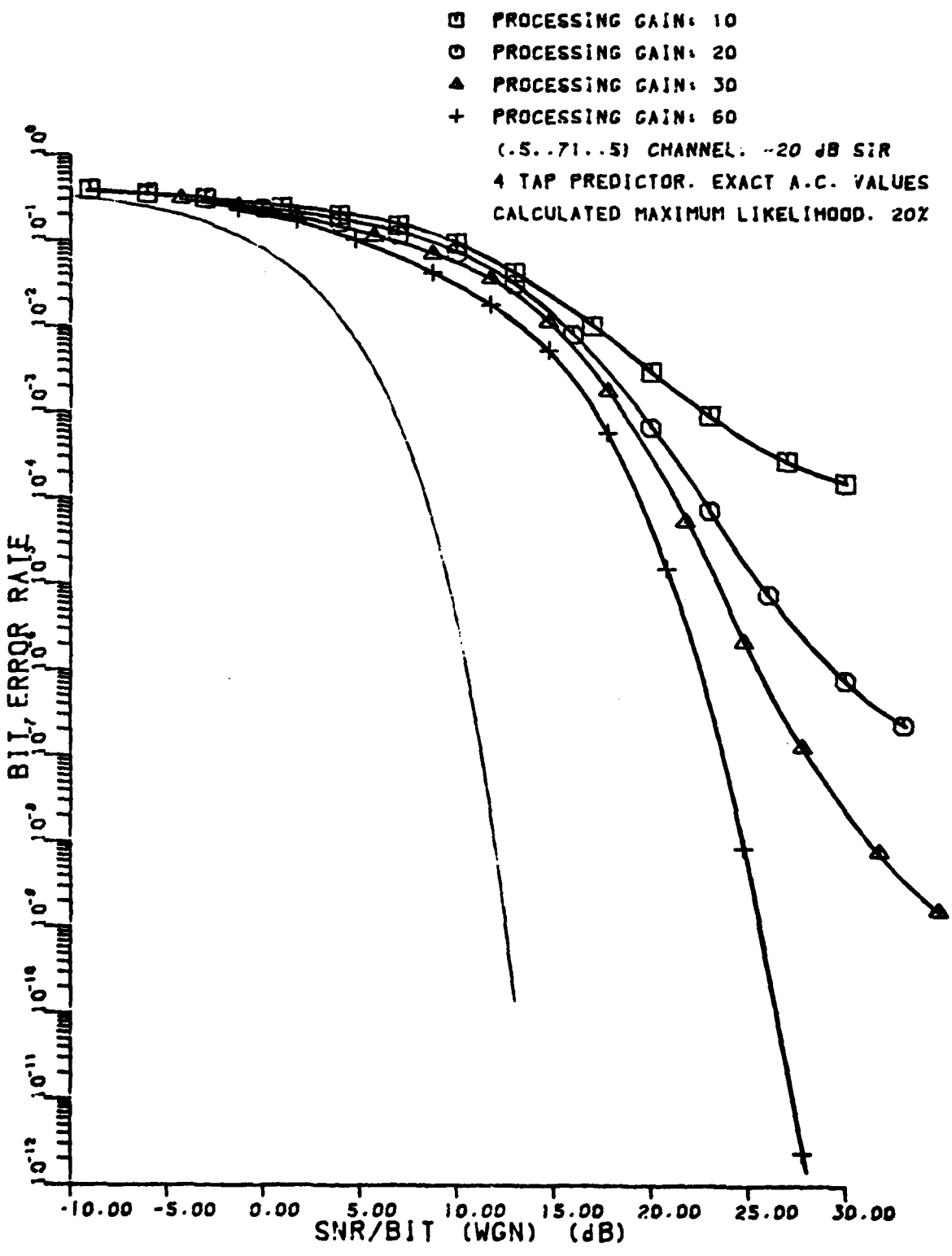
PROCESSING GAIN: 10
PROCESSING GAIN: 20
PROCESSING GAIN: 30
PROCESSING GAIN: 60
(.5..71..5) CHANNEL. -20 dB SIR
4 TAP PREDICTOR. EXACT A.C. VALUES
CALCULATED MAXIMUM LIKELIHOOD. 20%
BIT ERROR RATE
SNR/BIT (WGN) (dB)
-10.00
-5.00
0.00
5.00
10.00
15.00
20.00
25.00
30.00

Figure 35

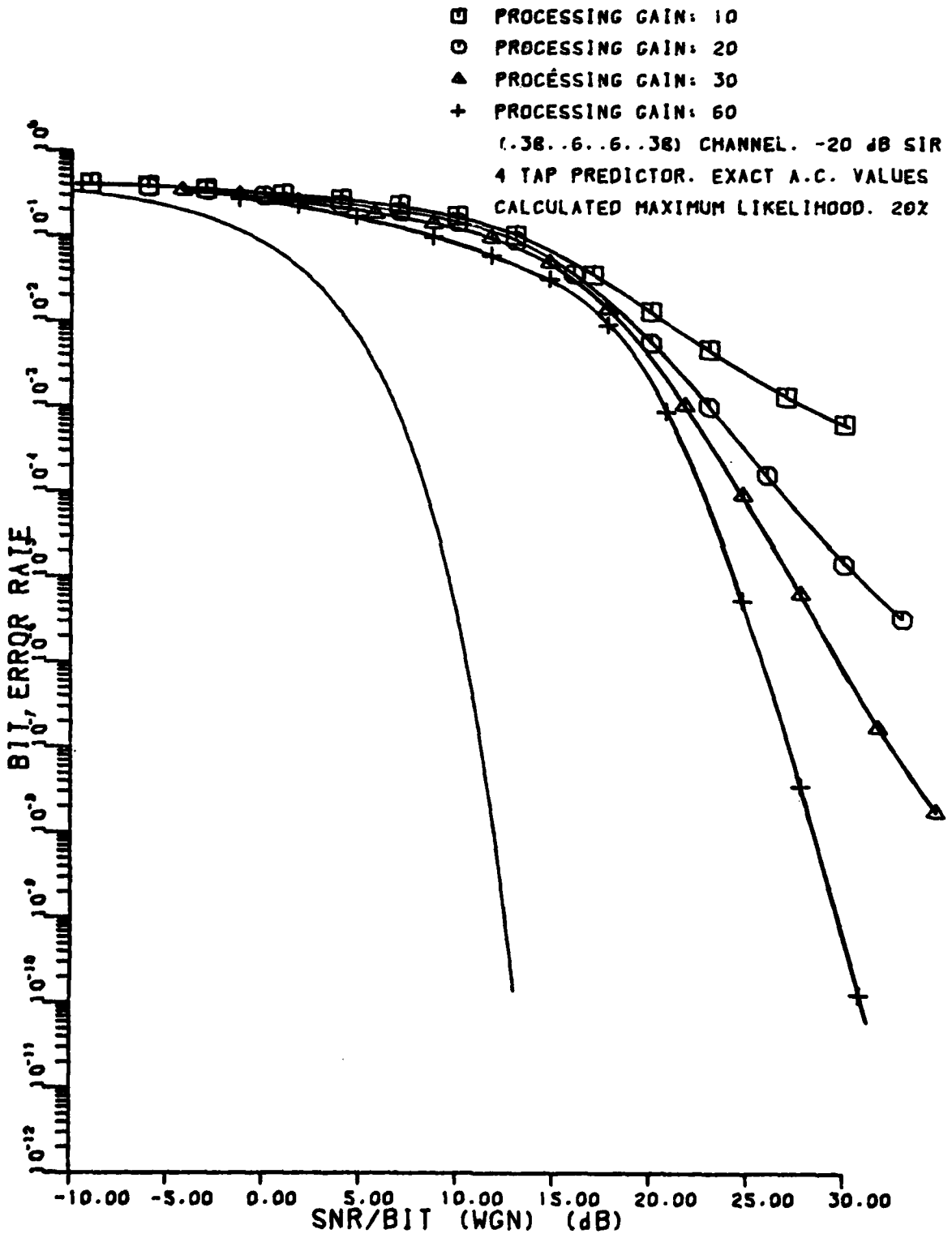
PROCESSING GAIN: 10
PROCESSING GAIN: 20
PROCESSING GAIN: 30
PROCESSING GAIN: 60
(.38..6..6..38) CHANNEL. -20 dB SIR
4 TAP PREDICTOR. EXACT A.C. VALUES
CALCULATED MAXIMUM LIKELIHOOD. 20%
BIT ERROR RATE
SNR/BIT (WGN) (dB)
-10.00 -5.00 0.00 5.00 10.00 15.00 20.00 25.00 30.00

Figure 36

Appendix A

In a previous report [2], the signal-to-noise ratio, defined as $E^2(z)/var(z)$, of the decision variable at the output of the sequence correlator shown in Figure 11 is shown to be:

$$SNR_o = \frac{L}{\sum_{\ell=1}^{P} h^2(\ell) + \sum_{\ell=0}^{P} \sum_{m=0}^{P} h(\ell)\, h(m)\, \rho_i(\ell - m) + \sigma_n^2 \sum_{\ell=0}^{P} h^2(\ell)} \tag{A.1}$$

This expression is limited for the following reasons: (1) it only applies when the suppression filter does not delay the desired signal, i.e., the first tap is the largest tap; (2) it only applies to baseband signaling. In this appendix we derive a more general formula for the signal-to-noise ratio for bandpass signaling, with a zero delay suppression filter and with a linear phase suppression filter.

When the whitening filter alone is used, the suppression filter has zero delay, and the decision variable is given by (35):

$$z_j = 2\alpha E_c\, Lh(0)\, u_j + 2\alpha E_c \sum_{k=jL}^{(j+1)L-1} \sum_{\ell=1}^{P} u_{\lfloor (k-\ell)/L \rfloor} \cdot c_k\, c_{k-\ell}\, h(\ell)$$

$$+ \sum_{k=jL}^{(j+1)L-1} \sum_{\ell=0}^{P} c_k \, h(\ell) \, \mathrm{Re}\left\{ \int_{-\infty}^{\infty} [n(\tau) + i(\tau)] \right.$$

$$\left. \cdot \, p^*[\tau - (k - \ell)\, \tau_c] \, d\tau \right\} \tag{34}$$

The mean of z_j is

$$E(z_j) = 2\alpha E_c \, Lh(0) \tag{A.2}$$

and the variance is

$$\mathrm{var}(z_j) = S_j + I_j + N_j \tag{A.3}$$

The first term in (A.3) is:

$$S_j = 4\alpha^2 E_c^2 \sum_{k=jL}^{(j+1)L-1} \sum_{m=jL}^{(j+1)L-1} \sum_{\ell=1}^{P} \sum_{n=1}^{P}$$

$$\cdot \, \overline{u_{\lfloor (k-\ell)/L \rfloor} \, u_{\lfloor (m-n)/L \rfloor}} \; \overline{c_k \, c_m \, c_{k-\ell} \, c_{m-n}} \; h(\ell) \, h(m) \tag{A.4}$$

Since $\{c_k\}$ is assumed to be a white sequence, c_k and c_ℓ are uncorrelated unless $k = \ell$. Thus $\overline{c_k \, c_\ell \, c_m \, c_n} = 0$ unless $k = \ell$ and $m = n$, $k = n$ and $\ell = m$, or $k = m$ and $\ell = n$, in which case $\overline{c_k \, c_\ell \, c_m \, c_n} = 1$. So $\overline{c_k \, c_m \, c_{k-\ell} \, c_{m-n}} = 0$ unless $k = m$ and $\ell = n$, $k = m - n$ and $m = k - \ell$, or $k = k - \ell$ and

$m = m - n$. The first condition is easily satisfied. The second condition is two equations in three unknowns which yields the following equality:

$$\ell = -n$$

which cannot be satisfied, since the intervals of summation of both ℓ and n are positive. Using the first condition in (A.4), we get

$$S_j = 4\alpha^2 E_c^2 L \sum_{\ell=1}^{P} h^2(\ell) \tag{A.5}$$

The second term in (A.3) is:

$$I_j = \frac{1}{2} \sum_{k=jL}^{(j+1)L-1} \sum_{m=jL}^{(j+1)L-1} \sum_{\ell=0}^{P} \sum_{n=0}^{P} \overline{c_k c_m}$$

$$\cdot \iint_{-\infty}^{\infty} \overline{i(t)\, i^*(\tau)}\, p^*[t - (k - \ell)\, \tau_c]$$

$$\cdot\, p[\tau - (m - n)\, \tau_c]\, dt\, d\tau$$

$$= \frac{1}{2} \sum_{\ell=0}^{P} \sum_{n=0}^{P} \sum_{k=jL}^{(j+1)L-1} \iint_{-\infty}^{\infty} 2\phi_{ii}(t - \tau)$$

$$\cdot\, p^*[t - (k - \ell)\, \tau_c)\, p[\tau - (k - n)\, \tau_c]\, dt\, d\tau \tag{A.6}$$

Equation (A.6) is evaluated in a manner similar to that used to evaluate (28), yielding

$$I_j = 2L\,\tau_c\,E_c \sum_{\ell=0}^{P} \sum_{n=0}^{P} h(\ell)\,h(n)\,\phi_{ii}[(n-\ell)\,\tau_c] \tag{A.7}$$

The third term, N_j, can be found in a straightforward manner to be:

$$N_j = 2L\,N_o\,E_c \sum_{\ell=0}^{P} h^2(\ell) \tag{A.8}$$

Summing (A.5), (A.7), and (A.8) gives the expression for $\mathrm{var}(z_j)$ given by (37):

$$\mathrm{var}(z_j) = 2L\,N_o\,E_c \sum_{\ell=0}^{P} h^2(\ell) + 2L\,\tau_c\,E_c \sum_{\ell=0}^{P} \sum_{m=0}^{P} h(\ell)\,h(m)\,\phi_{ii}[(m-\ell)\,\tau_c] + 4\alpha^2\,LE_c^2 \sum_{\ell=1}^{P} h^2(\ell) \tag{37}$$

The resulting SNR, now defined as $E^2(z_j)/2\,\mathrm{var}(z_j)$, is:

$$\gamma_j = \frac{L\,E_c\,h^2(0)\,\alpha^2}{N_o \sum_{\ell=0}^{P} h^2(\ell) + \tau_c \sum_{\ell=0}^{P} \sum_{m=0}^{P} h(\ell)h(m)\phi_{ii}[(m-\ell)\tau_c] + 2\alpha^2 E_c \sum_{\ell=1}^{P} h^2(\ell)} \tag{38}$$

This expression is similar to (A.1) with the exception that (38) is a bit more general than (A.1), and that when $\rho_i(0) = \phi_{ii}(0)$, the interference term in (38) contributes relatively half as much to the denominator in (38) as it does in (A.1). This is because a coherent bandpass receiver has a 3dB advantage over a baseband receiver against interference.

Next we consider the linear phase filter case. For convenience, we allow the linear phase filter to have an acausal impulse response. The linear phase interference suppression filter has coefficients $g(\ell)$, $\ell = -P, \ldots, P$, where $g(\ell) = g(-\ell)$, and the $g(\ell)$'s are real valued. The decision variable in this case is given by:

$$z_j = 2\alpha E_c Lg(0) u_j + 2\alpha E_c \sum_{k=jL}^{(j+1)L-1} \sum_{\substack{\ell=-p \\ \ell\neq 0}}^{P} u_{\lfloor (k-\ell)/L \rfloor} \cdot c_k c_{k-\ell} g(\ell)$$

$$+ \sum_{k=jL}^{(j+1)L-1} \sum_{\ell=-p}^{P} c_k g(\ell) \, \mathrm{Re}\left\{ \int_{-\infty}^{\infty} [n(\tau) + i(\tau)] \cdot p^*[\tau - (k-\ell)\tau_c] \, d\tau \right\} \qquad (34)$$

The mean of this decision variable is

$$E(z_j) = 2\alpha E_c Lg(0) \qquad (A.9)$$

and the variance is again given by

$$\text{var}(z_j) = S_j + I_j + N_j \tag{A.10}$$

The second two terms in (A.10) are found in a manner similar to that used to find the second two terms in (A.3). These terms are:

$$I_j = 2L\,\tau_c\,E_c \sum_{\ell=-p}^{P} \sum_{n=-p}^{P} g(\ell)\,g(n)\,\phi_{ii}[(n-\ell)\,\tau_c] \tag{A.11}$$

and

$$N_j = 2L\,N_o\,E_c \sum_{\ell=-p}^{P} g^2(\ell) \tag{A.12}$$

The self-noise variance, S_j, is found as follows:

$$S_j = 4\alpha^2 E_c^2 \left\{ \sum_{k=jL}^{(j+1)L-1} \sum_{\substack{\ell=-p \\ \ell\neq 0}}^{P} \sum_{m=jL}^{(j+1)L-1} \sum_{\substack{n=-p \\ n\neq 0}}^{P} \cdot \overline{u_{\lfloor (k-\ell)/L \rfloor}\, u_{\lfloor (m-n)/L \rfloor}}\ \overline{c_k\, c_{k-\ell}\, c_m\, c_{m-n}}\ g(\ell)\,g(n) \right\} \tag{A.13}$$

The three conditions outlined above under which $\overline{c_k\, c_{k-\ell}\, c_m\, c_{m-n}} = 0$ apply equally well for (A.13). However, in this case, the first condition as well as the second condition apply, i.e.,

we can set $k = m$ and $\ell = n$, but we can also set $m = k - \ell$ and $n = -\ell$. Thus we can write:

$$S_j = 4\alpha^2 E_c^2 \sum_{k=jL}^{(j+1)L-1} \sum_{\substack{\ell=-p \\ \ell\neq 0}}^{P} g^2(\ell)$$

$$+ 4\alpha^2 E_c^2 \sum_{k=jL}^{(j+1)L-1} \sum_{\substack{\ell=-p \\ \ell\neq 0}}^{P} g(\ell)\, g(-\ell)$$

$$jL \leq k-\ell \leq (j+1)L-1$$

$$= 4\alpha^2 E_c^2 \left\{ 2L \sum_{\ell=1}^{P} g^2(\ell) + 2 \sum_{\ell=1}^{P} (L - \ell)\, g^2(\ell) \right\}$$

$$= 8\alpha^2 E_c^2 \sum_{\ell=1}^{P} (2L - \ell)\, g^2(\ell) \qquad \text{(A.14)}$$

Summing these three terms yields the expression for $\text{var}(z_j)$ given by (39b), and the ratio $E^2(z_j)/2\ \text{var}(z_j)$ is given by (40).

An SNR improvement factor, defined as

$$\eta = \frac{\text{SNR with filter}}{\text{SNR without filter}}$$

was given in [2] as

$$\eta = \frac{\rho_i(0) + \sigma_n^2}{\sum_{\ell=1}^{P} h^2(\ell) + \sum_{\ell=0}^{P}\sum_{m=0}^{P} h(\ell)\, h(m)\, \rho_i(\ell-m) + \sigma_n^2 \sum_{\ell=0}^{P} h^2(\ell)} \tag{A.15}$$

A similar expression for improvement factor can be obtained by taking the ratio of (38) over (33):

$$\eta = \frac{[N_o + \tau_c\, \phi_{ii}(0)]\, h^2(0)}{N_o \sum_{\ell=0}^{P} h^2(\ell) + \tau_c \sum_{\ell=0}^{P}\sum_{m=0}^{P} h(\ell)h(m)\phi_{ii}[(m-\ell)\tau_c] + 2\alpha^2 E_c^2 \sum_{\ell=1}^{P} h^2(\ell)} \tag{A.16}$$

If $h(k)$, $k = 0, \ldots, P$ is normalized so that $h(0) = 1$, and we let $\sigma_n^2 = N_o/2$, $\alpha = 1$, $\tau_c = 1$, and $E_c = 1$, then (A.16) reduces to (A.15), with the exception that the interference terms in the numerator and denominator are a factor of 2 smaller than in (A.15). This is due to the fact that (A.15) applies to the baseband case, and (A.16) to bandpass signaling. The coherent bandpass receiver thus has a 3dB advantage over the baseband receiver against interference, as has been pointed out earlier.

The improvement factor given by (A.16) applies to the receiver with a zero delay interference suppression filter. The improvement factor for the receiver which contains a linear phase suppression filter can be obtained by taking the ratio of (40) over (33):

$$\eta =$$

$$\frac{[N_o + \tau_c \phi_{ii}(0)]\, g^2(0)}{N_o \sum_{\ell=-p}^{p} g^2(\ell) + \tau_c \sum_{\ell=-p}^{p} \sum_{m=-p}^{p} g(\ell) g(m) \phi_{ii}[(m-\ell)\tau_c] + \frac{1}{4}\alpha^2 E_c \sum_{\ell=1}^{p} \frac{(2L-\ell)}{L} g^2(\ell)}$$

(A.17)

Appendix B

In view of the results of Appendix A, some of the results given in [2] need to be modified. The improvement factor given by (A.15) was used in [2] both for the receiver with a zero delay suppression filter (whitening filter only) and for the receiver with a linear phase filter (whitening filter followed by its matched filter), and linear phase filter based on the Welch method. Given (A.17), however, this is clearly inappropriate. The improvement factors for these latter cases have been recalculated, and the results are given in this appendix.

Figure B.1 is the newly calculated improvement factor for the receiver with a whitening filter followed by its matched filter. In this figure the horizontal axis is the SNR/chip without filtering, given by

$$\frac{E_c \alpha^2}{\frac{N_o}{2} + \frac{\tau_c}{2} \phi_{ii}(0)}$$

This figure replaces Figure 3.16 in [2]. The curves in Figure B.1 are about 3dB below the corresponding curves in Figure 3.16 of [2]. This implies that the self-noise term in the improvement factor is in this case the dominant noise term, since we have increased the self-noise by almost 3dB, and the resulting change in the improvement factor is about 3dB.

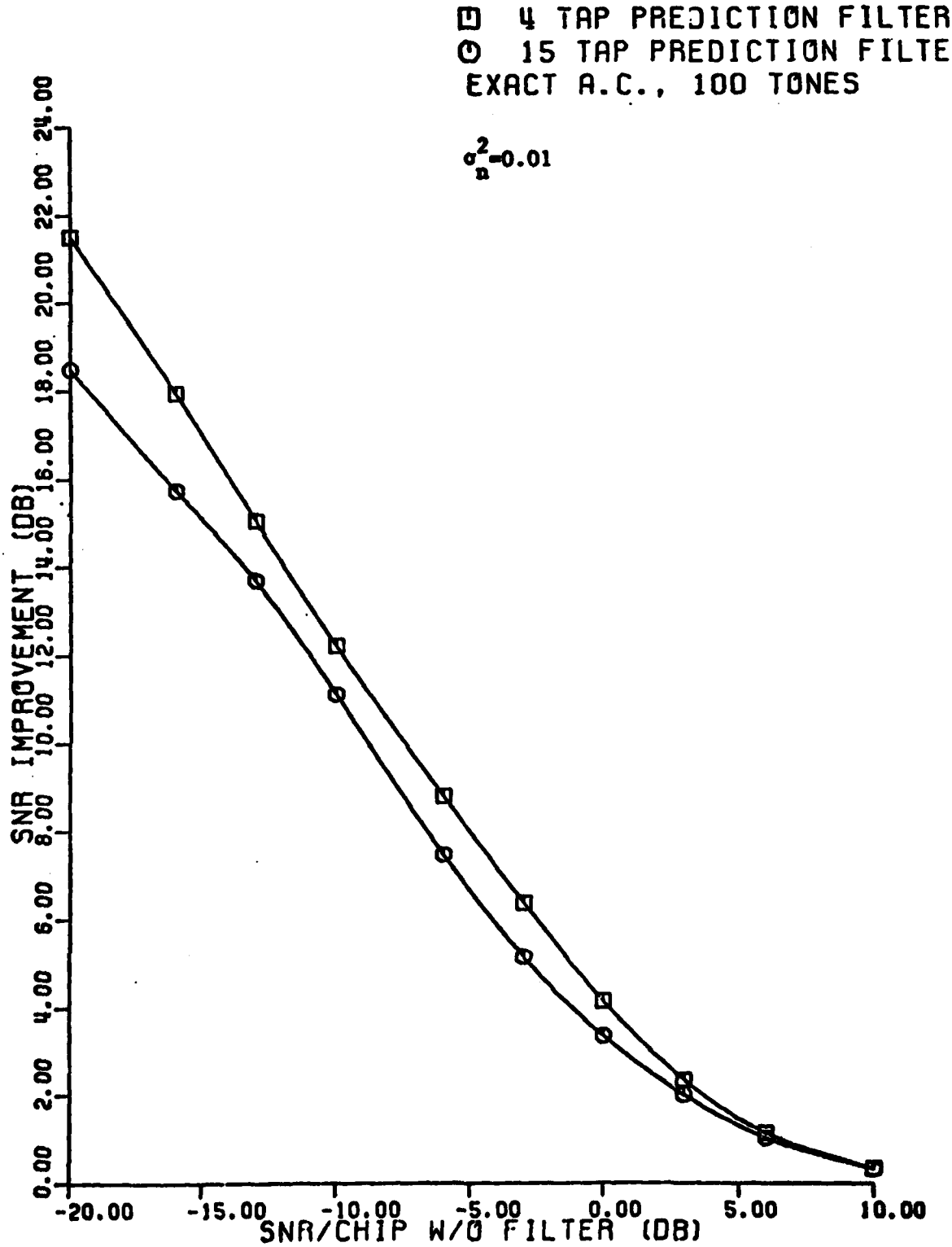
4 TAP PREDICTION FILTER
15 TAP PREDICTION FILTER
EXACT A.C., 100 TONES
σ_n^2=0.01
SNR IMPROVEMENT (DB)
0.00
2.00
4.00
6.00
8.00
10.00
12.00
14.00
16.00
18.00
20.00
22.00
24.00
-20.00
-15.00
-10.00
-5.00
0.00
5.00
10.00
SNR/CHIP W/O FILTER (DB)

Figure B.1

Figure 3.41 in [2] will also be affected by this correction, although we have not replotted it here. The single effect will be to increase the two self-noise curves in this figure by 3dB.

Figure B.2 is a figure which was not included in [2]. This figure contains plots of the improvement ratio for both the receiver with a matched filter and the receiver without the matched filter, plotted against the signal-to-white noise ratio, E_b/N_o.

Figure B.3 illustrates the improvement factor provided by the 15-tap linear phase filter obtained using the Welch method. This figure differs little from the corresponding figure in [2] (Figure 3.25). At the most, there is 1.5dB difference in the curves. This is because the self-noise term is not the dominant term with this filter because there is significant residual interference at the output.

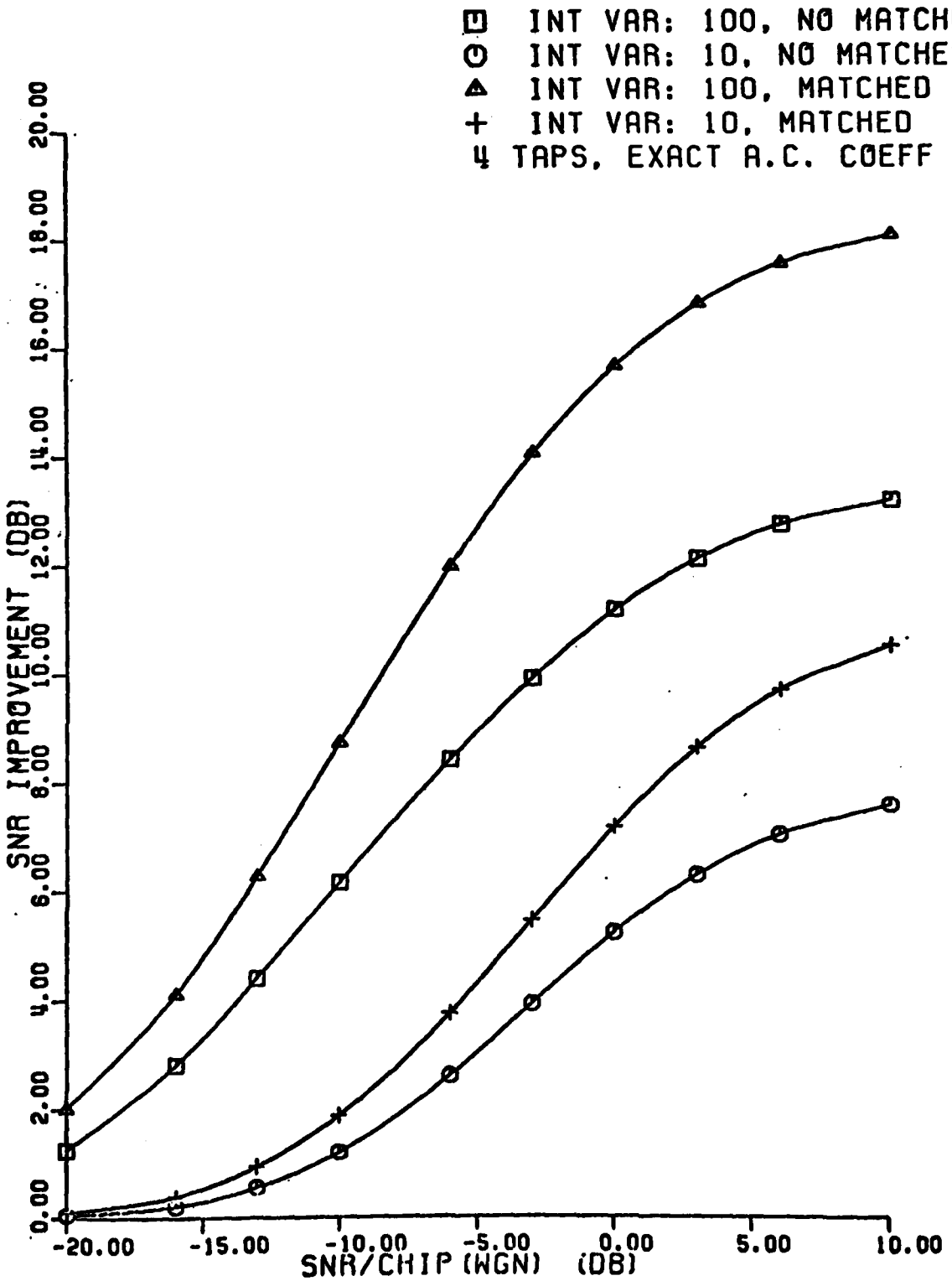
INT VAR: 100, NO MATCHED
INT VAR: 10, NO MATCHED
INT VAR: 100, MATCHED
INT VAR: 10, MATCHED
4 TAPS, EXACT A.C. COEFF
SNR IMPROVEMENT (DB)
0.00
2.00
4.00
6.00
8.00
10.00
12.00
14.00
16.00
18.00
20.00
-20.00
-15.00
-10.00
-5.00
0.00
5.00
10.00
SNR/CHIP (WGN) (DB)

Figure B.2

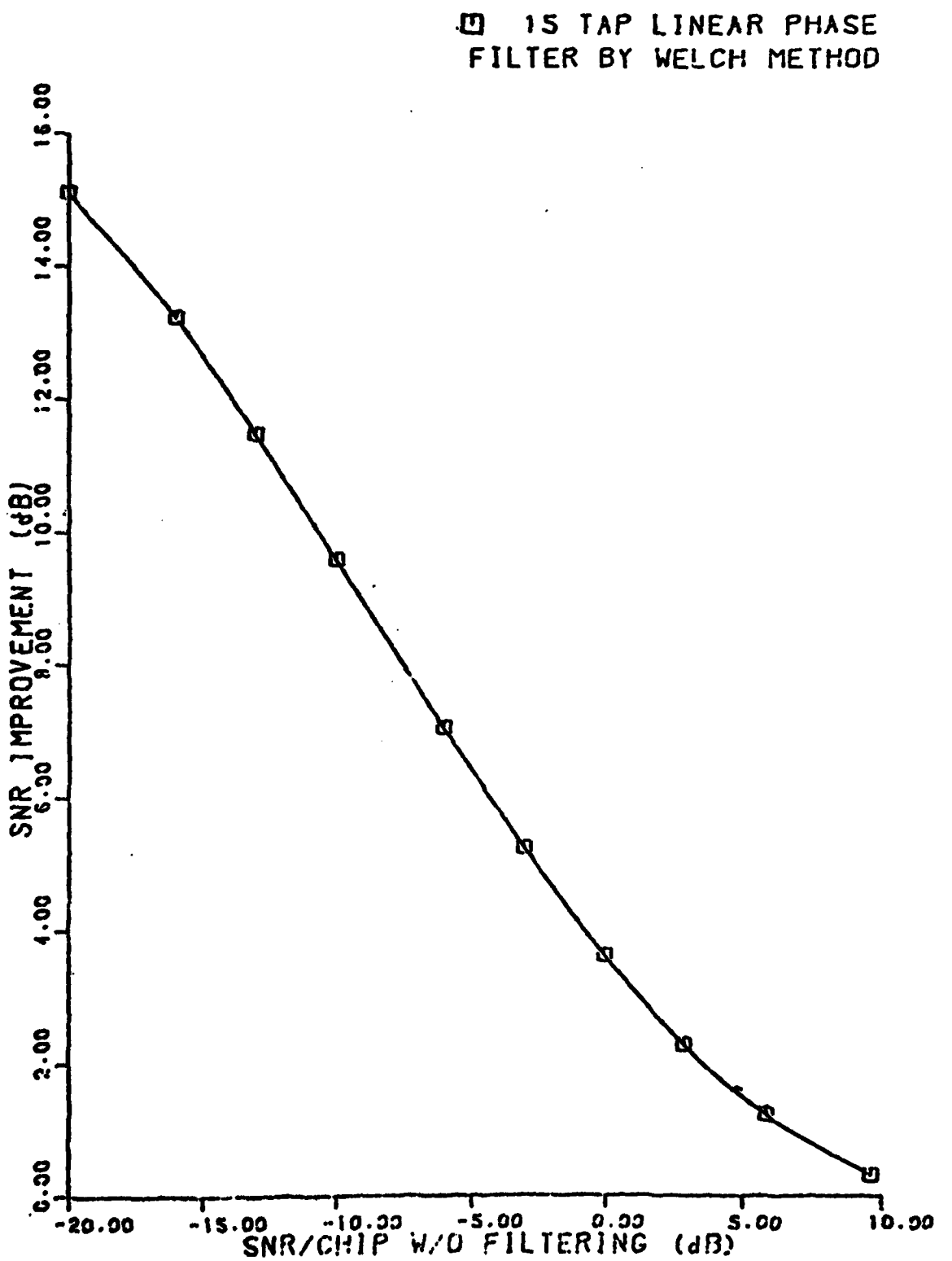
15 TAP LINEAR PHASE
FILTER BY WELCH METHOD
SNR IMPROVEMENT (dB)
16.00
14.00
12.00
10.00
8.00
6.00
4.00
2.00
0.00
-20.00
-15.00
-10.00
-5.00
0.00
5.00
10.00
SNR/CHIP W/O FILTERING (dB)

Figure B.3

References

[1] Hsu, F. M., Giordano, A. A., "Digital Whitening Techniques for Improving Spread Spectrum Communications Performance in the Presence of Narrowband Jamming and Interference," IEEE Trans. Com., Vol. COM-26, No. 2, pp. 209-216, February 1978.

[2] Proakis, J. G., Ketchum, J. W., "Suppression of Narrowband Interference in Pseudo-Noise Spread Spectrum Systems," Northeastern University, Final Technical Report, RADC-TR-81-6, Rome Air Development Center, Air Force Systems Command, Griffiss Air Force Base, New York 13441, February 1981.

[3] Proakis, J. G., Course notes for 03.9C1, 03.9C2, "Digital Communications," Northeastern University, 1979-1980.

[4] Price, R., Green, P. E. Jr., "A Communication Technique for Multipath Channels," Proc. IRE, Vol. 46, pp. 555-569, March 1958.

[5] Viterbi, A. J., Omura, J. K., Principles of Digital Communications and Coding, McGraw-Hill, 1979.

[6] Forney, G. D. Jr., "Maximum-Likelihood Sequence Estimation of Digital Sequences in the Presence of Intersymbol Interference," IEEE Trans. Inform. Theory, Vol. IT-18, No. 3, pp. 363-378, May 1972.

[7] Magee, F. R., Proakis, J. G., "An Estimate of the Upper Bound on Error Probability for Maximum Likelihood Sequence Estimation on Channels Having a Finite Duration Pulse Response," IEEE Trans. Inform. Theory, Vol. IT-19, No. 5, pp. 699-702, September 1973.

MISSION
of
Rome Air Development Center

RADC plans and executes research, development, test and selected acquisition programs in support of Command, Control Communications and Intelligence (C^3I) activities. Technical and engineering support within areas of technical competence is provided to ESD Program Offices (POs) and other ESD elements. The principal technical mission areas are communications, electromagnetic guidance and control, surveillance of ground and aerospace objects, intelligence data collection and handling, information system technology, ionospheric propagation, solid state sciences, microwave physics and electronic reliability, maintainability and compatibility.


DA
FILM